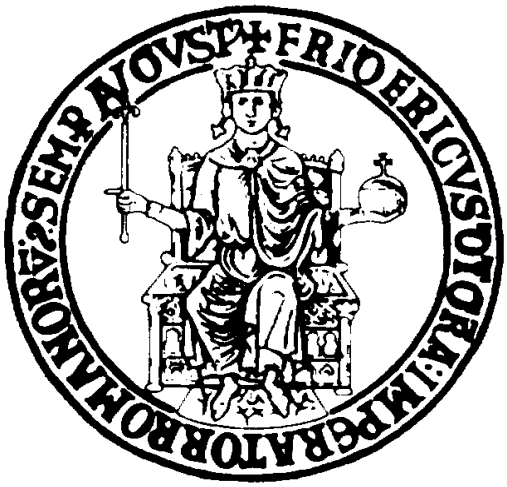

Dither for Smoothing Relay Feedback Systems: an Averaging Approach

Luigi Iannelli

Thesis for the Degree of Doctor of Philosophy
Department of Computer and Systems Engineering
University of Naples Federico II
Napoli, Italy

Submitted to the Faculty of Engineering, University of Naples Federico II, in partial fulfillment of the requirements for the degree of Doctor of Philosophy.

Printed in Italy.
Napoli, November 2002.

Abstract

Dither signals are commonly used for compensating nonlinearities in feedback systems in electronics and mechanics. The seminal works by Zames and Shneydor and more recently by Mossaheb present rigorous tools for systematic design of dithered systems. Their results rely however on a Lipschitz assumption on the nonlinearity and thus do not cover important applications with discontinuities.

The aim of this thesis is to provide some ideas and tools on how to analyse and design dither in nonsmooth systems. In particular, it is shown that a dithered relay feedback system can be approximated by a smoothed system. Guidelines are given for tuning the amplitude and the period time of the dither signal, in order to stabilize the nonsmooth system. Stability results based on Popov-like and Zames-Falb criteria jointly with some Linear Matrix Inequalities are proposed.

Moreover it is argued that in dithered relay feedback systems the shape of dither signals is relevant for stabilization. Some peculiar behaviours of relay feedback systems dithered with a particular class of dither signals are presented. When the dither signal is a square wave, the dithered system can exhibit an asymmetric periodic orbit, though the smoothed system is asymptotically stable. We even show an example in which, by using a trapezoidal dither signal, both systems have a stable oscillation, but the period time for the oscillation of the smoothed system is different from the one of the dithered system.

Finally some engineering applications are presented in order to show the usefulness of techniques and results discussed in the thesis.

Thesis Supervisor: Franco Garofalo, Professor of Automatic Control

Thesis Supervisor: Francesco Vasca, Associate Professor of Automatic Control

Acknowledgements

Yes, ...it's finally time for acknowledgements!! My PhD thesis is over and it is certainly a great joy for me. This thesis is the witness of the good (I hope...) things I learnt and I did, of course, but this period of my life was also full of some other important aspects and I wish to use this section to highlight what I mostly appreciated of my PhD studies...

I spent last three years at the Department of Computer and Systems Engineering of University of Naples Federico II within the Automatic Control group. When I started my career as a PhD student, I realized that I was in a special place, in which the work and studies could get strength supported by the friendly atmosphere due to people who worked there. I think that this atmosphere has a fundamental role for doing what I call a "good" work. So I would like to thank people who created this wonderful group: I wish to thank Prof. Franco Garofalo and Prof. Luigi Glielmo for doing all that possible.

A twofold acknowledgment goes to Prof. Franco Garofalo since he is also my advisor, and thus I would like to thank the second advisor of my thesis: Francesco Vasca who guided me through my PhD studies. I think that I couldn't get such results without his guide, suggestions and continuous support.

Then I thank two special persons, my first officemates Giovanni Fiengo and Stefania Santini. They gave me enjoyable working days and especially sincere friendship: it would have been a very different PhD period without their presence.

Thanks to all other colleagues and friends: Alessandro di Gaeta, with whom I began and finished my PhD studies; Mario di Bernardo, Oreste Riccardo Natale, Carmen del Vecchio, Osvaldo Barbarisi, Sabato Manfredi, Vladimiro Vacca. A special thanks to Maria Carmela De Gennaro for reading my manuscript and giving me many suggestions for improving it.

During my studies I spent a semester in a foreign University: the Royal Institute of Technology (KTH) in Stockholm, Sweden. This period have had a very important role for my thesis. I would like to thank all the people who contributed to make so enjoyable my staying at KTH. First I thank Karl Henrik Johansson and Ulf Jönsson for what I learnt and also for the wonderful dinners during the cold Swedish winter. Thanks to my KTH officemates Niklas Pettersson and Frank Lingelbach, and thanks to Henning Schmidt and my Italian friend Alberto Speranzon.

Then I would like to thank my parents and my sister Paola: I express my gratitude to them since they unconditionally supported and encouraged me during these years.

And above all I want to thank my sweet Antonella for her support, help and unlimited love.

Luigi Iannelli
November 27, 2002.

Contents

List of Figures

Chapter 1

Introduction

I heard for the first time the word "dither" during my Master thesis period. I was studying analog-to-digital converters and techniques for compensating nonlinearities due to the quantization effects. Dither was one of those techniques.

Later, during my PhD studies, it was a pleasant surprise to discover that dither was a word often used also in Automatic Control papers. So I decided to investigate how much of this technique was in common between the fields of Electronics and Automatics. I think it is a task worth to follow: studying a problem by different points of view and trying to bridge the gap (it often exists) among different approaches. In this process I got a broad view of the dither technique by looking at its several applications and I found some interesting problems to study. This thesis presents such topics.

As said above, dither has a wide class of applications. Here there are some of them:

- linearization of electrovalve characteristics;
- attenuation of friction effects (e.g. stick-slip);
- quenching of spurious tones in sigma-delta converters;
- suppression of limit cycles or chaos in nonlinear feedback systems.

The injection of a dither signal into nonlinear feedback system is widely used in practice for the purpose of modifying nonlinearities in order to make the stability more robust, to extinguish undesirable limit cycles, to reduce nonlinear distortion, to quench jump phenomena, etc. Much research has been published to treat this problem in recent years. Zames and Shneydor (1976) showed that the effect of dither on the behaviour of nonlinear systems depends on its amplitude distribution. Stability of the dithered system is related to that of its corresponding averaged system (defined by using an averaging operation on the original dithered nonlinearity). Zames and Shneydor (1977) showed that the averaged nonlinearity always lies in a nonlinear sector narrower than the original nonlinearity: the stabilizing effect of dither is thus explained in terms of reducing the size of the critical region and quenching jump phenomena.

Mossaheb (1983) displayed that the dither with a sufficiently high frequency may result in the smoothed system's output and the dithered system's output as close as desired. This phenomenon allows us for a rigorous prediction of the dithered system's stability by establishing that of its corresponding smoothed system when the dither has both sufficiently large amplitude and frequency, and the "linearized" feedback system

has the low-pass filter property. In general, dither is a periodic signal with a chosen frequency higher than the system cut-off frequency; as a result it is filtered out before reaching the output.

All these considerations are rigorously proven (Zames and Shneydor 1976, Zames and Shneydor 1977, Mossaheb 1983) only for Lipschitz nonlinearities. Indeed, discontinuous nonlinearities in feedback control systems with high-frequency excitations appear in a large variety of models, including systems with adaptive control (Åström and Wittenmark 1989), friction (Armstrong-Helouvry 1991, Armstrong-Helouvry *et al.* 1994), power electronics (Lehman and Bass 1996), pulse-width modulated converters (Peterchev and Sanders 2001), quantizers (Gray and Neuhoff 1998), relays (Tsypkin 1984), and variable-structure controllers (Utkin 1992).

In their paper on the analysis of the (smooth) LuGre friction model, Pervozvanski and Canudas-de-Wit (Pervozvanski and de Wit 2002) point out that a rigorous analysis of dither in discontinuous systems does not exist. Dither tuning of general nonsmooth systems is to our knowledge limited to approximate design methods mainly based on describing functions (Atherton 1975, Gelb and Vander-Velde 1968).

In power electronic systems, including various types of DC/DC converters, averaging theory is applied to separate the slow dynamics from the fast dynamics, which for example can be imposed by switching elements in pulse-width modulation, such as for dithered systems. Power electronics circuits is a class of systems with nonsmooth dynamics for which rigorous averaging analysis have been done, see (Lehman and Bass 1996, Gelig and Churilov 1998). Thus it is interesting to study dither applied to discontinuous nonlinearities.

In this thesis dithered relay feedback systems are investigated. The reason for considering this class of systems is that they are common. Early motivation for studying relay systems come from mechanical and electromechanical systems (Andronov *et al.* 1965, Tsypkin 1984). Recently, there has been renewed interest due to a variety of emerging applications, such as automatic tuning of PID controllers (Åström and Hägglund 1995), quantized control (Elia and Mitter 2001), and supervisory control (Morse 1995). The analysis of relay feedback systems is non-trivial, even if the dynamical part of the system is linear. Major progress in the study of various properties of autonomous linear systems with relay feedback was achieved in the last decade, particularly in the understanding of limit cycles in these systems, e.g., (Åström 1995, Johansson *et al.* 1999, di Bernardo *et al.* 2000, Gonçalves *et al.* 2001, Varigonda and Georgiou 2001, Johansson *et al.* 2002). Further historical remarks and references on relay feedback systems are reported in (Tsypkin 1984, Johansson *et al.* 1999).

1.1 Thesis outline

This thesis can be divided into three parts. The first part (Chapters 2 and 3) presents preliminary concepts on relay feedback systems and dither. The second part (Chapters 4 and 5) is the main contribution of the thesis with some theoretical results. The last part (Chapter 6) deals with engineering applications. The outline is the following.

Chapter 2 presents the basic concepts of relay feedback systems (RFSs). The more general framework of piecewise linear systems is introduced and RFSs are discussed in this framework. Some general definitions and properties are given and classical results on the existence of oscillations in relay feedback systems are discussed.

Chapter 3 gives an overview of the dithering technique: basic principles and some explicative examples are presented. Then dithering applied to feedback systems is

introduced with a literature overview of seminal works on dither in nonlinear systems. The problem of dither analysis in RFSs is highlighted and some motivating examples are presented. Those examples give a useful insight in open questions about the effects that different dither waveforms can induce in RFSs.

Chapter 4 (together with chapter 5) consists of the main original contribution of the thesis. In this chapter some ideas and tools for studying dithered RFSs are given. Some theorems are derived: an averaging theorem on finite time horizon, en extension to infinite time horizon, a theorem on practical stability of dithered relay feedback systems and some results on the analysis of limit cycles in RFSs with dither.

Chapter 5 uses general results of the previous chapter and, by using optimization techniques like Linear Matrix Inequalities, attacks the problem of finding good estimate of the approximation error defined as the difference between the state of the dithered system and the state of the corresponding smoothed system. In this way it is possible to design a dithered RFS by choosing a dither amplitude and frequency suitable for obtaining the desired performance of the overall system. Some design algorithms are given and discussed by examples.

Chapter 6 presents two possible applications of the theory derived in previous chapters. A DC/DC buck converter and a DC motor position control system are presented. It is shown how these systems can be considered dithered RFSs and some simulations show the effectiveness of dither theory.

1.2 Contributions

The main contributions of this thesis are given in Chapter 4 and Chapter 5. The main result is an extension of Mossaheb's work to relay feedback systems dithered with periodic triangular waveforms. In order to derive that, it is used an averaging approach. Since this classical theory is not valid for nonsmooth dynamical systems (Khalil 2002), some peculiarities of the relay nonlinearity are exploited for proving a finite time horizon theorem on the approximation error. This error is defined as the difference between states of the dithered system and the corresponding smoothed system (without dither) in which the relay nonlinearity is replaced by the corresponding averaged nonlinearity (for triangular dither, it is a saturation nonlinearity). It is shown that the error is a function of ordo p where p is the dither period. In this way it is always possible to increase the dither frequency in order to get the error smaller and smaller.

The theorem is extended to the infinite time horizon case (by adding some stability assumptions on the smoothed system) and this gives some useful considerations for deriving a bound on the approximation error less conservative than the finite time horizon case. The practically stability property of the dithered system is investigated in a successive theorem.

A more interesting and new problem is the investigation of how the dither's shape can affect performances in nonsmooth feedback systems. Examples with square wave and trapezoidal dither signals are studied and it is showed that this class of dither signals determines behaviours very different from the triangular case. In particular it is not possible to derive a corresponding averaging theorem such as for triangular dither. There are cases in which the smoothed system is asymptotically stable and the dithered system presents an asymmetric limit cycle that does not reduce its amplitude even by increasing the dither frequency. Dither signals with zero slope over nonzero time intervals (such as square wave and trapezoidal dither signals) generally fail to stabilize relay feedback system. The form of the dither signal is thus very critical in applications with

discontinuous dynamics. This is in stark contrast to systems with Lipschitz continuous dynamics for which it can be shown that the form of the dither signal is not critical at all, see (Zames and Shneydor 1976, Zames and Shneydor 1977).

Finally other original contributes are given about the design of dithered relay feedback systems: how to choose dither amplitude and frequency in order to get some desired performances? By exploiting theoretical results derived in averaging theorems, it is given a design procedure for dithered systems, where the dither signal is adjusted to the dynamics of the linear part of the system.

1.3 Publications

The work presented in this thesis has to date resulted in the following publications.

- L. Iannelli, K.H. Johansson, U. Jönsson and F. Vasca, "Analysis of Dither in Relay Feedback Systems". Accepted for presentation at IEEE Conference on Decision and Control, December 2002, Las Vegas, Nevada, USA.
- L. Iannelli, K.H. Johansson, U. Jönsson and F. Vasca, "Analysis of Dither in Relay Feedback Systems". Reglermöte, May 2002, Linköping, Sweden.

Moreover some papers have been submitted:

- L. Iannelli, K.H. Johansson, U. Jönsson and F. Vasca, "Dither for Smoothing Relay Feedback Systems". submitted to IEEE Transactions on Circuits and Systems, Part I.
- L. Iannelli, K.H. Johansson, U. Jönsson and F. Vasca, "Practical Stability and Smooth-Switching Trajectories in Dithered Relay Feedback Systems". submitted to European Control Conference 2003.

In addition, a technical report is available.

- L. Iannelli, K.H. Johansson, U. Jönsson and F. Vasca, "Analysis of Dither in Relay Feedback Systems". Internal report IR-S3-REG-0201, S3-Automatic Control, Royal Institute of Technology, 2002.

Chapter 2

Relay Feedback Systems

In this chapter we study *Relay Feedback Systems* (RFSs). We consider relays in feedback with a Linear Time Invariant (LTI) system (as shown in Figure 2.1).

Analysis of RFS is an old problem. The first works were motivated by the use of relays in electromechanical systems and simple models of dry friction (Andronov *et al.* 1965, Tsypkin 1984). Most recent examples and applications of RFSs are automatic tuning of PID regulators (Åström and Wittenmark 1989) and sigma-delta converters (Norsworthy *et al.* 1996).

Although they are simple devices, RFSs are quite complex to analyse. In fact RFSs are particular nonlinear systems: they belong to the so called nonsmooth systems class. In fact the characteristic of a relay isn't Lipschitz since the signum function is discontinuous in zero. This property doesn't allow to use the standard tools of analysis of nonlinear smooth systems so that analysis of RFSs has to be carried on more carefully. Moreover nonlinear phenomena typical of nonsmooth systems are present in RFSs (see (Johansson *et al.* 1999) and its references). A lot of work has been done on studying RFSs and, in particular, conditions for the existence and stability of oscillations. Åström (1995) derived some necessary and sufficient conditions for the existence of limit cycles in RFSs. Then Gonçalves *et al.* (2001) studied *global* stability conditions for the existence of these oscillations. Some other papers addressed the problem of oscillations and sliding (di Bernardo *et al.* 2000) or oscillations generated by external forcing (Varigonda and Georgiou 2001).

We will give here a brief overview of the basic problems in studying relay feedback systems.

2.1 Definition of RFS

Consider a SISO system represented in the state space as

$$\dot{x}(t) = Ax(t) + bu(t) \tag{2.1a}$$

$$u(t) = \mathrm{rel}(cx(t)) \tag{2.1b}$$

where the operator rel is defined as

$$\mathrm{rel}(z) = \begin{cases} 1 & z > 0 \\ 0 & z = 0 \\ -1 & z < 0 \end{cases} \tag{2.2}$$

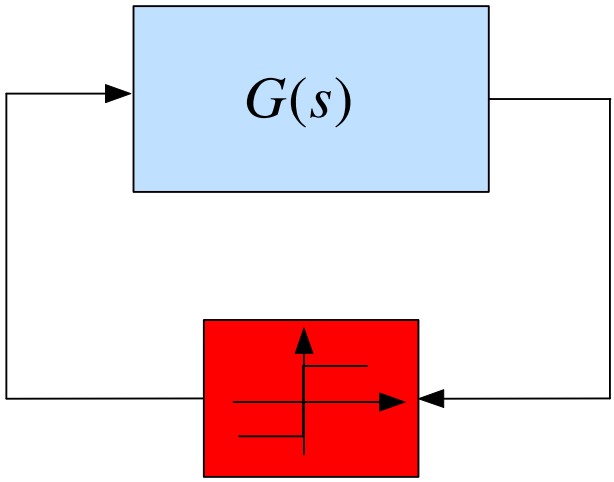

Figure 2.1: Relay Feedback System.

Equations (2.1) describe a relay feedback system. We will say that t is a *switching time instant* if u is discontinuous in t. Moreover we say that a trajectory of (2.1) *switches* at some time t if t is a switching time.

2.2 Piecewise Linear Systems

RFSs belong to the class of *piecewise linear systems* (PWL) (Johansson 1999, Chapter 2), (Gonçalves 2000, Chapter 3) defined as a set of affine (in the state) linear systems

$$\dot{x}(t) = A_q x(t) + a_q + B_q u(t), \tag{2.3}$$

where $x \in \mathbb{R}^n$ and $q \in \{1,2,\ldots,M\}$. A *switching rule* defines the current q (called *discrete state variable*) among the possible M values. The current q is a function of the current state x (in the case of a memoryless switching rule) or it depends on present and past values of x. The signal $q(t)$ is piecewise constant and we say that t^* is a switching time if $q(t)$ is discontinuous in t^*.

If the switching rule is memoryless, then q is function of the current state x and the state space is divided into M (possibly unbounded), sets X_i called *cells*:

$$X_i = \{x \,:\, q(x) = i\}.$$

Remark 2.2.1 *It could be worth to note that X_i are closed sets when the vector field of* (2.3) *is continuous on the boundaries of X_i (this is the case discussed in (Johansson 1999)). When we consider dynamic systems with discontinuous vector field, such as the RFSs, the cells X_i cannot be all closed sets in order to guarantee the well-posedness of the problem (for a discussion of the well-posedness in relay feedback systems see (Imura and van der Shaft 2000)).*

In the state space a switching occurs at *switching surfaces* (hyperplanes of dimension $n-1$) defined as

$$S_j = \{x \,:\, c_j x + d_j = 0\},\ j = 1,\ldots,N \tag{2.4}$$

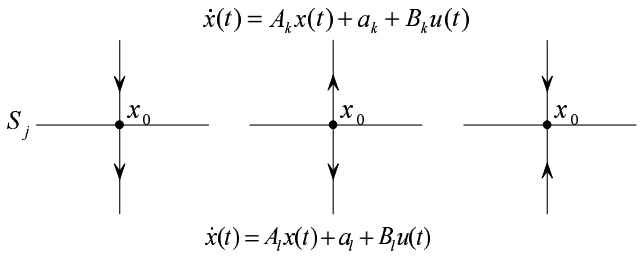

Figure 2.2: Existence of solutions in a PWL system.

where c_j is a row vector with n elements.

Definition 2.2.1 *Let $x(t)$ be an absolutely continuous function. We say that $x(t), u(t)$ is a trajectory of the system* (2.3) *on $[t_0, t_f]$ if, for* almost all $t \in [t_0, t_f]$, *the equation $\dot{x}(t) = A_q x(t) + a_q + B_q u(t)$ holds for all q with $x(t) \in X_q$.*

It is clear that if t^* is a switching time, the time derivative of $x(t)$ could not be defined if $\dot{x}(t^*)$ is discontinuous (nonsmooth systems). But if $x(t)$ does not remain on a switching surface for any time, the time interval in which the time derivative is not defined has measure equal to zero so $x(t)$ is still a trajectory (in the definition it is required that the differential equation holds for *almost all* t). On the other hand in the definition of PWL systems we required that $q(t)$ is a piecewise constant function: this means that arbitrarily fast switches (Johansson *et al.* 1999) are not possible.

Example 2.2.1
The RFS defined in Equations(2.1) *can be viewed as a PWL defined by three cells $X_1 = \{x : cx > 0\}, X_2 = \{x : cx < 0\}$ and X_3 that coincides with the switching surface $S = \{x : cx = 0\}$. Moreover $A_1 = A + bc, A_2 = A - bc, A_3 = A, a_{1,2,3} = 0, B_{1,2,3} = 0$.*

Let us give a deeper look at conditions for the existence of solution in a PWL system. If the initial condition x_0 is in the interior[1] of a cell X_i then there exists a solution at least from the initial condition to the first intersection of the trajectory with a switching surface. In fact in X_i the system dynamics is affine in the state. The problem is when the initial condition is on a switching surface and we can have unique solution, multiple solution, or no solution, depending on the vector field in the neighborhood of the switching surface S_j.

In Figure 2.2 on the left we have a situation in which the vector field does not change signum switching from cell X_k to cell X_l through S_j. In this case, if $x_0 \in S_j$ the solution is unique since the trajectory necessarily passes from X_k to X_l.

In the center of Figure 2.2 we could have multiple solutions since the trajectory can either move upwards or downwards.

In the last case (Figure 2.2, on the right) the vector field points toward the switching surface on both sides of the switching surface. Since we cannot have arbitrarily fast switchings (or, in other words, $\dot{x}$ has to be defined almost for all t), the solution does not exist. One way to overcome this problem is to define a dynamical system on the switching surface S_j (so that this dynamical system is $n-1$ dimensional) and let the trajectory evolve on the switching surface satisfying the differential equation of this new dynamical system until $x(t)$ "escapes" from one of the sides of S_j. This behaviour

[1] x is an *interior point of X if there exists a neighborhood W of x such that $W \subset X$ (see Appendix A).*

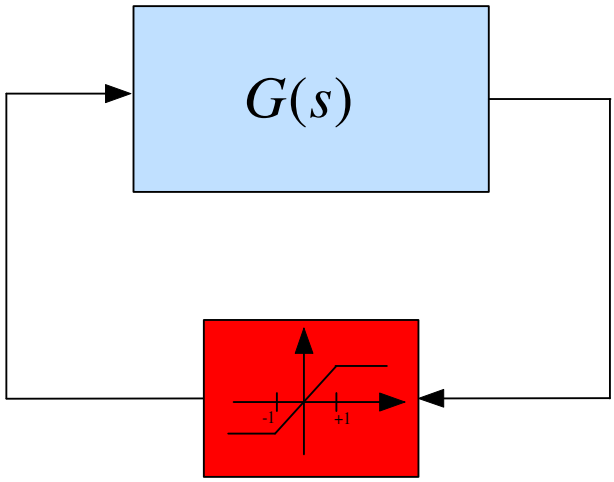

Figure 2.3: Saturation system.

is called *sliding mode*. In this thesis we will not consider the possibility of sliding mode (we exclude the case in which vector field points toward the switching surface on both sides of it).

Example 2.2.2
Let us consider the saturation system (Figure 2.3)

$$\dot{x}(t) = Ax(t) + b\,\mathrm{sat}(cx(t)), \tag{2.5}$$

where the operator sat *is defined as*

$$\mathrm{sat}(z) = \begin{cases} 1 & z > 1, \\ z & |z| \le 1, \\ -1 & z < -1. \end{cases} \tag{2.6}$$

In this case we have three cells:

$$\begin{aligned} X_1 &= \{x \,:\, cx > 1\} \\ X_2 &= \{x \,:\, |cx| \le 1\} \\ X_3 &= \{x \,:\, cx < -1\}. \end{aligned}$$

The corresponding systems are

$$\begin{aligned} \dot{x}(t) &= Ax(t) + b \quad \text{for } x \in X_1, \\ \dot{x}(t) &= (A + bc)x(t) \quad \text{for } x \in X_2 \\ \dot{x}(t) &= Ax(t) - b \quad \text{for } x \in X_3. \end{aligned}$$

The switching surfaces are

$$\begin{aligned} S_1 &= \{x \,:\, cx = +1\} \\ S_2 &= \{x \,:\, cx = -1\}. \end{aligned}$$

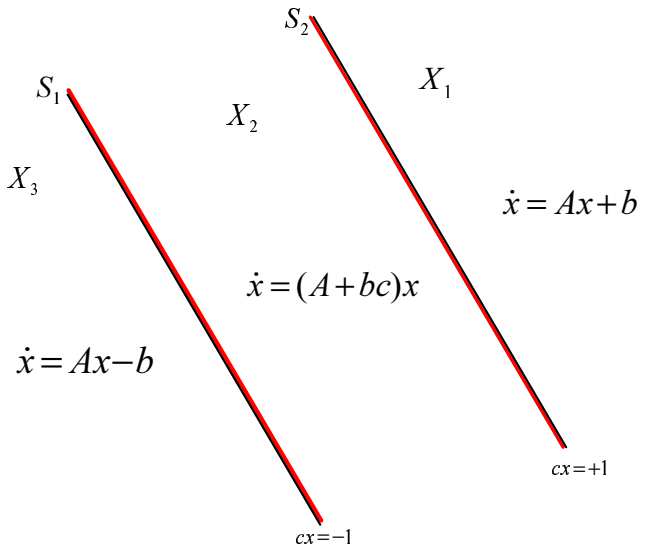

Figure 2.4: State space partition for a saturation system.

In this case the cells X_1 and X_3 are open and unbounded sets while X_2 is a closed (and unbounded) set (Figure 2.4). The vector field is continuous on S_1 and S_2 (with S_1, $S_2 \subset X_2$) so we have no problems for the existence of solutions. On the other hand the sat *operator is Lipschitz and the existence theorem (Theorem A.4.1) guarantees the existence and uniqueness of the solution.*

2.2.1 Equilibrium points

PWL systems can present none, one or multiple equilibrium points. By looking at Equation (2.3) we can say that $\bar{x} \in X_i$ is an equilibrium point for the constant input $\bar{u}$ if and only if

$$A_i \bar{x} + a_i + B_i \bar{u} = 0. \tag{2.7}$$

An important task is to investigate the local stability of equilibrium points. If the equilibrium point is an interior point of a cell, it is straightforward to analyse its local stability by using the standard tools (eigenvalues computation) of linear systems.

Example 2.2.3
Let us consider the saturation system in the Example 2.2.2 with

$$A = \begin{pmatrix} -0.5 & 0 \\ 0 & -1 \end{pmatrix} \qquad b = \begin{pmatrix} 1 \\ -\beta \end{pmatrix} \qquad c = \begin{pmatrix} 0 & 1 \end{pmatrix}. \tag{2.8}$$

In this case $cA^{-1}b = \beta$. In cells X_1 and X_3 we have, respectively, $\bar{x}_1 = -A^{-1}b$ and $\bar{x}_3 = A^{-1}b$ as points that make null the time derivative of x. Moreover $c\bar{x}_1 = -\beta$ and $c\bar{x}_3 = \beta$. So if $-\beta > 1$ (i.e. $\beta < -1$) x_1 and x_3 are equilibrium points of, respectively, X_1 and X_3, otherwise they are not. In the first case we have three equilibrium points (the origin and $(\pm 2 \quad \mp\beta)^T$) and in the second case only the origin is an equilibrium point of the saturation system. In general if A is invertible and $1 + cA^{-1}b < 0$ (it is possible to show that this inequality implies $A + bc$ invertible) , then we have three equilibrium points: the origin and two points symmetric with respect to the origin.

Some problems arise when an equilibrium point $\bar{x}$ belongs to a switching surface. In this case the equilibrium point belongs to a boundary of one or more cells (if there is a nonempty intersection among some cells): it is a *limit point*[2] of two or more cells. The local stability is not simple to be shown. Let us consider the following

Example 2.2.4
We have a second order PWL system defined as

$$\dot{x}(t) = A_1 x(t), \quad x \in X_1$$
$$\dot{x}(t) = A_2 x(t), \quad x \in X_2$$

with X_1 the first and third quadrant and X_2 the second and fourth quadrant and

$$A_1 = \begin{pmatrix} -0.1 & 1 \\ -10 & -0.1 \end{pmatrix} \qquad A_2 = \begin{pmatrix} -0.1 & 10 \\ -1 & -0.1 \end{pmatrix}.$$

Both matrices A_1 and A_2 have the same stable eigenvalues ($-0.1 \pm j\sqrt{10}$) and the origin (belonging to the intersection of two switching surfaces) is an equilibrium point for both the systems. It can be shown that the origin is globally stable but if we swap X_1 with X_2 (X_1 second and fourth quadrant and X_2 first and third quadrant), the origin is unstable.

As we saw in the previous example, we have to consider carefully the case in which some equilibrium points are on a switching surface. For discontinuous PWL systems this is more relevant with respect to PWL systems that have a continuous vector field such as the case of saturation systems.

Example 2.2.5
If we consider again the saturation example 2.2.2 we can investigate when an equilibrium point is on a switching surfaces. If $cA^{-1}b = 1$ the two equilibrium points different from the origin lie on the switching surfaces. If we introduce an external constant reference $R > 0$ (analogous results can be derived for $R < 0$) the system looses the symmetry so that we can have cases in which only one equilibrium point is on a switching surface. Let us consider the saturation system

$$\dot{x} = Ax + b\,\mathrm{sat}(cx + R). \tag{2.9}$$

Now the switching surfaces are $S_1 = \{x : cx + R = 1\}$ and $S_2 = \{x : cx + R = -1\}$. Moreover $X_1 = \{x : cx + R > 1\}$, $X_2 = \{x : |cx + R| \leq 1\}$ and $X_3 = \{x : cx + R < -1\}$. Assuming that A and $A + bc$ are invertible we can now find the condition for the existence of none, one or more equilibrium points. Since in cell X_2 the dynamics are $\dot{x} = (A + bc)x + bR$, we can compute the inverse of the matrix $A + bc$ by using the inversion lemma *(Ljung 1999)*

$$(F + GHK)^{-1} = F^{-1} - F^{-1}G(KF^{-1}G + H)^{-1}KF^{-1}. \tag{2.10}$$

By applying the inversion lemma we obtain

$$\begin{aligned}(A + bc)^{-1} =& A^{-1} - A^{-1}b(cA^{-1}b + 1)^{-1}cA^{-1} \\ =& A^{-1} - \frac{A^{-1}bcA^{-1}}{1 + cA^{-1}b},\end{aligned} \tag{2.11}$$

then if $1 + cA^{-1}b \neq 0$, $A + bc$ is invertible.

[2] x is a limit point of the set X if every neighborhood of x contains a point $y \neq x$ such that $y \in X$.

- *The point* $\bar{x}_2 = -(A+bc)^{-1}bR$ *is an equilibrium point of* (2.9) *only if* $|c\bar{x}_2 + R| \leq 1$. *By simple substitutions and algebraic computations this condition becomes* $|R/(1+cA^{-1}b)| \leq 1$.
- *The point* $\bar{x}_1 = -A^{-1}b$ *is an equilibrium point if* $-cA^{-1}b+R > 1$ *(or* $1+cA^{-1}b < R$*).*
- *The point* $\bar{x}_3 = A^{-1}b$ *is an equilibrium point if* $cA^{-1}b+R < -1$ *(or* $1+cA^{-1}b < -R$*).*

If we look at the expression $1+cA^{-1}b$ *we have different cases as reported in Table 2.1. We see that the only two cases when an equilibrium point is on a switching surface are when* $1+cA^{-1}B = \pm R$. *In both the cases we have two coincident equilibrium points and it is not possible to have a single equilibrium point.*

2.3 RFSs as PWL systems

Let us consider now the RFS defined in equations (2.1). We can divide the state space into two cells $X_1 = \{x : cx > 0\}$ and $X_2 = \{x : cx < 0\}$ and a third cell X_3 that coincides with the switching surface $S = \{x : cx = 0\}$. Of course the origin is an equilibrium point and we have two more equilibrium points only if $cA^{-1}b < 0$. When $cA^{-1}b > 0$ only origin is an equilibrium point and the trajectory could diverge or could present a globally stable limit cycle (see Section 2.4).

In RFSs the vector field is discontinuous at the switching surface so it could happen that there is no solution. In cell X_1 the dynamics is $\dot{x} = Ax + b$ (in the following, for the sake of simplicity, we will forget the time-dependance of x) so the trajectory tends towards the switching surface (from a region with $cx > 0$ towards a surface with $cx = 0$) only if $c\dot{x} < 0$. This means that the vector field points towards the switching surface if $cAx + cb < 0$. The hyperplane $p_+ = \{x : x \in S,\ cAx + cb = 0\}$ is a $n-2$ dimensional surface that identifies the boundary between the region in which the vector field in X_1 points towards the switching surface and the region in which it points opposite to the switching surface. In an analogous way we can define $p_- = \{x : x \in S,\ cAx - cb = 0\}$. Hence the vector field in X_1 points towards S if and only if $cAx < -cb$ while the vector field in X_2 points towards S if and only if $cAx > cb$. Considering the signum of cb we have the cases reported in Figure 2.5.

If $cb = 0$ we have $p_- \equiv p_+$ but it could be that there are still multiple fast switches (Johansson *et al.* 1999). So, in order to guarantee the existence of a solution for the relay feedback systems, we need that the first non-vanishing Markov parameter is positive: $cA^k b > 0$ where $k = 0, 1, \ldots, n-1$ is the smallest number such that $cA^k b \neq 0$. In this thesis we will assume that the previous condition always is satisfied.

$1 + cA^{-1}b$	Equilibrium points
$< -R$	x_1, x_2, x_3
$> -R$, and $< R$	x_1
$> R$	x_2
$= -R$	$x_2 \equiv x_3$
$= R$	$x_2 \equiv x_1$

Table 2.1: Different cases of equilibrium points for an asymmetric saturation system.

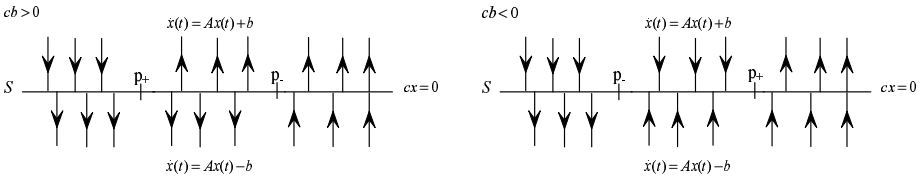

Figure 2.5: Existence of solutions in RFSs.

2.4 Periodic solutions

RFSs, as several others nonlinear systems, can present limit cycles (see Section A.6). The RFS defined in equations (2.1) can present symmetric (see Section A.6) limit cycle. In fact if $x^*(t)$ is a solution of equations (2.1), also $-x^*(t)$ is solution. We call *unimodal* limit cycle a periodic solution that presents only two switchings per period.

However a symmetric RFS can present also asymmetric limit cycles(Varigonda and Georgiou 2001).

Let us assume that the RFS has a symmetric unimodal periodic solution of period p, which means that

$$x(t + p/2) = -x(t), \quad \forall\, t \geq 0,$$

and that the solution switches only twice per period. To analyse this oscillation, it is no restriction to consider the system

$$\dot{x}(t) = Ax(t) + b\,\mathrm{rel}(cx),$$

with initial conditions at $t = 0$ such that $cx(0) = 0$ and $c\dot{x}(0) < 0$. Then,

$$\dot{x}(t) = Ax(t) - b, \quad 0 \leq t < p/2 \tag{2.12a}$$

$$\dot{x}(t) = Ax(t) + b, \quad p/2 \leq t < p. \tag{2.12b}$$

It follows that

$$x(p/2) = e^{Ap/2}x(0) - A^{-1}(e^{Ap/2} - I)b, \tag{2.13}$$

where we assume that A is invertible. (If A is not invertible, one can still derive $x(p/2)$ but for simplicity we do not consider that case.) Since the periodic solution is assumed to be symmetric, we have

$$x(p/2) = -x(0) = e^{Ap/2}x(0) - A^{-1}(e^{Ap/2} - I)b, \tag{2.14}$$

and thus

$$x(0) = (e^{Ap/2} + I)^{-1}A^{-1}(e^{Ap/2} - I)b. \tag{2.15}$$

It is now possible to derive the following existence result, cf., (Åström 1995, Varigonda and Georgiou 2001).

Proposition 2.4.1 *The RFS has a symmetric unimodal periodic solution with period p if and only*

$$c(e^{Ap/2} + I)^{-1}A^{-1}(e^{Ap/2} - I)b = 0$$

and

$$ce^{At}(e^{Ap/2}+I)^{-1}A^{-1}(e^{Ap/2}-I)b - cA^{-1}(e^{At}-I)b < 0, \quad 0 < t < \frac{p}{2}.$$

Next we investigate the stability of the periodic solution. Introduce the maps

$$g(t,x) = e^{At}x - A^{-1}(e^{At}-I)b, \qquad \mu(t,x) = cg(t,x).$$

For an initial point $x(0) = x_0$, denote the first switching instant for RFS by $t^* = t^*(x_0)$. Then,

$$x(t^*) = g(t^*,x_0) = e^{At^*}x_0 - A^{-1}(e^{At^*}-I)b =: N(t^*)x_0 - M(t^*), \tag{2.16}$$

where notations N and M are introduced for convenience. The switching constraint is

$$\mu(t^*,x_0) = 0. \tag{2.17}$$

Since the switching instant $t^* = t^*(x_0)$ is a function of the initial condition x_0, we can evaluate the partial derivative of (2.16) with respect to x_0 by using the theorem of implicit functions, and thus derive the following Jacobian evaluated at $(t,x) = (t^*,x_0)$:

$$J = \frac{\partial g}{\partial x} - \frac{\partial g}{\partial t}\left(\frac{\partial \mu}{\partial t}\right)^{-1}\frac{\partial \mu}{\partial x} \tag{2.18}$$

where

$$\frac{\partial g}{\partial x} = N(t^*) \tag{2.19}$$

$$\frac{\partial g}{\partial t} = \frac{\partial N(t^*)}{\partial t}x_0 - \frac{\partial M(t^*)}{\partial t} \tag{2.20}$$

$$\frac{\partial \mu}{\partial t} = c\frac{\partial g}{\partial t} \tag{2.21}$$

$$\frac{\partial \mu}{\partial x} = c\frac{\partial g}{\partial x} = cN(t^*). \tag{2.22}$$

By evaluating the equations above, we obtain the following stability result.

Proposition 2.4.2 *A symmetric unimodal periodic solution defined by Proposition 2.4.1 is stable if all eigenvalues of the Jacobian*

$$J = \left(I - \frac{wc}{cw}\right)e^{At^*}, \qquad w = \left(I + e^{At^*}\right)^{-1}e^{At^*}(-2b)$$

are in the open unit disc. It is unstable if at least one eigenvalue of J is outside.

By applying Propositions 2.4.1 and 2.4.2, we can thus prove the existence and the stability of a periodic solution for the RFS.

Chapter 3

Dithered Relay Feedback Systems

Dithering is a commonly used technique that engineers apply in several fields usually in order to overcome bad effects due to the presence of nonlinearities in a system.

For example dithering is used to reduce the effects of quantization noise on speech and visual signals converted by an Analog-to-Digital Converter (ADC). ADCs have a static characteristic (quantizer) strongly nonlinear. The nonlinearity introduces effects such as harmonics, spurious tones, chaos, etc. Dithering contributes to reduce this effects (Gray and Stockham 1993, Wannamaker 1997, Wannamaker *et al.* 2000*b*). The technique consists in adding a signal (dither) to the input of the quantizer nonlinearity such that the averaged output has a "more linear" behaviour (Wagdy 1989, Wagdy and Goff 1994). In this way we can attenuate spurious tones, we can eliminate chaotic effects or quenching limit cycles. Dither signal can be a deterministic or a stochastic signal (Carbone and Petri 2000).

Dithering is used also in feedback control systems (Zames and Shneydor 1976, Zames and Shneydor 1977, Mossaheb 1983) in which some nonlinearities are intrinsically present in physical systems or control devices. For example friction is a typical nonlinear phenomena that induces a "stick-slip" behaviour. Dithering contributes to reduce this problem (Feeny and Moon 2000). In physics literature a phenomena known as stochastic resonance can be viewed also as an effect due to dithering that "linearize" nonlinearities (Wannamaker *et al.* 2000*a*). Dither is often used in physics also for controlling chaotic systems (Fuh and Tung 1997, Morgül 1999).

3.1 Dithering principles

The basic principle of dithering is that if we add a suitable high frequency signal to the input of a nonlinearity, the averaged input-output relation is "smoothed". Of course this effect depends on the features of the dither signal. In fact, by sweeping quickly back and forth across the domain of the nonlinear element, a dither smoothes the nonlinear element prior to being filtered out, in effect making it less nonlinear in some sense.

There are two different approaches to dithering: *stochastic* and *deterministic* dithering. The stochastic approach consists in adding a random signal with some statistical properties (mean value, variance, probability density function, etc.). The performance

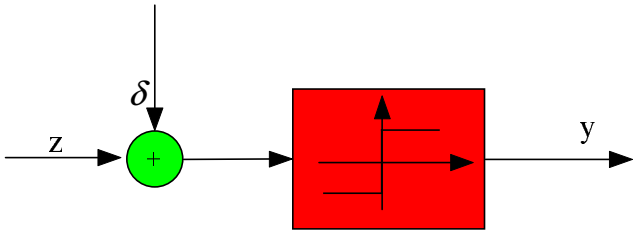

Figure 3.1: Relay nonlinearity with dither.

of a stochastic dithering system is evaluated by using the expectation value of the nonlinearity's output. For stationary and ergodic stochastic processes, the expectation is computed by the usual time average operation. The deterministic approach consists in adding a periodic (or quasi periodic) signal with some properties (mean value, shape of the signal, amplitude distribution, etc.). In this case the performance is evaluated by computing the time average (on a dither period) of the nonlinearity's output.

Both approaches are used in practice even if in signal processing applications (in particular analog-to-digital conversion) the stochastic approach is more immediate for the evaluation of parameter such as signal-to-noise ratio, power spectrum, etc. It is clear that in both cases an averaging operation (time averaging for deterministic case and expectation for stochastic case) is the basic cause of the smoothing effect.

3.2 Smoothed nonlinearity and Amplitude Density Function

Let us consider a relay nonlinearity with a dither signal δ added at the input z (Figure 3.1). In the deterministic approach the dither signal δ is periodic (or quasi-periodic, (Zames and Shneydor 1976)) of period p. We evaluate the time averaging of the output y on a dither period p by assuming z constant:

$$N(z) = \frac{1}{p}\int_0^p \mathrm{rel}(z+\delta(t))dt. \tag{3.1}$$

Of course the function $N(z)$ (called averaged or *smoothed* nonlinearity) depends on the signal δ and its shape (if it is a square wave, a sawtooth, a sinusoid, etc.).

By using a stochastic approach we consider z a deterministic variable and δ a random variable with a given *Probability Density Function* (PDF) $f_\delta(\delta)$. Then the expected output is

$$E[y] = \int_{-\infty}^{\infty} \mathrm{rel}\,(z+\delta) f_\delta(\delta) d\delta. \tag{3.2}$$

If $\delta(t)$ is a *stationary stochastic process*, since rel is a static nonlinearity, then $y(t)$ is a stationary stochastic process (Papoulis 1991). Then

$$E[y(t)] = \int_{-\infty}^{\infty} \mathrm{rel}\,(z+\delta(t)) f_\delta(\delta) d\delta. \tag{3.3}$$

If, moreover, $y(t)$ is *ergodic* (Papoulis 1991), we can evaluate the expectation as

$$E[y(t)] = \lim_{p\to\infty} \frac{1}{2p} \int_{-p}^{p} \mathrm{rel}\,(z+\delta(t))dt. \tag{3.4}$$

If we introduce the *Amplitude Density Function* (ADF[1]) of the periodic deterministic signal $\delta(t)$, we can obtain an expression similar to (3.2) which is valid in a deterministic framework and replaces (3.1).

The dither signal δ is a periodic function of time so we can consider its restriction to a single period:

$$\delta : [0, p] \mapsto D.$$

By considering the integral in (3.1) as a Lebesgue integral, it follows (Taylor 1966) that

$$N(z) = \int_D \mathrm{rel}\,(z+a) f_\delta(a) da \tag{3.5}$$

where $f_\delta(a)$ is the Amplitude Density Function of δ and it is defined as

$$f_\delta(a) = \frac{dF_\delta(a)}{da} \tag{3.6}$$

where $F_\delta(a)$ is the Amplitude Distribution Function:

$$F_\delta(a) = \frac{1}{p}\mu\{\delta \le a\} \tag{3.7}$$

with $\mu\{\delta \le a\}$ Lebesgue measure of the time sets in which $\delta(t) \le a$.

The Amplitude Density Function and Amplitude Distribution Function satisfy the same property of, respectively, Probability Density Function and Cumulative Distribution Function (for example, F_δ is right continuous). It is clear that if we use (3.5) instead of (3.1), we have no difference in operating for the computation of the (time or stochastic) averaging of the nonlinearity. In general, if $n(z)$ is the static nonlinearity and we add a dither δ at the input, the averaged nonlinearity is

$$\begin{aligned} N(z) &= \int_D n(z+\delta) f_\delta(\delta) d\delta \\ &= \int_{-\infty}^{\infty} n(z+\delta) f_\delta(\delta) d\delta \end{aligned} \tag{3.8}$$

where f_δ is the ADF (or PDF) of δ if we use a deterministic (or stochastic) dithering.

In this thesis we will consider only deterministic dithering. Similar tools can be used for stochastic dithering analysis.

If we consider dither signals symmetrically distributed with respect to the origin, i.e. $f_\delta(-\delta) = f_\delta(\delta)\ \forall\delta$, (3.8) assumes a particular form:

$$N(z) = \int_{-\infty}^{\infty} n(z-\delta) f_\delta(\delta) d\delta = n(z) * f_\delta(z). \tag{3.9}$$

Equation (3.9) shows that the averaged nonlinearity can be computed as the convolution of the original nonlinearity and the ADF of the dither signal.

[1] In (Zames and Shneydor 1976) ADF acronym is used instead for denoting the *Amplitude Distribution Function*.

When the original nonlinearity is the relay nonlinearity $\mathrm{rel}(z)$, Equation (3.8) becomes

$$\begin{aligned} N(z) &= \int_{-\infty}^{\infty} \mathrm{rel}(z+\delta) f_\delta(\delta) d\delta \\ &= \int_{-z^+}^{\infty} f_\delta(\delta) d\delta - \int_{-\infty}^{-z^-} f_\delta(\delta) d\delta \\ &= 1 - 2\int_{-\infty}^{-z^-} f_\delta(\delta) d\delta - \int_{-z^-}^{-z^+} f_\delta(\delta) d\delta. \end{aligned} \tag{3.10}$$

In this way, given $F_\delta(z)$ the Amplitude Distribution Function (or Cumulative Distribution Function) of the dither signal δ, the smoothed nonlinearity of a relay dithered with δ is

$$N(z) = 1 - [F_\delta(-z^+) + F_\delta(-z^-)]. \tag{3.11}$$

If $F(z)$ is continuous in $-z$ then $N(z) = 1 - 2F_\delta(-z)$ otherwise, when f_δ is impulsive in $-z$, we have to take into account the left and right limits of F_δ in $-z$.

In conclusion we have three different approaches for computing the smoothed nonlinearity for a relay dithered with a deterministic periodic signal: we can compute the time averaging (3.1), we can use the convolution operation (3.9) or relation (3.11).

3.2.1 Triangular

An example of a dither signal, which we will study in detail, is a triangular waveform of amplitude $A > 0$ and period $p > 0$, i.e., $\delta(t+p) = \delta(t)$ for all t and

$$\delta(t) = \begin{cases} \dfrac{4A}{p} t, & t \in [0, p/4) \\ -\dfrac{4A}{p} t + 2A, & t \in [p/4, 3p/4) \\ \dfrac{4A}{p} t - 4A, & t \in [3p/4, p). \end{cases} \tag{3.12}$$

Triangular waveform is an odd function ($\delta(t) = -\delta(-t)$) so it has a zero mean value (as all other dither signals we consider in this thesis). It is not difficult to show that the Amplitude Density Function for triangular waveform is the *rectangular window function* reported in Figure 3.2:

$$\Pi_A(z) = \begin{cases} \frac{1}{2A} & |z| \le A \\ 0 & |z| > A \end{cases}. \tag{3.13}$$

Of course the corresponding stochastic dither is a random variable with a uniform PDF.

For the triangular dither, it is easy to show (by applying the time averaging definition or by using the convolution product or the Equation (3.11)) that

$$N(z) = \mathrm{sat}(z/A) = \begin{cases} -1, & z < -A \\ z/A, & |z| \le A \\ +1, & z > A. \end{cases} \tag{3.14}$$

We can note that now $N(z)$ is Lipschitz (with Lipschitz constant equal to $1/A$) while the original relay nonlinearity was discontinuous. Dither has "smoothed" the relay, and,

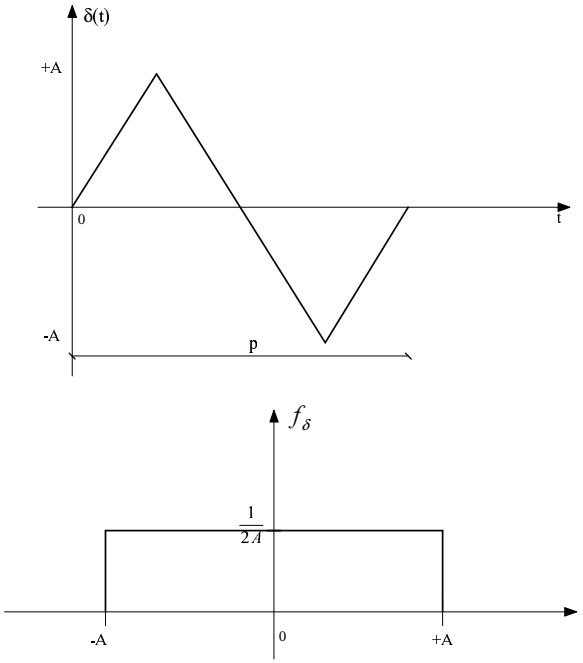

Figure 3.2: Triangular dither: waveform and its ADF.

in fact, the equivalent or averaged nonlinearity is called *smoothed nonlinearity*[2] since the smoothness property of dither is a general property (Zames and Shneydor 1976).

3.2.2 Sawtooth

In this case a sawtooth waveform dither of amplitude A and period p is the signal (restricted to the single period):

$$\delta(t) = \frac{2A}{p}t - A, \quad t \in [0, p). \tag{3.15}$$

The signal has the same ADF of the triangular dither. It presents a discontinuity in $t = kp$ and has a time derivative constant and equal to $2A/p$ while for triangular dither the time derivative oscillates between $4A/p$ and $-4A/p$.

Since the sawtooth dither has the same ADF of the triangular dither, the corresponding smoothed nonlinearity is the same. We have smoothed the original nonlinearity (that is discontinuous) obtaining a continuous nonlinearity. It is worth to note that the dither amplitude A affects the gain of the saturation: higher the amplitude is, lower is the gain.

[2] It is worth to note that the attribute *smoothed* is not referred to functions infinitely continuous with their derivatives.

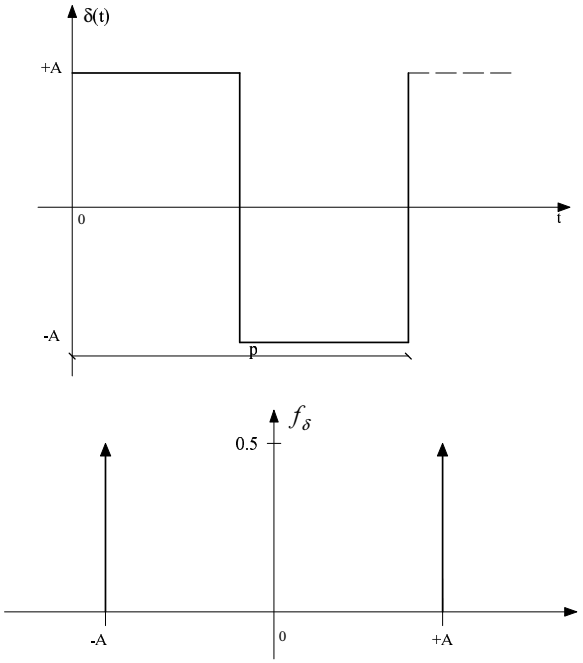

Figure 3.3: Square wave dither: waveform and its ADF.

3.2.3 Square wave

A square wave dither of period p is

$$\delta(t) = \begin{cases} +A & t \in [0, p/2) \\ -A & t \in [p/2, p). \end{cases} \tag{3.16}$$

In this case the Amplitude Density Function is $f_\delta(z) = 0.5\tilde{\delta}(z+A) + 0.5\tilde{\delta}(z-A)$ where $\tilde{\delta}$ is the Dirac impulse (see Figure 3.3). The presence of Dirac impulses is due to the fact that the Amplitude Distribution Function is discontinuous. That is similar to the case of random variables where the presence of impulses in the PDF is due to the discontinuity of the CDF.

In general if a signal assumes a constant value for a time interval of non zero measure, the ADF presents some Dirac impulses (analogously to discrete random variables). So dither signals with zero-slope time interval, generate Dirac impulses in their Amplitude Density Functions.

In this case, given the impulsive Amplitude Density Function of the square wave dither, the smoothed nonlinearity can be simply computed (by using the convolution product) as $N(z) = 0.5n(z+A) + 0.5n(z-A)$ (see Figure 3.4):

$$N(z) = \begin{cases} -1, & z < -A \\ -0.5 & z = -A \\ 0, & |z| < A \\ 0.5 & z = +A \\ +1, & z > A. \end{cases} \tag{3.17}$$

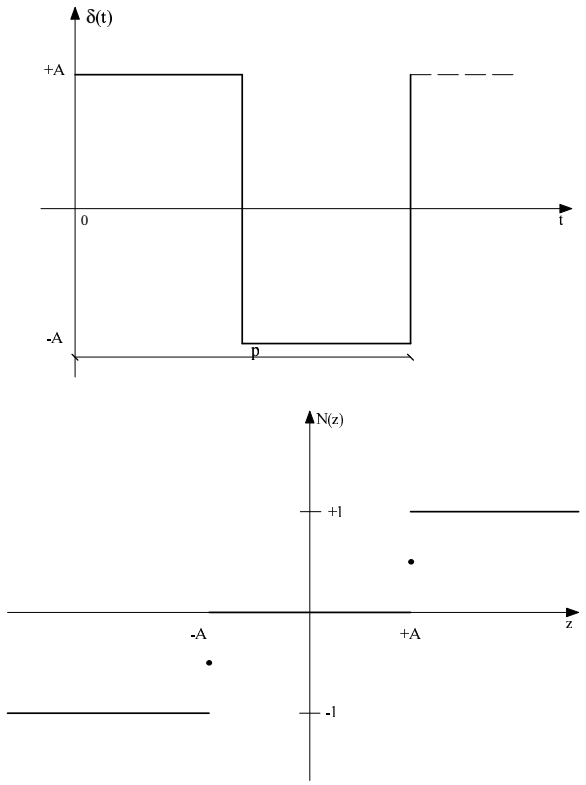

Figure 3.4: Square wave dither signal (upper diagram) and the corresponding smoothed nonlinearity $N(z)$ (lower diagram).

The smoothed nonlinearity is still discontinuous: now we have two jumps in $z = -A$ and $z = +A$. On the other hand, $N(z)$ lies in a nonlinear sector narrower than the original one ($n(z)$ lies in $[0,\infty)$) such as predicted by (Zames and Shneydor 1976). When the ADF of a dither signal presents some impulses, the smoothed nonlinearity of the dithered relay has some discontinuities. Since a dither with time intervals in which the signal is constant (dithers with zero-slope intervals, see Section 4.5) has Dirac impulses in its ADF, this class of dither signals has to be carefully used in Relay Feedback Systems.

3.2.4 Trapezoidal

A trapezoidal signal is a square waveform without discontinuities: we have a high slope from the positive value to the negative.

$$\delta(t) = \begin{cases} +A & t \in [0, p/2 - \Delta) \\ -2\dfrac{A}{\Delta}t + \dfrac{Ap}{\Delta} - A & t \in [p/2 - \Delta, p/2) \\ -A & t \in [p/2, p - \Delta) \\ 2\dfrac{A}{\Delta}t - \dfrac{2Ap}{\Delta} + A & t \in [p - \Delta, p). \end{cases} \tag{3.18}$$

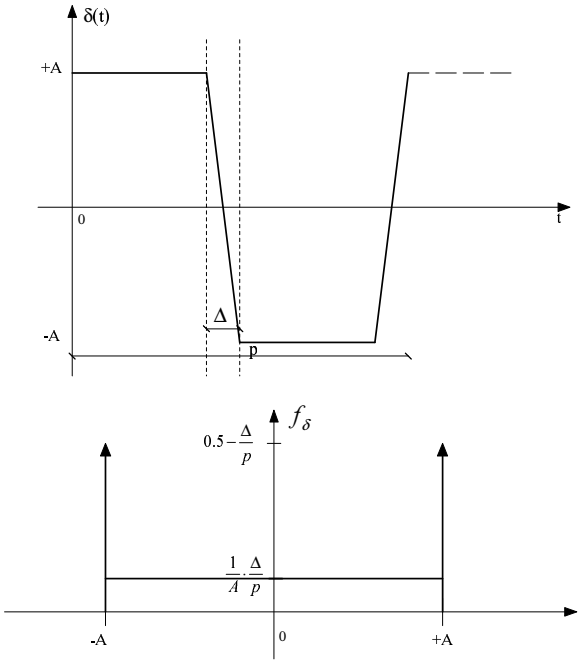

Figure 3.5: Trapezoidal dither: waveform and its ADF.

In this case the ADF is (see Figure 3.5) the sum of two Dirac impulses in $-A$ and $+A$ (due to the zero slope time interval as for the square wave case) and a rectangular windows due to the high slope time interval:

$$f_\delta(z) = (0.5 - \Delta/p)\left[\tilde{\delta}(z+A) + 0.5\tilde{\delta}(z-A)\right] + (2\Delta/p)\Pi_A(z).$$

We have both the effects of a triangular and a square wave dither; the smoothed nonlinearity, computed again by using the convolution, is (see Figure 3.6):

$$N(z) = \begin{cases} -1, & z < -A \\ -0.5 - \Delta/p & z = -A \\ 2\Delta z/(pA), & |z| < A \\ 0.5 + \Delta/p & z = +A \\ +1, & z > A. \end{cases} \tag{3.19}$$

3.2.5 Sinusoidal

Of course a sinusoidal dither is

$$\delta(t) = A\sin\left(\frac{2\pi}{p}t\right). \tag{3.20}$$

It is a continuous signal without zero-slope time interval: the time derivative is zero only in some time instants ($t = p/4$ and $t = 3p/4$), so their Lebesgue measure

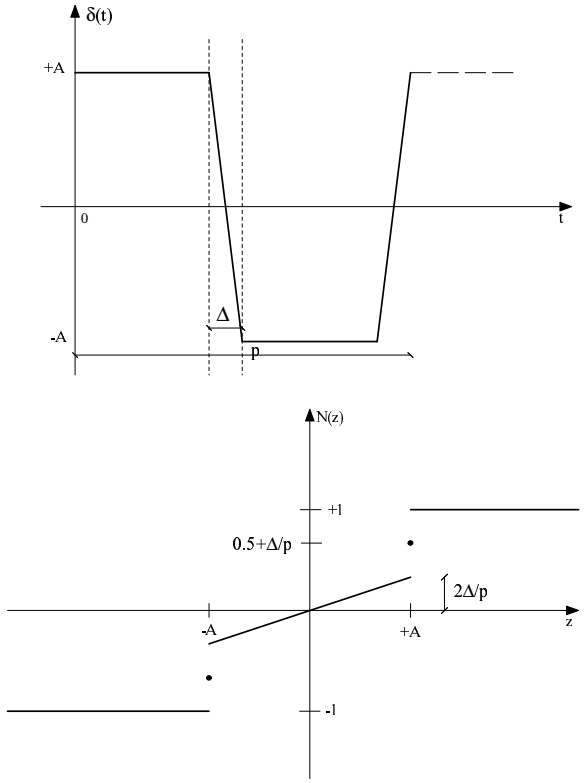

Figure 3.6: Trapezoidal dither signal (upper diagram) and the corresponding smoothed nonlinearity $N(z)$ (lower diagram).

is zero. Then we expect an ADF without impulses. We can compute the Amplitude Distribution Function and then differentiate it in order to obtain the ADF.

It is not difficult to show that

$$F_\delta(z) = \begin{cases} 0 & z < -A \\ \frac{1}{2}\left(1 + \frac{2}{\pi}\sin^{-1}\frac{z}{A}\right) & |z| \le A \\ 1 & z > A \end{cases} \tag{3.21}$$

and, by differentiating (3.21),

$$f_\delta(z) = \begin{cases} 0 & |z| > A \\ \frac{1}{A\pi}\frac{1}{\sqrt{1-\left(\frac{z}{A}\right)^2}} & |z| < A. \end{cases} \tag{3.22}$$

Since in this case the Amplitude Distribution Function is continuous, we can use

the third way for computing the smoothed nonlinearity:

$$N(z) = 1 - 2F(-z) = \begin{cases} -1 & z < -A \\ \frac{2}{\pi} \sin^{-1} \frac{z}{A} & |z| \leq A \\ 1 & z > A. \end{cases} \tag{3.23}$$

It should be noticed that in some cases computations of averaged (or equivalent) nonlinearities are simpler if we use the convolution rule (3.9) or the rule of Equation (3.11) valid for relay nonlinearities.

3.3 Dither in Feedback Systems

We saw that the averaged effect of injecting a dither signal at the input of a nonlinearity can be analysed by looking at the equivalent nonlinearity. In practice, if we put an averaging operation at the output of the nonlinearity, the overall system is equivalent to the averaged nonlinearity.

But what happens when we put dither in feedback systems? Intuition suggests that a Linear Time Invariant System can operate as a smoothing and thus also as an averaging operator if it is sufficiently low pass, so it seems interesting to study effects of dither in feedback systems.

The seminal work for studying dither in feedback systems was carried on by Zames and Shneydor (Zames and Shneydor 1976, Zames and Shneydor 1977).

In their work Zames and Shneydor use an input-output framework to prove that dither affects stability of nonlinear systems. Essentially they show that an input-output analysis of the dithered system can be derived by looking at the smoothed system. In practice the dithered system is $\mathcal{L}_2$ bounded if the smoothed system is bounded on the Sobolev space[3] S_{2p} and the dither period is sufficiently high with respect to some parameters function of the frequency response of the linear part of the dithered system.

A different approach for studying dither in nonlinear system was used by Mossaheb. In (Mossaheb 1983) it has not been used an input-output approach but a classical averaging method for showing that a sufficiently high frequency dither can make arbitrarily close the state of the dithered system and the state of the smoothed system. Mossaheb studied in particular the class of triangular dither signals showing that a triangular signal always linearizes a saturating odd nonlinearity. Zames and Shneydor's work and Mossaheb's work are valid only for Lipschitz nonlinearities[4]. But in control systems some non Lipschitz nonlinearities are used. For example the relay is a typical non Lipschitz nonlinearity.

The main contribute of this thesis is to extend Mossaheb's results to the case of relay feedback systems. So in this Section we will give some notations for dithered RFSs.

The *dithered system* is the relay feedback system

$$\dot{x}(t) = Lx(t) + bn(cx(t) + r(t) + \delta(t)), \qquad x(0) = x_0. \tag{3.24}$$

[3]The Sobolev space S_{2p} is the set of functions $f(t)\ S_{2p} = \{f : f(0) = 0,\ f(t) \in \mathcal{L}_2\ \dot{u}(t) \in \mathcal{L}_2\}$ with norm $\|f\|_{2p} = (\|f\|_2 + p^{-1}\|f\|_2^2)^{1/2}$.

[4]For sake of truth Mosshaeb assumes that the original nonlinearity is absolutely continuous, but a relay does not satisfy this property.

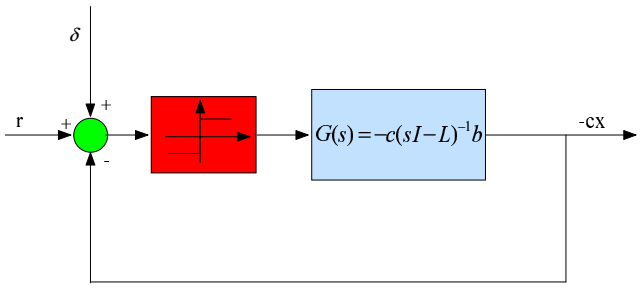

Figure 3.7: Dithered system.

Here L, b, and c are constant matrices of dimensions $q \times q$, $q \times 1$, and $1 \times q$, respectively. The nonlinearity $n : \mathbb{R} \to \mathbb{R}$ is given by the relay characteristic

$$n(z) = \mathrm{rel}(z) = \begin{cases} 1, & z > 0 \\ 0, & z = 0 \\ -1, & z < 0. \end{cases}$$

In Figure 3.7 a block diagram of the dithered system is reported. It is worth to note that the negative feedback is highlighted by defining the transfer function of the linear system $G(s) = -c(sI - L)^{-1}b$ and considering as output $y(t) = -cx(t)$.

The signal $r(t)$ is the external reference and it is assumed to be Lipschitz continuous, i.e., there exists a constant $M_r > 0$ such that $|r(t_1) - r(t_2)| \leq M_r|t_1 - t_2|$, $\forall t_1, t_2$.

The dither signal $\delta : [0, \infty) \to \mathbb{R}$ is periodic and of high frequency compared to the linear dynamics. It should be pointed out that the results that will be presented in this thesis depend on the shape of the dither signal. Dither signals with zero slope for non-vanishing time intervals, such as the square wave, are sometimes unpredictable. This is in contrast to systems with Lipschitz continuous dynamics, where the form of the dither signal is not critical (Zames and Shneydor 1976, Zames and Shneydor 1977).

The relay feedback system is assumed to have a solution $x : [0, \infty) \to \mathbb{R}^n$ (in a classical sense), which on every compact subinterval of $[0, \infty)$ is C^1 everywhere except at finitely many points. We sometimes use the notation $x(t, x_0)$ for the solution of (3.24). We use $|\cdot|$ to denote the Euclidean norm of a vector and $\|\cdot\|$ to denote the corresponding induced matrix norm.

The *smoothed relay feedback system* is defined as

$$\dot{w}(t) = Lw(t) + bN(cw(t) + r(t)), \qquad w(0) = w_0, \tag{3.25}$$

where the smoothed nonlinearity $N : \mathbb{R} \to \mathbb{R}$ is the average $N(z) = p^{-1} \int_0^p n(z + \delta(t))dt$. If the dither signal has an even Amplitude Density Function, we can evaluate the smoothed nonlinearity also as a convolution product: $N(z) = n(z) * f_\delta(z)$.

It will be shown in Chapter 4 that the smoothed system in many cases is a good approximation of the dithered relay feedback system. Therefore analysis and design can be performed on the smoothed system, which is often easier to treat, and then be carried over to the dithered system.

Note that the term "smoothed system" (which is standard in the literature on dither) refers to that the nonlinear sector is narrowed by the dither signal. The nonlinearity is not necessarily C^∞, as illustrated above by different dither signals.

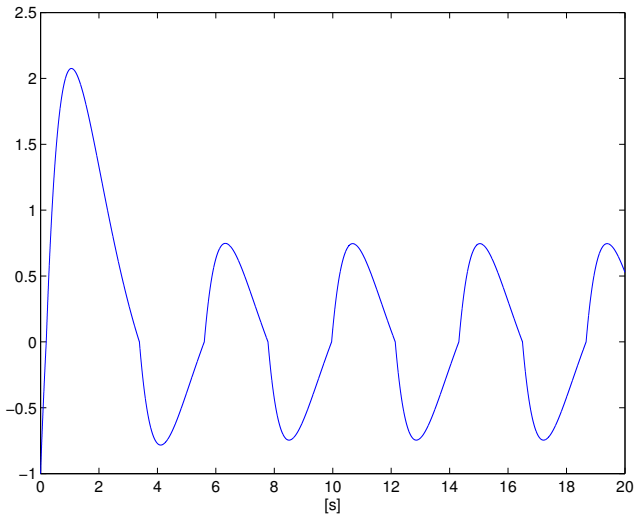

Figure 3.8: Output $-cx$ of the relay feedback system (3.24) with (3.26) but without dither signal ($\delta \equiv 0$).

3.4 Motivating examples

We present here some examples and simulations to illustrate effects of different dither signals on relay feedback systems.

3.4.1 Averaging

A second-order relay feedback system is used as a representative example. Consider the system (3.24) with

$$L = \begin{pmatrix} -2 & -1 \\ 1 & 0 \end{pmatrix}, \quad b = \begin{pmatrix} 1 \\ 0 \end{pmatrix}, \quad c = \begin{pmatrix} 1 & -1 \end{pmatrix}. \tag{3.26}$$

The linear part of the relay feedback system thus has a nonminimum-phase zero at 1 and a double pole at -1. When no dither is present ($\delta(t) \equiv 0$), the relay feedback system presents a limit cycle as reported in Figure 3.8. The output [5] of the linear part $-cx$ of (3.24) is plotted for a solution with initial condition $x_0 = \begin{pmatrix} 2 & 1 \end{pmatrix}^T$.

If we apply a triangular dither signal δ with amplitude $A = 1$ and period $p = 1/50$, the limit cycle in Figure 3.8 is dissolved as shown in Figure 3.9. Hence, the dither in a sense attenuates the oscillations present in the original system. Figure 3.9 shows also the output $-cw$ of the smoothed system (3.25). The two systems have almost identical responses. Hence, although the output of the dithered system oscillates due to the presence of the dither, the smoothed system provides an accurate approximation of the dithered system for $p = 1/50$. Figure 3.10 shows the responses when the dither signal has a larger period: $p = 1$. The responses are no longer close but the oscillations in the output of the dithered system (solid) are still due to the forcing dither and not to a limit cycle such as that in Figure 3.8.

[5] It is worth to note that the minus signum introduced in the output (as previously said in Section 3.3) gives the opposite of the typical response of a nonmimimum-phase linear system.

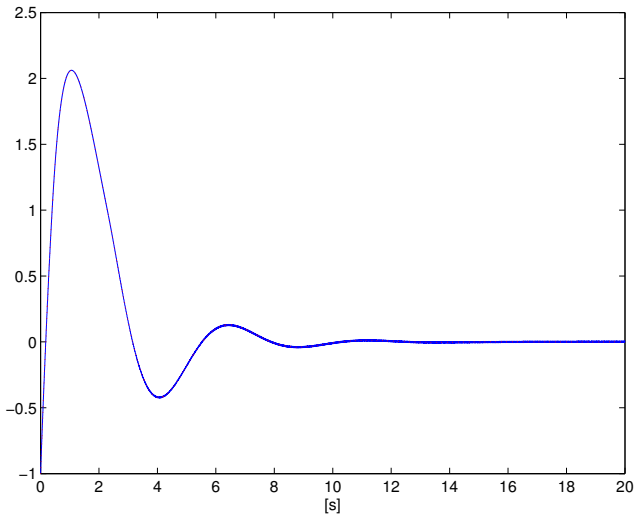

Figure 3.9: Outputs of the dithered relay feedback system (3.24) (solid) and the smoothed system (3.25) (dashed). The responses are almost identical.

The simulations suggest that the dither period p is related to how accurately the smoothed system approximates the dithered system. In next section it is shown that by choosing p sufficiently small the approximation can be made arbitrarily tight (Theorem 4.1.1). Regarding the dither amplitude A, note that the smoothed system above is unstable for $A < 1/2$, since the closed-loop system is linear with characteristic polynomial equal to $s^2 + (2 - A^{-1})s + 1 + A^{-1}$ when $|cw| < A$. The dither amplitude hence defines the response dynamics. This is shown in next chapter by relating A to the stability of the dithered system (Theorem 4.2.1).

3.4.2 Zero slope dither signals

Some interesting effects arise when relay feedback systems are dithered with signals that have zero time derivative in a time interval of nonzero measure. A well known class of such signals is the square wave. As a motivating example let us consider the system (3.24) with δ a square wave dither of period p and amplitude A, and a constant external reference $r = R$.

Figure 3.11 shows the output of the relay feedback system dithered with a square wave and the output of the corresponding smoothed system. By decreasing the dither period the shape of the waveforms doesn't change and the limit cycle (that presents a smooth interval and a switching interval) still remains. This example shows that in this case the dither does not give a similar result as in the triangular dither case (i.e., the error between the dithered and smoothed system does not decrease as p becomes smaller and smaller).

One could conjecture that the averaging doesn't work for a dither signal with time derivative equal to zero in a time interval of non null measure. In fact this is the case of the just shown square wave dither signal. With similar considerations we can consider the case of a dither signal that isn't discontinuous (as the square wave) but presents some zero derivative time intervals.

Let us consider the trapezoidal dither signal (Figure 3.6). The smoothed and the

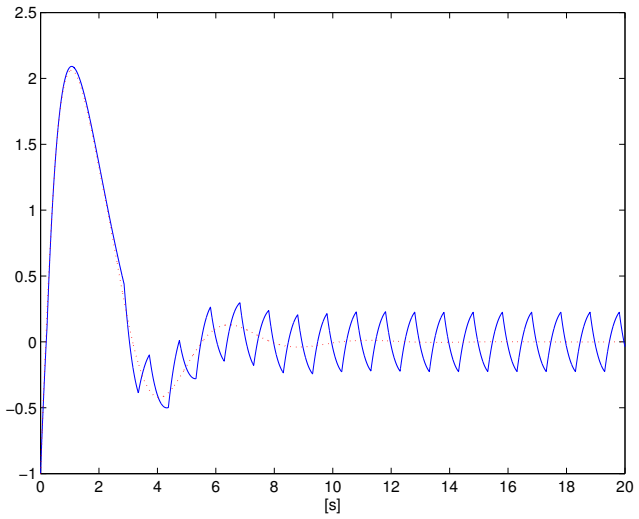

Figure 3.10: Outputs of the dithered relay feedback system (3.24) (solid) and the smoothed system (3.25) (dashed). Similar simulation as in Figure 3.9 but with dither signal having 50 times longer period. Note the deviation between the responses.

dithered system outputs waveforms are highly different in time, see Figure 3.12. We can see that the stationary behaviour of the systems is periodic and the period of the smoothed system output is different from the period of the dithered system output. On the other hand it is simple to show that the trajectories of the smoothed and dithered systems present phase plane portraits close to each other. This example will inspire the investigation of the averaging analysis also in the presence of limit cycles for the smoothed system.

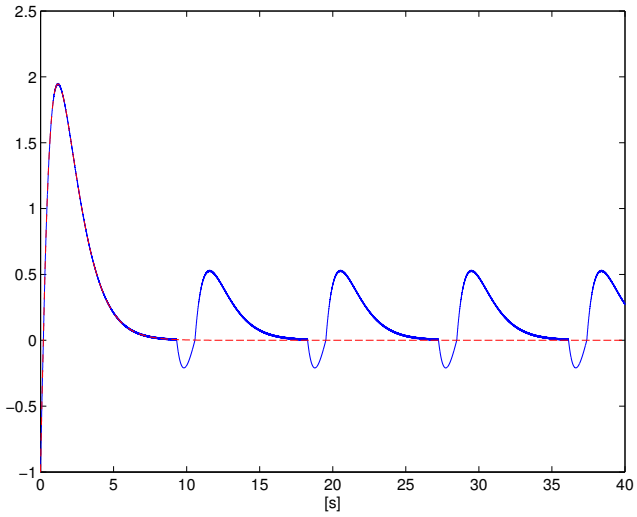

Figure 3.11: Outputs of the dithered relay feedback system (solid) and the smoothed system (dashed) with dither period $p = 1/50$, dither amplitude $A = 1$ and external reference $r(t) = R = 1$. The dither signal is a squarewave.

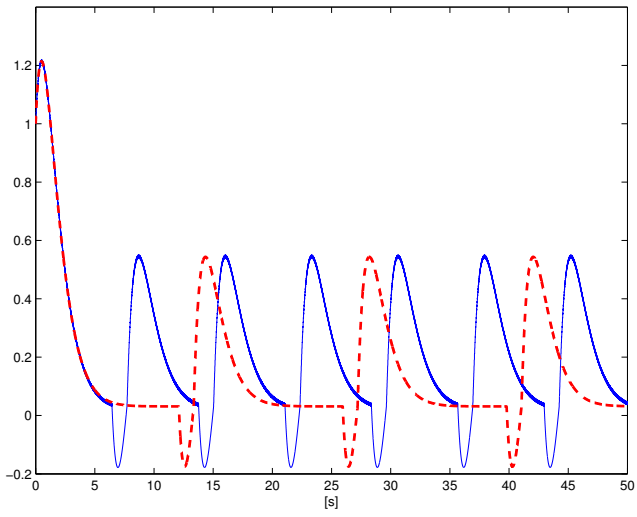

Figure 3.12: Outputs of the dithered relay feedback system (solid) and the smoothed system (dashed) with the trapezoidal dither of Figure 3.6 ($p = 1/50, A = 1, \Delta = p/10$) and external reference $r(t) = R = A + 2\Delta/p$.

Chapter 4

Averaging analysis of dithered Relay Feedback Systems

In this chapter we will derive the main results on the analysis of dithered relay feedback system by looking at the smoothed system:

$$\dot{x}(t) = Lx(t) + bn(cx(t) + r(t) + \delta(t)), \qquad x(0) = x_0 \tag{4.1a}$$

$$\dot{w}(t) = Lw(t) + bN(cw(t) + r(t)), \qquad w(0) = x_0, \tag{4.1b}$$

where $n(\cdot)$ is a relay and

$$N(z) = \frac{1}{p}\int_0^p n(z+\delta)dt = \text{sat}(z/A).$$

The smoothed nonlinearity depends on the dither signal (as shown in Chapter 3).

By considering triangular dither signal, the first result is on accurate approximation over compact time intervals and the second is on practical stability. These two results are then combined to obtain a result on approximation over infinite time horizon. The proofs do not fully exploit the particular structure of the smoothed system and the resulting bounds on the dither period are conservative. In Theorem 5.2.1 we obtain much tighter bounds by using linear matrix inequalities (LMI) to characterize the structural properties of the system. The same averaging and stability results for dithered systems with sawtooth dither signals can be proved also in the case of sawtooth waveforms (see Remark 4.1.1 in Section 4.1). As an interesting point in Section 4.6 we show that the averaging approach eventually fails for square wave dither signals.

4.1 Averaging theorem

The following theorem states that by choosing the dither period p of the triangular dither sufficiently small, it is possible to make the solution $x(t)$ of the relay feedback system arbitrarily close to the solution $w(t)$ of the smoothed system on any compact time interval.

Theorem 4.1.1 *Let $T, \varepsilon > 0$ and $x_0 \in \mathbb{R}^n$ be given. Assume that $r(t)$ is Lipschitz on $[0,T]$ with Lipschitz constant M_r. There exists $p_0 > 0$ such that if $p \in (0, p_0)$, then $|x(t,x_0) - w(t,x_0)| \leq \varepsilon$ for all $t \in [0,T]$.*

Proof: Consider the dithered system and the smoothed system on the time interval $[0,T]$ and with $w(0) = x(0) = x_0$:

$$\dot{x}(t) = Lx(t) + bn(cx(t) + r(t) + \delta(t)), \qquad x(0) = x_0 \tag{4.2a}$$

$$\dot{w}(t) = Lw(t) + bN(cw(t) + r(t)), \qquad w(0) = x_0, \tag{4.2b}$$

with $N(z) = \text{sat}(z/A)$.

Note that the right-hand side of (4.2a) is bounded on every compact time interval $[0,T]$, so there exists a positive constant M_y such that $|c\dot{x}(t)| \leq M_y$, for all $t \in [0,T]$:

$$\begin{aligned} |c\dot{x}(t)| &= |cLx(t) + cbn\left(\delta(t) + cx(t) + r(t)\right)| \\ &\leq |cLe^{Lt}| \cdot |x_0| + \int_0^t \left|cLe^{L(t-s)}b\right| ds + |cb|. \end{aligned} \tag{4.3}$$

$$M_y(x_0) := \sup_{t\in[0,T]} \left[|cLe^{Lt}| \cdot |x_0| + \int_0^t \left|cLe^{L(t-s)}b\right| ds + |cb| \right]. \tag{4.4}$$

Moreover by hypothesis $r(t)$ is Lipschitz:

$$|r(t_1) - r(t_2)| \leq M_r |t_1 - t_2|, \quad \forall t_1, t_2$$

Then we introduce $M = M_y + M_r$.

By integrating the two members of (4.2), we obtain

$$\begin{aligned} x(t) - w(t) =& \int_0^t [Lx(s) + bn(cx(s) + r(s) + \delta(s))]ds \\ &- \int_0^t [Lw(s) + bN(cw(s) + r(s))]ds \\ =& L\int_0^t [x(s) - w(s)]ds \\ &+ b\int_0^t [n(cx(s) + r(s) + \delta(s)) - N(cw(s) + r(s))]ds. \end{aligned} \tag{4.5}$$

The idea now is to show that the integral $\int_0^t [n(cx(s) + r(s) + \delta(s))]ds$ can be approximated by $\int_0^t N(cx(s) + r(s))ds$. The error introduced by this approximation is a function of the dither period p. We will show that it can be made small by decreasing the period p. This is not obvious, particularly, since n is a discontinuous nonlinearity.

We first evaluate the term $\int_0^t [n(cx(s) + r(s) + \delta(s))]ds$. If we introduce $m = \lfloor T/p \rfloor$, the largest integer such that $mp \leq T$, then

$$\begin{aligned} \int_0^t n(cx(s) + r(s) + \delta(s))ds = &\sum_{k=0}^{m-1} \int_{kp}^{(k+1)p} n(cx(s) + r(s) + \delta(s))ds \\ &+ \int_{mp}^{mp+\Delta t} n(cx(s) + r(s) + \delta(s))ds, \end{aligned} \tag{4.6}$$

with $\Delta t = T - mp$. Since n is a bounded function and the time interval of the last integral in (4.6) has a Lebesgue measure less than p, we can write

$$\int_0^t n(cx(s) + r(s) + \delta(s))ds = \sum_{k=0}^{m-1} \int_{kp}^{(k+1)p} n(cx(s) + r(s) + \delta(s))ds + V_0(t) \tag{4.7}$$

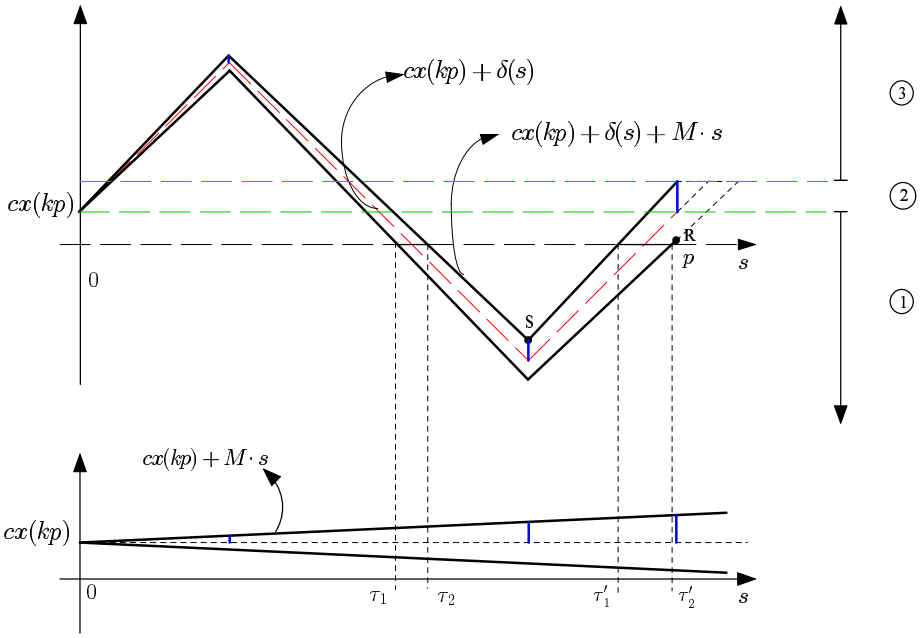

Figure 4.1: Time diagrams of the signals.

with $|V_0(t)| \le p$. Each term in the sum can be written as

$$\begin{aligned}
&\int_{kp}^{(k+1)p} n(cx(s)+r(s)+\delta(s))ds \\
&\quad = \int_{kp}^{(k+1)p} n(cx(kp)+r(kp)+\delta(s))ds \\
&\qquad + \int_{kp}^{(k+1)p} [n(cx(s)+r(s)+\delta(s)) - n(cx(kp)+r(kp)+\delta(s))]ds \\
&\quad = pN(cx(kp)+r(kp)) \\
&\qquad + \int_0^p [n(cx(s+kp)+r(s+kp)+\delta(s)) - n(cx(kp)+r(kp)+\delta(s))]ds. \qquad (4.8)
\end{aligned}$$

Figure 4.1 illustrates the evolution for one dither period interval. In the top diagram, the solid lines bound $cx(s+kp)+r(s+kp)+\delta(s)$, $0 \le s \le p$. The dashed line is $cx(kp)+r(kp)+\delta(s)$. The figure presents all possible cases for the evolution of $cx+r+\delta$, in the sense that the envelope has the same characteristics as long as the point **R** is above the point **S**. It is not difficult to show that this is equivalent to that the relation

$$p < \frac{1}{7}\cdot\frac{4A}{M} =: \bar{p} \qquad (4.9)$$

holds. In the following we assume that p is chosen such that (4.9) holds.

All possible cases correspond to different values of $cx(kp)+r(kp)$ or, equivalently, all possible cases can be obtained by shifting the horizontal s-axis upward and down-

ward in the top diagram of Figure 4.1. We have three cases:

$$\begin{cases} 0 \le cx(kp) + r(kp) & \text{Region 1,} \\ cx(kp) + r(kp) \le 0 \le cx(kp) + r(kp) + Mp & \text{Region 2,} \\ cx(kp) + r(kp) + Mp \le 0 & \text{Region 3.} \end{cases}$$

The regions are illustrated on the right side of Figure 4.1 by the location of the s-axis for the three cases. The partition identifies the time intervals, during which the signal $cx(s+kp)+r(s+kp)+\delta(s)$ can have a zero-crossing. It is only during these intervals the integrand function in (4.8) can be non-zero. Introduce I_i to denote the sum of the lengths of these intervals for Region i, as further described below. Next we discuss each region separately.

Region 1: For the first region, I_1 can be the sum of at most two time intervals: $[\tau_1, \tau_2]$ and $[\tau_1', \tau_2']$, say. Since the considered signals are piecewise linear, the time instants τ_1 and τ_2 can be derived as

$$\tau_1 = \left(\frac{1}{2} + \frac{cx(kp) + r(kp)}{4A}\right) \frac{p}{1 + Mp/(4A)} \tag{4.10a}$$

$$\tau_2 = \left(\frac{1}{2} + \frac{cx(kp) + r(kp)}{4A}\right) \frac{p}{1 - Mp/(4A)}, \tag{4.10b}$$

and, analogously,

$$\tau_1' = \left(1 - \frac{cx(kp) + r(kp)}{4A}\right) \frac{p}{1 + Mp/(4A)} \tag{4.11a}$$

$$\tau_2' = \left(1 - \frac{cx(kp) + r(kp)}{4A}\right) \frac{p}{1 - Mp/(4A)}. \tag{4.11b}$$

Note that if the s-axis is below the point **S**, we have only one time interval. However, since we are only interested in an upper bound of I_1, we can consider the worst case, i.e., the case discussed previously. Moreover, if the s-axis is above the point **R**, then τ_2' is less than p. However, we can still consider the previous expression, since the time interval $[\tau_1', \tau_2']$ derived above is greater than the effective one.

By considering the Lebesgue measures of the time intervals, we have

$$\tau_2 - \tau_1 = \left(\frac{1}{2} + \frac{cx(kp) + r(kp)}{4A}\right) \frac{M}{2A} \cdot \frac{p^2}{1 - (Mp/(4A))^2}, \tag{4.12}$$

and

$$\tau_2' - \tau_1' = \left(1 - \frac{cx(kp) + r(kp)}{4A}\right) \frac{M}{2A} \cdot \frac{p^2}{1 - (Mp/(4A))^2}. \tag{4.13}$$

Note two facts now: (i) the inequality (4.9) assures that $Mp/(4A)$ is always less than one, and (ii) if $Mp/(4A) \ll 1$ (i.e., $p \ll 4A/M$) the region in which the signal $cx(s+kp)+r(s+kp)+\delta(s)$ can lie is very small, so we can approximate the signal by $cx(kp)+r(kp)+\delta(s)$.

Hence, we have shown that the worst case (largest estimate of I_1) is when the integrand function in (4.8) is different from zero in both intervals $[\tau_1, \tau_2]$ and $[\tau_1', \tau_2']$. In that case we have

$$I_1 = \tau_2 - \tau_1 + \tau_2' - \tau_1' = \frac{3}{2} \cdot \frac{M}{2A} \cdot \frac{p^2}{1 - (Mp/(4A))^2}. \tag{4.14}$$

Region 3: Now we can consider the case in which the s-axis lies in the third region. The time interval $[\tau_1, \tau_2]$ is the same as previously in this case. The other possible time interval $[\tau_1'', \tau_2'']$ can be identified by considering the crossing of the first increasing part of the envelope through the s-axis. In an analogous way we can calculate the Lebesgue measure of the interval as

$$\tau_2'' - \tau_1'' = -\frac{cx(kp) + r(kp)}{4A} \cdot \frac{M}{2A} \cdot \frac{p^2}{1 - (Mp/(4A))^2}. \tag{4.15}$$

The worst case (through similar arguments as above) is given by

$$I_3 = \tau_2'' - \tau_1'' + \tau_2 - \tau_1 = \frac{1}{2} \cdot \frac{M}{2A} \cdot \frac{p^2}{1 - (Mp/(4A))^2}. \tag{4.16}$$

Note that both I_1 and I_3 are independent from the value of $cx(kp) + r(kp)$. The Lebesgue measure of the worst-case time interval is the same for all points in the corresponding region.

Region 2: Finally, we consider the second region. Here we can have a subtle behaviour because it might happen that we have to consider three different time intervals. One of these, however, corresponds to the time interval considered in both Regions 1 and 3. Since we are carrying on a worst case analysis, it is possible to overcome the "loss of symmetry" by the following bound:

$$I_2 \leq I_1 + I_3 = 2 \cdot \frac{M}{2A} \cdot \frac{p^2}{1 - (Mp/(4A))^2}. \tag{4.17}$$

To conclude the discussion on Regions 1–3, note that the worst case I, say, for all three of them is bounded by the right-hand side of (4.17). It is easy to see that there exists $p^* > 0$ such that for all $p \leq p^*$, we have I of ordo p^2, i.e., $I = O(p^2)$. In particular, we may choose

$$p^* = \frac{4A}{M} \cdot \frac{\sqrt{2}}{2}, \tag{4.18}$$

so that

$$I \leq 4 \cdot \frac{M}{2A} p^2, \quad \forall p \leq p^*. \tag{4.19}$$

Note that (4.19) follows from (4.9). In conclusion, the estimate of the upper bound (4.19) is valid for all cases, so hence we have that (4.8) is equal to

$$\int_{kp}^{(k+1)p} n(cx(s) + r(s) + \delta(s))ds = pN(cx(kp) + r(kp)) + Z_1(k), \qquad p \leq \bar{p}, \tag{4.20}$$

with $|Z_1(k)| \leq 8 \cdot \frac{M}{2A} p^2$.

So far we have mainly considered one period p. Since in (4.7) we have $m = \lfloor T/p \rfloor$ terms, we have

$$\int_0^t n(cx(s) + r(s) + \delta(s))ds = \sum_{k=0}^{m-1} pN(cx(kp) + r(kp)) + V_0(t) + V_1(t), \tag{4.21}$$

with $|V_1(t)| \leq 8 \cdot \frac{M}{2A} Tp$. For p sufficiently small (or, equivalently, for m sufficiently large) the sum can be approximated by an integral. The maximum error of the approximation is related to the maximum slope of the signal $N(cx(s)+r(s))$. But N satisfies the slope condition

$$0 \leq \left|N(cx(s_1)+r(s_1)) - N(cx(s_2)+r(s_2))\right| \leq \frac{M}{A}\left|s_1 - s_2\right|, \qquad \forall\, s_1, s_2 \in [0,T], \tag{4.22}$$

which implies

$$\int_{kp}^{(k+1)p} N(cx(s)+r(s))ds = pN(cx(kp)+r(kp)) + Z_2(k) \tag{4.23}$$

(with $|Z_2(k)| \leq \frac{M}{2A}p^2$) and, thus,

$$\begin{aligned}\sum_{k=0}^{m-1} pN(cx(kp)+r(kp)) &= \int_0^{mp} N(cx(s)+r(s))ds + V_2(t) \\ &= \int_0^t N(cx(s)+r(s))ds + V_2(t) + V_3(t)\end{aligned} \tag{4.24}$$

with $|V_2(t)| \leq \frac{M}{2A}Tp$ and $|V_3(t)| \leq p$.

We have up to now proved that (4.5) can be written as

$$\begin{aligned}x(t) - w(t) =& L\int_0^t [x(s) - w(s)]ds + b\int_0^t [N(cx(s)+r(s)) - N(cw(s)+r(s))]ds \\ &+ V(t), \quad \forall p \leq \bar{p}\end{aligned} \tag{4.25}$$

where $V(t) = b(V_0(t) + V_1(t) + V_2(t) + V_3(t))$ and $|V(t)| \leq |b|(p + 8 \cdot \frac{M}{2A}Tp + \frac{M}{2A}Tp + p) = |b|(\frac{9}{2}\frac{M}{A}T + 2)p$. Since N has Lipschitz constant equal to $1/A$, we get

$$|x(t) - w(t)| \leq \left(\|L\| + \frac{|b|\cdot|c|}{A}\right)\int_0^t |x(s) - w(s)|ds + O(p),\ p \leq \bar{p}, \tag{4.26}$$

where

$$O(p) = \left(\frac{9}{2}\cdot\frac{M}{A}T + 2\right)|b|p. \tag{4.27}$$

Now, by applying the Grönvall-Bellman Lemma (Sastry 1999) to (4.26), we get for all $p \leq \bar{p}$,

$$\begin{aligned}|x(t) - w(t)| \leq& O(p) + \int_0^t \left[\left(\|L\| + \frac{|b|\cdot|c|}{A}\right) \quad \times O(p)e^{\int_\tau^t \left(\|L\| + \frac{|b|\cdot|c|}{A}\right)d\sigma}\right] d\tau \\ =& O(p) + \left(\|L\| + \frac{|b|\cdot|c|}{A}\right)O(p)\int_0^t e^{\left(\|L\| + \frac{|b|\cdot|c|}{A}\right)(t-\tau)}d\tau \\ =& O(p) + O(p)\left[e^{\left(\|L\| + \frac{|b|\cdot|c|}{A}\right)t} - 1\right].\end{aligned} \tag{4.28}$$

Hence,

$$\begin{aligned}|x(t) - w(t)| \leq& O(p)e^{(\|L\| + |b|\cdot|c|/A)t} \\ \leq& O(p)e^{(\|L\| + |b|\cdot|c|/A)T} = \varepsilon, \quad \forall t \in [0,T].\end{aligned} \tag{4.29}$$

This concludes the proof of the theorem. ∎

Note that from (4.27), we have an estimate of p_0 of the theorem, namely,

$$p_0 = \min\left(\frac{4A}{7M}, \frac{\varepsilon}{(9MT/(2A)+2)\,|b|e^{(\|L\|+|b|\cdot|c|/A)T}}\right) \tag{4.30}$$

Corollary 4.1.1 *If the smoothed system has an initial condition different from the dithered system, the approximation error is not a linear function of p but it is only affine. It can be proven that*

$$|x(t)-w(t)| \le |x_0-w_0|e^{(\|L\|+|b|\cdot|c|/A)T} + O(p)e^{(\|L\|+|b|\cdot|c|/A)T} = \varepsilon, \quad \forall t \in [0,T]. \tag{4.31}$$

Remark 4.1.1 *If the dither signal $\delta(t)$ is a sawtooth waveform of period p*

$$\delta(t) = \begin{cases} \dfrac{2A}{p}t - A, & t \in [0,p). \end{cases} \tag{4.32}$$

Theorem 4.1.1 is still valid but expression (4.30) *becomes*

$$p_0 = \min\left(\frac{A}{M}, \frac{\varepsilon}{(9MT/(2A)+2)\,|b|e^{(\|L\|+|b|\cdot|c|/A)T}}\right). \tag{4.33}$$

Theorem 4.1.1 can be interpreted as an extension of Theorem 1 in (Mossaheb 1983) to a class of nonsmooth systems. The result in (Mossaheb 1983) relies on continuity properties of the solutions of the original and the smoothed systems. This argument cannot be used here, since a relay feedback system in general do not have solutions that depend continuously on initial conditions or system parameters. Instead, we pay particular attention in the proof to the system evolution at and between relay switchings. For pulse-width modulated systems, which is a class of nonsmooth systems that shows some similarities to the dithered relay feedback system, averaging techniques are applied in (Lehman and Bass 1996, Gelig and Churilov 1998).

The proof of Theorem 4.1.1 is constructive, so a bound for p_0 is also derived. It shows that p_0 should be chosen to be of the order of ε. The bound on p_0 depends on system data and T. It is conservative, since the derivation is done without taking system data into particular consideration. Tighter bounds can be obtained by exploiting more of the problem structure, see Section 5.2.1. Heuristic tuning rules for the design of p_0 will be presented in Section 5.3.

4.2 Practical stability

In this section we discuss the stability of the dithered system (4.1a). We assume that $r(t) \equiv 0$.

We will use Theorem 4.1.1 to obtain conditions for practical stability of the dithered system. The idea is the following. First we choose the amplitude A of the dither signal, such that the smoothed system is stable. Then if the period p of the dither signal is chosen small enough, the output of the dithered system closely follows the output of the smoothed system. This implies that the output of the dithered system converges

close to zero. Note that we cannot obtain convergence strictly to zero, since the dither signal always cause small fluctuations of the output. We use the following definition of stability.

Definition 4.2.1 (Practical stability) *The system in* (4.1a) *with the triangular dither and a given amplitude $A > 0$ is called practically (exponentially) stable if for any $\varepsilon > 0$ there exists $\alpha > 0$ and $\beta \geq 1$, and $p_0 > 0$ such that*

$$|x(t)| \leq \beta e^{-\alpha t}|x_0| + \varepsilon, \quad \forall t \in [0, \infty)$$

for any dither period $p \in (0, p_0)$.

Theorem 4.2.1 *Suppose $r(t) \equiv 0$ and that the smoothed system* (4.1b) *is exponentially stable. Then there exists p_0 such that for $p \in (0, p_0)$ the dithered system* (4.1a) *is practically stable.*

Proof: By hypothesis the system (4.1b) with $r(t) \equiv 0$ is exponentially stable. Hence, there exists $\alpha_0 > 0$ and $\beta_0 \geq 1$ such that

$$|w(t)| \leq \beta_0 e^{-\alpha_0 t}|x_0|, \quad \forall t \geq 0.$$

We will use this to prove practical stability of (4.1a). We iteratively consider time intervals of length T and, in order to guarantee a decay rate of 0.1, we choose $T = -{\alpha_0}^{-1} \ln(0.1/\beta_0)$. Then, if p_0 is sufficiently small (see (4.30)), we have

$$|x(t) - w(t)| \leq \varepsilon_0$$

on $t \in [0, T]$. If we consider a new smoothed system satisfying (4.1b) on the time interval $[kT, (k+1)T]$, $k = 0, 1, 2, \ldots$, with initial condition $w(kT) = x(kT)$, then it follows from the above arguments that

$$|w(t)| \leq \beta_0 e^{-\alpha_0 (t-kT)}|x(kT)|, \quad \forall t \geq kT,$$

and, by applying Theorem 4.1.1 again,

$$\begin{aligned} |x(t)| =& |x(t) - w(t) + w(t)| \leq \varepsilon_0 + |w(t)| \\ \leq& \beta_0 e^{-\alpha_0 (t-kT)}|x(kT)| + \varepsilon_0 \end{aligned} \tag{4.34}$$

on $t \in [kT, (k+1)T]$. By evaluating (4.34) in $t = (k+1)T$,

$$|x((k+1)T)| \leq 0.1|x(kT)| + \varepsilon_0. \tag{4.35}$$

Hence

$$|x(kT)| \leq 0.1^k |x_0| + \varepsilon_0 \frac{1 - 0.1^k}{1 - 0.1}. \tag{4.36}$$

Then (4.34) becomes

$$\begin{aligned} |x(t)| &\leq \beta_0 e^{-\alpha_0 (t-kT)} \left(e^{-\alpha kT}|x_0| + \frac{\varepsilon_0}{0.9} \right) + \varepsilon_0 \\ &\leq \beta_0 e^{-\alpha_0 (t-kT)} e^{-\alpha kT} |x_0| + \underbrace{\beta_0 \frac{\varepsilon_0}{0.9} + \varepsilon_0}_{\varepsilon}, \end{aligned} \tag{4.37}$$

where $\alpha = -T^{-1}\ln 0.1$. Since $\alpha_0 > \alpha$ and $t \geq kT$, (4.37) becomes

$$|x(t)| \leq \beta_0 e^{-\alpha t}\,|x_0| + \varepsilon. \tag{4.38}$$

We have thus shown practical stability with $\alpha = -T^{-1}\ln 0.1$ and $\beta = \beta_0$. ∎

There are many available results for stability analysis of the smoothed system. We will here use a criterion by Zames and Falb (1968), which generalizes the Popov criterion.

Corollary 4.2.1 *Assume L is Hurwitz and let $G(j\omega) = -c(j\omega I - L)^{-1}b$. Further let $H(j\omega) = \int_{-\infty}^{\infty} h(t)e^{-j\omega t}dt$, where $h : \mathbb{R} \to \mathbb{R}$ satisfies $\int_{-\infty}^{\infty} |h(t)|dt \leq 1$. If there exists $\varepsilon > 0$ such that*

$$\mathrm{Re}\,(G(j\omega) + A)(1 + H(j\omega)) \geq \varepsilon, \quad \forall \omega \in (0,\infty), \tag{4.39}$$

then there exists p_0 such that for $p \in (0, p_0)$ the dithered system (4.1a) *is practically stable.*

Proof: The saturation nonlinearity $N(z)$ satisfies the integral quadratic constraint

$$\int_0^{\infty} [z(t) - AN(z(t))][N(z(t)) - (h * N(z))(t)]\,dt \geq 0, \qquad \forall z \in \mathbf{L}_2[0,\infty),$$

where $*$ indicates the convolution product. If the criterion (4.39) holds, then it follows from the main result in (Zames and Falb 1968, Megretski and Rantzer 1997) that the smoothed system in (4.1b) is $\mathfrak{L}_2$-stable. Moreover, since the vector field of (4.1b) is Lipschitz continuous it can be shown that $\mathfrak{L}_2$-stability implies exponential stability (Megretski and Rantzer 1997, Vidyasagar 1993). By applying Theorem 4.2.1 we proved the corollary. ∎

Note that the criterion (4.39) corresponds to one of the least conservative conditions for stability available for systems with a slope restricted nonlinearity. However, it does not give any immediate information on the performance (e.g., the exponential decay parameters for the smoothed system α and β), and it is not convex in the pair (A, H). The most straightforward use of the theorem is to put $H = 0$, which then corresponds to the circle criterion. From the Kalman–Yakubovich–Popov Lemma one can for that case derive a linear matrix inequality that verifies (4.39) and results in explicit estimates of the exponential decay parameters. In Section 5.1 we will show how a suitable choice of H can help to obtain better tuning for A.

4.3 Infinite time horizon

The next result shows that the dithered system can track the averaged system arbitrarily well over an infinite time horizon provided that the dither signal is chosen appropriately.

Let us call $x(t, r, x_0)$ the solution of the problem (4.1a) with initial condition $x(0) = x_0$ and $w(t, r, w_0)$ the solution of the problem (4.1b) with initial condition $w(0) = w_0$. We want to evaluate the approximation error $|x(t, r, x_0) - w(t, r, x_0)|$, $\forall t \geq 0$ for any Lipschitz continuous reference signal $r(t)$. We will assume the dither amplitude is tuned such that the smoothed system is incrementally exponentially stable.

Definition 4.3.1 *The system* (4.1b) *is incrementally exponentially stable if there exists $\beta \geq 1$ and $\alpha > 0$ such that for any given initial conditions w_1 and w_2, the corresponding solutions satisfy*

$$|w(t, r, w_1) - w(t, r, w_2)| \leq \beta e^{-\alpha t}|w_1 - w_2| \quad \forall t \geq 0. \tag{4.40}$$

A simple and often very useful criterion for incremental exponential stability is given by the next lemma.

Lemma 4.3.1 *Assume there exists $Q > 0$ and $\alpha > 0$ such that the matrix inequality*

$$\begin{pmatrix} L^T Q + QL + 2\alpha Q & Qb + c^T \\ b^T Q + c & -2A \end{pmatrix} \leq 0 \tag{4.41}$$

holds. Then the smoothed system is incrementally exponentially stable with decay rate α and gain $\beta = \sqrt{\lambda_{\max}(Q)/\lambda_{\min}(Q)}$.

Proof: Let $\Delta w(t) = w(t,r,w_1) - w(t,r,w_2)$ and $\Delta u(t) = N(cw(t,r,w_1)+r) - N(cw(t,r,w_2)+r)$. If we let $V(t) = \Delta w(t)^T Q \Delta w(t)$ and use (4.41) then

$$\frac{d}{dt}V(t) \leq -2\alpha V(t) - 2(c\Delta w(t) - A\Delta u(t))\Delta u(t) \leq -2\alpha V(t) \tag{4.42}$$

because

$$(c\Delta w(t) - A\Delta u(t))\Delta u(t) = (cw(t,r,w_1) + r(t) - (cw(t,r,w_2) + r(t)) - A\Delta u(t))\Delta u(t) \geq 0$$

due to the slope condition on the saturation nonlinearity. Inequality (4.42) gives

$$|\Delta w(t)| \leq \beta e^{-\alpha t}|w_1 - w_2|$$

with β given in the lemma. ∎

Theorem 4.3.1 *Let $\varepsilon > 0$ and $x_0 \in \mathbb{R}^n$ be given. Suppose that the smoothed system* (4.1b) *is incrementally exponentially stable and assume $r(t)$ is globally Lipschitz with Lipschitz constant M_r. There exists $p_0 > 0$ such that if $p \in (0, p_0)$, then $|x(t,x_0) - w(t,x_0)| \leq \varepsilon$ for all $t \in [0,\infty)$.*

Proof: We will need to consider the dithered and the smoothed system from arbitrary initial time $t_0 \geq 0$. Hence, for the proof we consider the dithered system

$$\begin{cases} \dot{x}(t) &= Lx(t) + bn(cx(t) + \delta(t) + r(t)) \qquad \forall t \geq t_0 \\ x(t_0) &= x_0 \end{cases} . \tag{4.43}$$

and the smoothed system

$$\begin{cases} \dot{w}(t) &= Lw(t) + bN(cw(t) + r(t)) \qquad \forall t \geq t_0 \\ w(t_0) &= w_0 \end{cases} \tag{4.44}$$

where $N(z) = \text{sat}(z/A)$. We suppress the variable $r(t)$ and denote $x(t,t_0,x0)$ the solution of (4.43) with initial condition $x(t_0) = x_0$ and $w(t,t_0,w_0)$ the solution of (4.44) with initial condition $w(t_0) = w_0$. We want to evaluate the approximation error $|x(t,t_0,x_0) - w(t,t_0,x_0)|, \quad \forall t \geq t_0$. For this we will make critical use of the incremental exponential stability assumption which means that

$$|w(t,t_0,w_1) - w(t,t_0,w_2)| \leq \beta e^{-\alpha(t-t_0)}|w_1 - w_2| \tag{4.45}$$

Let us indicate as $w^0(t)$ the solution $w(t,t_0,x_0)$ of the problem (4.44). The idea is to show that for each time interval $[kT,(k+1)T], \quad k \geq 0, \ T > 0$ the approximation error $|x(t,t_0,x_0) - w^0(t)| \quad t \in [kT,(k+1)T]$ is bounded by a function of ordo p_0.

Let us call $\tilde{w}(t,\bar{t}) = w(t,\bar{t},x(\bar{t}))\quad t \geq \bar{t}$ the solution of the smoothed system (4.44) when the initial condition (at the time instant $t_0 = \bar{t}$) is equal to the value that the state of dithered system assumes at $t = \bar{t}$. In other words during each time interval $[kT,(k+1)T]$, $\tilde{w}(t)$ is the solution of the smoothed system when the initial condition is equal to $x(kT)$.

By the triangle inequality we have

$$|x(t,0,x_0) - w^0(t)| \leq |x(t,0,x_0) - \tilde{w}(t)| + |\tilde{w}(t) - w(t,0,x_0)| \qquad \forall t \in [0,+\infty) \quad (4.46)$$

Let us consider the first time interval $[0,T]$. In this case $\tilde{w}(t) = w^0(t)$ since the initial condition is the same for both the solutions. Hence (4.46) reduces to

$$|x(t,0,x_0) - w^0(t)| = |x(t,0,x_0) - \tilde{w}(t)|.$$

We can apply Theorem 4.1.1 and choose a $p_0 = p_0(x_0,T,M_r,\mu\xi)$ (where x_0,T,M_r, and $\varepsilon = \mu\xi$ are the parameters that define p_0 in equation (4.30) since $M = M_y(x_0) + M_r$ and $M_y(x_0)$ is defined in (4.4)) such that the approximation error is bounded by the value $\mu\xi$ with $0 < \mu < 1$ and $\xi > 0$:

$$|x(t,0,x_0) - w^0(t)| = |x(t,0,x_0) - \tilde{w}(t)| \leq \mu\xi < \xi \quad \forall t \in [0,T]. \qquad (4.47)$$

In particular

$$|x(T,0,x_0) - w^0(T)| \leq \xi. \qquad (4.48)$$

Now let us consider a generic time interval $[kT,(k+1)T]$ with

$$|x(kT,0,x_0) - w^0(kT)| \leq \xi$$

(note that this inequality holds for $k = 1$):

$$\begin{aligned} |x(t,0,x_0) - w^0(t)| =& |x(t,kT,x(kT)) - w(t,kT,w(kT))| \\ \leq& |x(t,kT,x(kT)) - \tilde{w}(t,kT)| \\ &+ |\tilde{w}(t,kT) - w(t,kT,w(kT))| \quad \forall t \in [kT,(k+1)T]. \end{aligned} \qquad (4.49)$$

For the first term we apply Theorem 4.1.1 on the finite time horizon on the interval $[kT,(k+1)T]$. It shows that there exists $p_0(x(kT),T,M_r,\mu\xi)$, which gives the upper bound $\mu\xi$. For the second term we use the incremental exponential stability condition in (4.45), which implies

$$\begin{aligned} |\tilde{w}(t,kT) - w(t,kT,w(kT))| &\leq \beta e^{-\alpha(t-kT)}|x(kT) - w(kT)| \\ &\leq \beta e^{-\alpha(t-kT)}\xi \leq \beta\xi \quad \forall t \in [kT,(k+1)T]. \end{aligned} \qquad (4.50)$$

In the time instant $t = (k+1)T$ we have

$$\begin{aligned} |x((k+1)T,0,x_0) - w^0((k+1)T)| =& |x((k+1)T,kT,x(kT)) - w((k+1)T,kT,w(kT))| \\ \leq& |x((k+1)T,kT,x(kT)) - \tilde{w}((k+1)T,kT)| \\ &+ |\tilde{w}((k+1)T,kT) - w((k+1)T,kT,w(kT))| \\ \leq& \mu\xi + \beta e^{-\alpha T}\xi. \end{aligned} \qquad (4.51)$$

If we choose a

$$T \geq \frac{1}{\alpha}\ln\frac{\beta}{(1-\mu)} \qquad (4.52)$$

then the inequality (4.51) can be written

$$|x((k+1)T,0,x_0) - w^0((k+1)T)| \leq \mu\xi + (1-\mu)\xi = \xi. \tag{4.53}$$

We have shown that there exists $T > 0$ and $p_0(x(kT), T, M_r, \mu\xi)$ such that if

$$|x(kT,0,x_0) - w^0(kT)| \leq \xi$$

, then the approximation error is bounded from above by the value $\xi(\mu+\beta)$ on $[kT,(k+1)T]$and $|x((k+1)T,0,x_0) - w^0((k+1)T)| \leq \xi$. The infinite horizon theorem now follows by continuing this process inductively. Indeed, the incremental exponential stability assumption can be used to show that

$$\|w\|_\infty = \sup_{t\in[0,\infty)} |w(t,0,x_0)| < \infty.$$

Hence, we can use the bound $p_0 = p_0(\|w\|_\infty + \xi, T, M_r, \varepsilon)$ in each inductive step. ■

Remark 4.3.1 *If we introduce* $\kappa = \left(\|L\| + \frac{|b|\cdot|c|}{A}\right)$ *and use* $T = \frac{1}{\alpha}\ln\frac{\beta}{1-\mu}$, *by using formula* (4.27) *and* (4.29) *we obtain the approximation error*

$$\begin{aligned}\varepsilon = (\mu+\beta)\xi &= \left(1+\frac{\beta}{\mu}\right)\left(4.5\frac{M}{A}\frac{1}{\alpha}\ln\frac{\beta}{1-\mu}+2\right)|b|e^{\kappa\frac{1}{\alpha}\ln\frac{\beta}{1-\mu}}p_0 \\ &= \left(1+\frac{\beta}{\mu}\right)\left(4.5\frac{M}{A}\frac{1}{\alpha}\ln\frac{\beta}{1-\mu}+2\right)|b|\left(\frac{\beta}{1-\mu}\right)^{\frac{\kappa}{\alpha}}p_0. \end{aligned}\tag{4.54}$$

where $M = M_y(\|w\|_\infty + \mu\xi) + M_r$, *where* $M_y(\cdot)$ *is defined in* (4.4).

The approximation error is independent from the length of the time interval and depends only on the free parameter μ *that can be chosen such that the expression* (4.54) *is minimized.*

The constructive proof of Theorem 4.3.1 provides also bound on the dither period p_0. This bound is shown to be independent from the length of the time interval and depends only on a free parameter and on the desired approximation error ε (see Remark 4.3.1 in the proof of Theorem 4.3.1). It turns out, however, that this p_0 bound in general is conservative. The problem is that the bound was derived using only a minimum information about the structure of the linear part of the system. We will in the next chapter improve this bound for the case when the smoothed system is incrementally stable.

4.4 Periodic solutions in dithered RFSs

The dithered system will in many cases exhibit a periodic solution. In Chapter 3 we saw some examples where the solution of the dithered system converges to an oscillation with a period equal to the period p of the dither signal, while the smoothed system is asymptotically stable. The existence and stability of periodic solutions in dithered systems are analysed in this section. Particularly, we are interested in solutions with period equal to p. The results are useful in the tuning of dither signals discussed in previous section, because given estimates on the dither period p and amplitude A from the tuning algorithm, we can use the results below to prove that the dithered system

will have a (locally) stable oscillation. The results in this section lead to an analytical expression for the ripple in the output of the dithered system. This expression can improve the heuristic tuning algorithm introduced in the previous section.

The results presented next cover both symmetric and asymmetric oscillations and they hold for any (piecewise smooth) periodic dither signal. The mathematical tools used in this section for the analysis of periodic solutions are based on Poincaré maps. For similar results and derivations, but for relay feedback systems with no dither ($\delta \equiv 0$), see (Åström 1995, Johansson *et al.* 1999, di Bernardo *et al.* 2000, Varigonda and Georgiou 2001, Johansson *et al.* 2002).

4.4.1 Symmetric periodic solutions

First we consider the case of symmetric periodic solutions. Consider the dithered relay feedback system (4.1a), with zero reference $r(t) \equiv 0$ and a symmetric dither signal so that $\delta(t + p/2) = -\delta(t)$, $\forall t$. Let us assume that this system has a symmetric unimodal periodic solution of period p, which means that

$$x(t + p/2) = -x(t), \quad \forall\, t \geq 0,$$

and that the solution switches only twice per period. To analyse this oscillation, it is no restriction to consider the system

$$\dot{x}(t) = Lx(t) + b\,\mathrm{sgn}(z(t)), \quad z(t) = cx(t) + R + \delta(t - \alpha))$$

with initial conditions at $t = 0$ such that $z(0) = 0$ and $\dot{z}(0) < 0$. The dither signal δ has been translated α time units. We assume that $\delta(t)$ is differentiable at $t = -\alpha$. Then,

$$\dot{x}(t) = Lx(t) - b, \quad 0 \leq t \leq p/2 \tag{4.55a}$$

$$\dot{x}(t) = Lx(t) + b, \quad p/2 < t \leq p. \tag{4.55b}$$

It follows that

$$x(p/2) = e^{Lp/2}x(0) - L^{-1}(e^{Lp/2} - I)b, \tag{4.56}$$

where we assume that L is invertible (if L is not invertible, one can still derive $x(p/2)$ but for simplicity we do not consider that case). Since the periodic solution is assumed to be symmetric, we have

$$x(p/2) = -x(0) = e^{Lp/2}x(0) - L^{-1}(e^{Lp/2} - I)b, \tag{4.57}$$

and thus

$$x(0) = (e^{Lp/2} + I)^{-1}L^{-1}(e^{Lp/2} - I)b. \tag{4.58}$$

It is now possible to derive the following existence result, cf., (Åström 1995, Varigonda and Georgiou 2001).

Proposition 4.4.1 *The dithered system has a symmetric unimodal periodic solution with period p if and only if there exists α such that*

$$c(e^{Lp/2} + I)^{-1}L^{-1}(e^{Lp/2} - I)b + \delta(-\alpha) = 0$$

and

$$ce^{Lt}(e^{Lp/2} + I)^{-1}L^{-1}(e^{Lp/2} - I)b - cL^{-1}(e^{Lt} - I)b + \delta(t - \alpha) < 0, \quad 0 < t < \frac{p}{2}.$$

Next we investigate the stability of the periodic solution. Introduce the maps

$$g(t,x) = e^{Lt}x - L^{-1}(e^{Lt} - I)b, \qquad \mu(t,x) = cg(t,x) + \delta(t-\alpha).$$

For an initial point $x(0) = x_0$, denote the first switching instant for the dithered system by $t^* = t^*(x_0)$. As pointed out above, we assume that $\delta(t-\alpha)$ does not have a discontinuity in its time derivative at the switching instants. Then,

$$x(t^*) = g(t^*,x_0) = e^{Lt^*}x_0 - L^{-1}(e^{Lt^*} - I)b =: N(t^*)x_0 - M(t^*), \tag{4.59}$$

where notations N and M are introduced for convenience. The switching constraint is

$$\mu(t^*,x_0) = 0. \tag{4.60}$$

Since the switching instant $t^* = t^*(x_0)$ is a function of the initial condition x_0, we can evaluate the partial derivative of (4.59) with respect to x_0 by using the theorem of implicit functions, and thus derive the following Jacobian evaluated at $(t,x) = (t^*,x_0)$:

$$J = \frac{\partial g}{\partial x} - \frac{\partial g}{\partial t}\left(\frac{\partial \mu}{\partial t}\right)^{-1}\frac{\partial \mu}{\partial x} \tag{4.61}$$

where

$$\frac{\partial g}{\partial x} = N(t^*) \tag{4.62}$$

$$\frac{\partial g}{\partial t} = \frac{\partial N(t^*)}{\partial t}x_0 - \frac{\partial M(t^*)}{\partial t} \tag{4.63}$$

$$\frac{\partial \mu}{\partial t} = c\frac{\partial g}{\partial t} + \frac{\partial \delta}{\partial t} \tag{4.64}$$

$$\frac{\partial \mu}{\partial x} = c\frac{\partial g}{\partial x} = cN(t^*). \tag{4.65}$$

By evaluating the equations above, we obtain the following stability result.

Proposition 4.4.2 *A symmetric unimodal periodic solution defined by Proposition 4.4.1 is stable if all eigenvalues of the Jacobian*

$$J = \left(I - \frac{wc}{cw + \partial\delta/\partial t}\right)e^{Lt^*}, \qquad w = \left(I + e^{Lt^*}\right)^{-1}e^{Lt^*}(-2b)$$

are in the open unit disc. It is unstable if at least one eigenvalue of J is outside.

By applying Propositions 4.4.1 and 4.4.2, we can thus prove the existence and the stability of a periodic solution for the dithered system. This information can be used to guide the dither tuning introduced in previous section, since for appropriate application of the dither the feedback system should exhibit a (fast) oscillation with period p. If such oscillation does not exist, the period of the dither could be modified.

4.4.2 Asymmetric periodic solutions and bias

Dither may give rise also to asymmetric periodic solutions. By following a procedure similar to that presented above, it is easy to derive sufficient and necessary conditions for the existence of asymmetric periodic solutions.

Consider the dithered relay feedback system (4.1a) again, but now with (possibly non-zero) constant reference $r(t) = R$ and (possibly) asymmetric dither signal. Let us assume that this system has a asymmetric unimodal periodic solution of period p. Then,

$$\dot{x}(t) = Lx(t) - b, \quad 0 \le t \le T_- \tag{4.66a}$$
$$\dot{x}(t) = Lx(t) + b, \quad T_- < t \le T_- + T_+, \tag{4.66b}$$

where $T_- \neq T_+$ are the lengths of the two asymmetric parts of the periodic solution, so that $T_- + T_+ = p$. Define $\xi = x(0)$ as the initial condition and $\eta = x(T_-)$ the value of the state at the switching instant time T_-. If L is invertible, then

$$\eta = e^{LT_-}\xi - L^{-1}(e^{LT_-} - I)b, \tag{4.67}$$

and since $\xi = x(p/2)$,

$$\xi = e^{LT_+}\eta + L^{-1}(e^{LT_+} - I)b. \tag{4.68}$$

Hereby,

$$(I - e^{Lp})\xi = L^{-1}(-e^{Lp} + 2e^{LT_+} - I)b \tag{4.69a}$$
$$(I - e^{Lp})\eta = L^{-1}(e^{Lp} - 2e^{LT_-} + I)b. \tag{4.69b}$$

Similar to Proposition 4.4.1, these equations lead to the following result.

Proposition 4.4.3 *The dithered system has an asymmetric unimodal periodic solution with period p if and only if there exist α and a positive $T_- \neq T_+$, with $p = T_- + T_+$, such that*

$$c(I - e^{Lp})^{-1}L^{-1}(-e^{Lp} + 2e^{LT_+} - I)b + \delta(-\alpha) + R = 0$$
$$c(I - e^{Lp})^{-1}L^{-1}(-e^{LT_-} + e^{LT_+})b + \frac{1}{2}\delta(T_- - \alpha) + R = 0,$$

and

$$ce^{Lt}\xi - cL^{-1}(e^{Lt} - I)b + \delta(t - \alpha) + R > 0, \quad 0 < t < T_-$$
$$ce^{Lt}\eta + cL^{-1}(e^{Lt} - I)b + \delta(t + T_- - \alpha) + R < 0, \quad 0 < t < T_+,$$

where ξ and η are defined above.

Compared to the symmetric case we have an extra parameter to determine when establishing the existence of an asymmetric periodic solution.

It is straightforward to derive the stability condition corresponding to Proposition 4.4.2 also for asymmetric periodic solutions.

Note that the existence of a unimodal asymmetric periodic solution implies that the average of some of the state variables must be nonzero. Such a dithered system, could present a bias in the output while the output of corresponding smoothed system may tend to zero. A rigorous analysis of the bias phenomena is out of the scope of this thesis, but will be investigated in a future work.

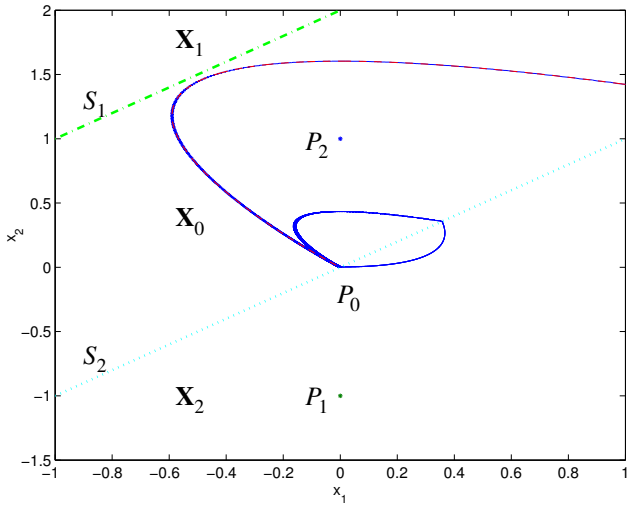

Figure 4.2: Phase plane portrait of the simulation of Figure 3.11. The dash-dotted line is the switching plane $cx + A + R = 0$ and the dotted line is the switching plane $cx - A + R = 0$. In the diagram the equilibrium points $\bar{x} = \pm L^{-1}b$ are also plotted.

4.5 Zero-slope dither signals

One of the key point in the proof of the average theorem is the assumption on shape of the dither signal. The analysis used in the proof cannot be directly extended to dither signals that have zero time derivative in a time interval of nonzero measure. In this Section we will discuss and analyse simulations presented in Chapter 3 related to the relay feedback system dithered with square wave signals.

A phase plane picture of the space evolution of the dithered system can help to justify the shape of the limit cycle of the dithered system in this case. In Figure 4.2 we plotted the switching lines $cx + A + R = 0$ and $cx - A + R = 0$, for $R = A$. In fact the square wave dither assumes only the values $+A$ and $-A$ so that we have only two switching hyperplanes. When the trajectory is in the region between these two switching lines, dither affects the system. When the trajectory is below the line $cx - A + R$ we have a smooth behaviour: no switching occurs until the trajectory intersects this line again. In order to analyse this behaviour, let us consider Figure 4.3 in which we focus our attention on four points of the trajectory:

1 Starting point of our analysis: the trajectory tends towards the upper equilibrium point. In fact $\delta(t) = +A$ and the upper switching line is active. Since the trajectory is below this line ($cx + \delta + r > 0$), the output of the relay is $+1$ and the equilibrium point is $\bar{x} = -L^{-1}b = \begin{pmatrix} 0 & 1 \end{pmatrix}^T$.

2 The square wave dither switches from $+A$ to $-A$. The trajectory is now above the active switching line so the output of the relay is -1 and the trajectory tends towards the equilibrium point $\begin{pmatrix} 0 & -1 \end{pmatrix}^T$ (see Figure 4.2).

3 The square wave dither switches again from $-A$ to $+A$ and we have the same behaviour as of the point 1.

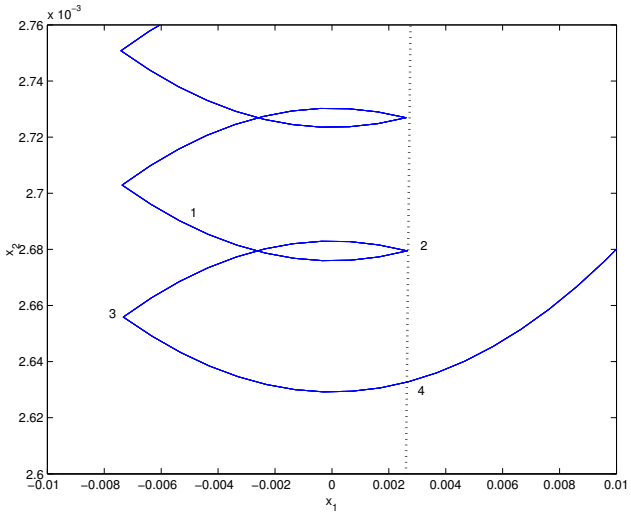

Figure 4.3: Zoom of Figure 4.2. The dotted line is the switching plane $cx - A + R = 0$.

4 Now the trajectory passes through the switching line $cx - A + R = 0$ although the active switching line is the upper one ($cx + A + R = 0$). When the dither switches to the value $-A$ so that the active switching line is $cx - A + R = 0$, the trajectory is now below this line and the output of the relay doesn't change even when the dither switches again. We have a smooth behaviour until the trajectory passes again through the plane $cx - A + R = 0$. This behaviour (switching-smooth) still remains even if we increase the dither frequency.

This simulation, together with the example of trapezoidal dither (see Chapter 3), shows the validity of the conjecture derived from the geometrical approach of the average theorem proof. In order to understand this key point it is necessary to give a look at the proof of Theorem 4.1.1: when we have a dither signal with some time interval of zero slope, it can be shown that the time interval during which the argument of the integral in (4.8) can be non-zero is not bounded by p^2 (so as required for the proof) but only by p.

4.6 Averaging for smooth-switching trajectories

In the previous section we have just pointed out that the geometrical approach could be used in deriving some conjectures about the dither effectiveness in smoothing the relay nonlinearity. We discussed the example of the square wave dither and we saw how this class of signals can induce a smooth-switching behaviour in the dithered system.

In this section we will give a deeper look at the cause of such a behaviour. First of all we generalize the case of square wave dithered RFS.

Let us consider a phase plane approach. We can divide the phase plane into three regions: two regions in which the dither has no effects since the argument of the signum function is always greater than or less than the dither signal ($cx + R < -A$ or $cx + R > A$) and a third region (included between the two hyperplanes S_1 and S_2) in which the dither affects the system behaviour:

- Region $\mathbf{X}_1 = \{x : cx + R + A < 0\}$. In this region $u = -1$ and the dithered system coincides with the smoothed system: $\dot{x} = Lx - b$. The equilibrium point is P_1 : $\bar{x} = L^{-1}b$ (by assuming L invertible).
- Region $\mathbf{X}_2 = \{x : cx + R - A > 0\}$. In this region $u = +1$ and the dithered system coincides with the smoothed system: $\dot{x} = Lx + b$. The equilibrium point is P_2 : $\bar{x} = -L^{-1}b$ (by assuming L invertible).
- Region $\mathbf{X}_0 = \{x : |cx + R| < A\}$. In this region the dithered system has an input that switches periodically between -1 and $+1$ (note that while $x \in \mathbf{X}_0$ the switches are periodic because only depend on the dither signal and are independent from the state x). The smoothed system has an input equal to zero: $\dot{w} = Lw$. The equilibrium point of the smoothed system is the origin (L is assumed to be invertible).

In what follows we will consider the different situations due to the position of the equilibrium points P_0 with respect to the hyperplane S_2. A similar analysis can be carried out by considering P_0 close to S_1.

Case $P_2 \in \mathbf{X}_0$, $P_0 \in S_2$, $P_1 \in \mathbf{X}_2$

By looking at Figure 4.2 it is clear that the smooth-switching behaviour is due to the fact that the state trajectory lies in the regions $\mathbf{X}_0$ and $\mathbf{X}_2$. Starting from a point $x_0 \in \mathbf{X}_2$, since the equilibrium point (asymptotically stable since L is Hurwitz) $P_2 \notin \mathbf{X}_2$, the trajectory goes again in the $\mathbf{X}_0$ region. In this region the dithered system "follows" the smoothed system behaviour: w asymptotically tends to the origin $P_0 \in S_2$ and, in the case under investigation, the smoothed state does not pass through the S_2 hyperplane. However, due to the nonzero ripple, the "dithered" state x crosses S_2 and passes into the region $\mathbf{X}_2$ and here the cycle repeats.

Case $P_2 \in \mathbf{X}_0$, $P_0 \in \mathbf{X}_0$, $P_1 \in \mathbf{X}_2$

When $P_0 \in S_2$ only an infinite dither frequency can avoid that the state x crosses S_2; therefore for finite dither frequency the smoothed state w tends to the origin P_0 and the dithered state x escapes from the "entrapment" region $\mathbf{X}_0$. If the origin is inside the region $\mathbf{X}_0$, a sufficiently high dither frequency can avoid the presence of a smooth-switching trajectory (it can be shown that in the $\mathbf{X}_0$ region the averaging theorem is still valid).

In order to validate our conjecture, we can change the position of the origin P_0 with respect to the switching line S_2: if we choose $A = 1$ and $R = 0.99$ the origin P_0 is inside the region $\mathbf{X}_0$. In Figure 4.4 we have the time diagram of the outputs (dithered system and smoothed system) and in Figure 4.5 we have the phase plane diagram. The smooth-switching behaviour is still present since the ripple is sufficiently high to escape from the $\mathbf{X}_0$ region.

If we increase the dither frequency, the ripple decreases and in the case $p = 1/50$ the dithered state x cannot escape from the region $\mathbf{X}_0$ so smoothed system and dithered system have the same behaviour (see Figure 4.6 and Figure 4.7).

Case $P_2 \in \mathbf{X}_0$, $P_0 \in \mathbf{X}_2$, $P_1 \in \mathbf{X}_2$

This is the straightforward case in order to obtain a smooth-switching behaviour. In fact the averaged system isn't stable and its trajectory oscillates between $\mathbf{X}_0$ and $\mathbf{X}_2$

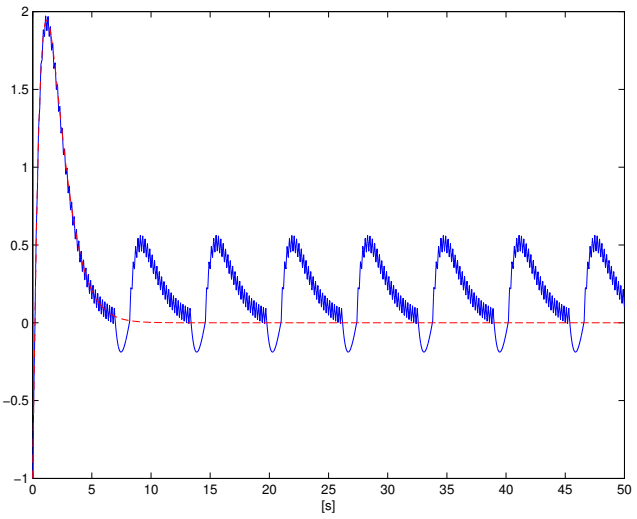

Figure 4.4: Outputs of the dithered relay feedback system (solid) and the smoothed system (dashed) with dither period $p = 1/5$, dither amplitude $A = 1$ and external reference $r(t) = R = 0.99$. The dither signal is a squarewave.

region. When the state is in $\mathbf{X}_1$ or $\mathbf{X}_2$, the trajectory tends toward the equilibrium point and necessarily passes into the region $\mathbf{X}_0$. So the trajectory of the dithered system has a smoothed behaviour in this phase. When the state of the dithered system is in $\mathbf{X}_0$ we have a switching behaviour but again the trajectory passes into the region $\mathbf{X}_2$ since the equilibrium point of the averaged system is in $\mathbf{X}_2$ and the dithered trajectory follows the averaged one. Then the cycle restarts.

4.6.1 Triangular dither

Inspired by the previous analysis it could be interesting to investigate the possibility for obtaining a smooth-switching behaviour also in the case of a triangular dither waveform.

Let us define the regions $\mathbf{X}_0$, $\mathbf{X}_1$ and $\mathbf{X}_2$ and the equilibrium points P_1 and P_2 as above. In order to avoid the convergence of the trajectory towards an equilibrium point, it is necessary that $P_1 \notin \mathbf{X}_1$ and $P_2 \notin \mathbf{X}_2$. These conditions can be satisfied by suitably choosing the parameters A and R.

In the case of a square wave dither we have shown that if $P_0 \in S_2$ it is possible to have smooth-switching trajectories also with high dither frequency. Instead, in order to have smooth-switching trajectory with triangular dither it is not sufficient to put the equilibrium point P_0 (equilibrium point of the smoothed system in the region $\mathbf{X}_0$) close to S_2 (or S_1). In fact, in this case the smoothed system (saturation as equivalent nonlinearity) has a vector field non discontinuous on S_2. The continuity of the vector field does not allow to have a cyclic behaviour of the dithered system because the equilibrium point $P_2 \to P_0$ when P_0 tends towards S_2. In fact P_0 is $\bar{w} = -(L + bc/A)^{-1} bR/A$, a continuous (and linear) function of R and P_2 is $-L^{-1}b$. It can be shown (see Example 2.2.5) that when $P_0 \in S_2$ (i.e. $c\bar{w} + R - A = 0$), $P_0 \equiv P_2$. In the case of the square dither, indeed, both P_0 and P_2 didn't depend on R and they were always different points.

Inspired by the averaging theorem we can conjecture that a smooth-switching tra-

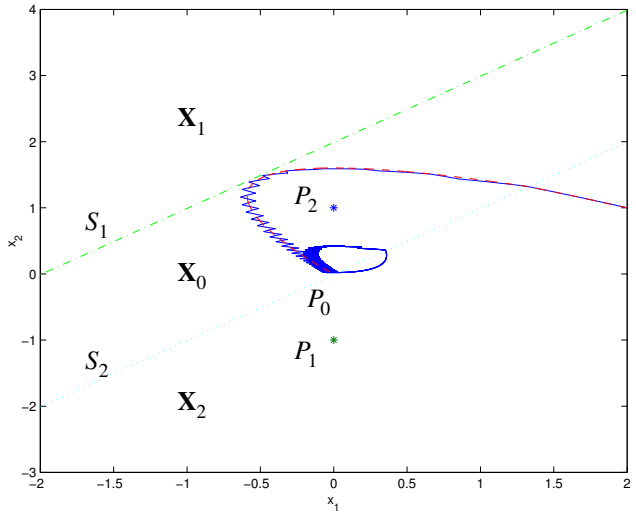

Figure 4.5: Phase plane portrait of the simulation of Figure 4.4. The dash-dotted line is the switching plane $cx + A + R = 0$ and the dotted line is the switching plane $cx - A + R = 0$. In the diagram the equilibrium points $\bar{x} = \pm L^{-1}b$ are also plotted.

jectory in a relay feedback system with triangular dither may exist if the smoothed system has a limit cycle that crosses the switching line S_2. This intuition derives from the averaging theorem although the theorem has not been proved (for infinite time horizon) in the case of an unstable smoothed system (the case in which it presents a limit cycle). Figures 4.8, 4.9 and 4.10 confirm our intuition. In what follows we show in which cases the averaging theorem can be applied also when the smoothed system has a limit cycle.

Definition 4.6.1 (Practical stability) *The dithered system* (4.1a) *with the triangular dither and a given amplitude $A > 0$ has a practically (exponentially) stable limit cycle γ if for any $\varepsilon > 0$ there exists $\alpha > 0$ and $\beta \geq 1$, and $p_0 > 0$ such that*

$$\mathrm{d}(x(t), \gamma) \leq \beta e^{-\alpha t}\, \mathrm{d}(x_0, \gamma) + \varepsilon, \quad \forall t \in [0, \infty)$$

for any dither period $p \in (0, p_0)$, where $\mathrm{d}(x, \gamma) = \inf_{y \in \gamma} |x - y|$.

Theorem 4.6.1 *Suppose $r(t) = R$ and that the smoothed system* (4.2b) *has an exponentially stable limit cycle. Then there exists p_0 such that for $p \in (0, p_0)$ the dithered system* (4.1a) *has a practically stable limit cycle.*

Proof: By hypothesis the system (3.25) with $r(t) = R$ has a limit cycle γ exponentially stable. Hence, there exists $\alpha_0 > 0$ and $\beta_0 \geq 1$ such that

$$\mathrm{d}(w(t), \gamma) \leq \beta_0 e^{-\alpha_0 t}\, \mathrm{d}(w_0, \gamma), \quad \forall t \geq 0.$$

We iteratively consider time intervals of length T and, in order to guarantee a decay rate of 0.1, we choose $T = -{\alpha_0}^{-1} \ln(0.1/\beta_0)$. Then, if p_0 is sufficiently small, we have

$$|x(t) - w(t)| \leq \varepsilon_0$$

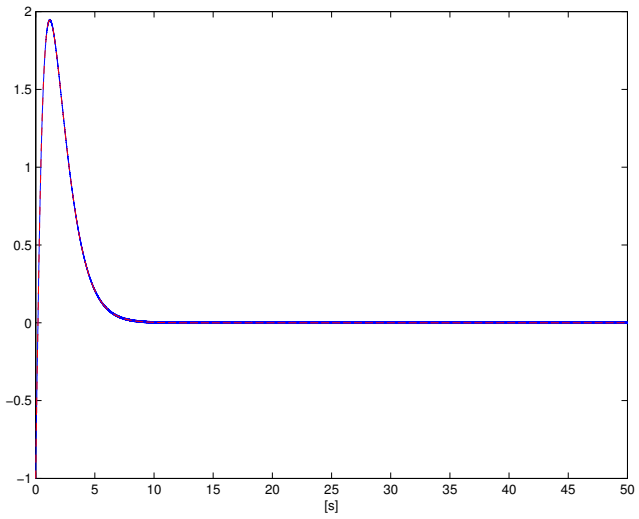

Figure 4.6: Outputs of the dithered relay feedback system (solid) and the smoothed system (dashed) with dither period $p = 1/50$, dither amplitude $A = 1$ and external reference $r(t) = R = 0.99$. The dither signal is a squarewave.

on $t \in [0,T]$. If we consider a new smoothed system satisfying (3.25) on the time interval $[kT,(k+1)T]$, $k = 0,1,2,\ldots$, with initial condition $w(kT) = x(kT)$, then it follows from the above arguments that

$$\mathrm{d}(w(t),\gamma) \leq \beta_0 e^{-\alpha_0(t-kT)}\,\mathrm{d}(x(kT),\gamma), \quad \forall t \geq kT,$$

and, by applying the averaging theorem on finite time horizon again,

$$\begin{aligned}\mathrm{d}(x,\gamma) \leq& |x(t)-w(t)| + \mathrm{d}(w,\gamma) \leq \varepsilon_0 + \mathrm{d}(w(t),\gamma)\\ \leq& \beta_0 e^{-\alpha_0(t-kT)}\,\mathrm{d}(x(kT),\gamma) + \varepsilon_0\end{aligned} \tag{4.70}$$

on $t \in [kT,(k+1)T]$. By evaluating (4.70) in $t = (k+1)T$,

$$\mathrm{d}(x((k+1)T),\gamma) \leq 0.1\,\mathrm{d}(x(kT),\gamma) + \varepsilon_0. \tag{4.71}$$

Hence

$$\mathrm{d}(x(kT),\gamma) \leq 0.1^k\,\mathrm{d}(x_0,\gamma) + \varepsilon_0\frac{1-0.1^k}{1-0.1}. \tag{4.72}$$

Then (4.70) becomes

$$\begin{aligned}\mathrm{d}(x(t),\gamma) &\leq \beta_0 e^{-\alpha_0(t-kT)}\left(e^{-\alpha kT}\,\mathrm{d}(x_0,\gamma) + \frac{\varepsilon_0}{0.9}\right) + \varepsilon_0\\ &\leq \beta_0 e^{-\alpha_0(t-kT)} e^{-\alpha kT}\,\mathrm{d}(x_0,\gamma) + \underbrace{\beta_0\frac{\varepsilon_0}{0.9} + \varepsilon_0}_{\varepsilon},\end{aligned} \tag{4.73}$$

where $\alpha = -T^{-1}\ln 0.1$. Since $\alpha_0 > \alpha$ and $t \geq kT$, (4.73) becomes

$$\mathrm{d}(x(t),\gamma) \leq \beta_0 e^{-\alpha t}\,\mathrm{d}(x_0,\gamma) + \varepsilon. \tag{4.74}$$

We have thus shown practical stability with $\alpha = -T^{-1}\ln 0.1$ and $\beta = \beta_0$. ■

Figure 4.11 shows the validity of the theorem even if $w_0 \neq x_0$. In Figure 4.12 we can see what happens in the time domain.

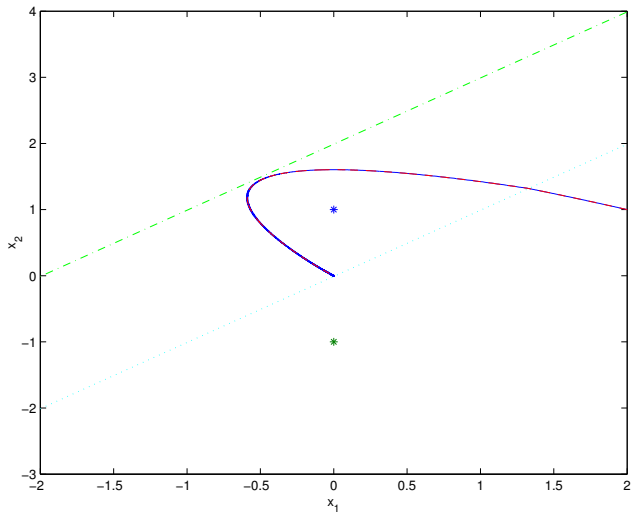

Figure 4.7: Phase plane portrait of the simulation of Figure 4.6. The dash-dotted line is the switching plane $cx + A + R = 0$ and the dotted line is the switching plane $cx - A + R = 0$. In the diagram the equilibrium points $\bar{x} = \pm L^{-1}b$ are also plotted.

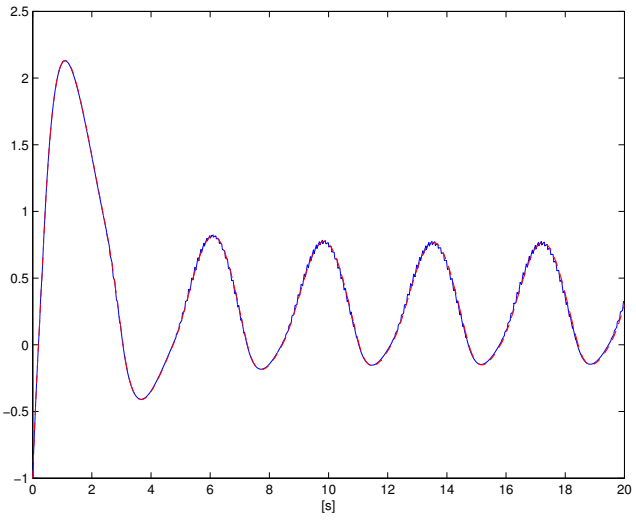

Figure 4.8: Outputs of the dithered relay feedback system (solid) and the smoothed system (dashed) with dither period $p = 1/10$, dither amplitude $A = 0.45$ and external reference $r(t) = R = 0.45$. The dither signal is triangular.

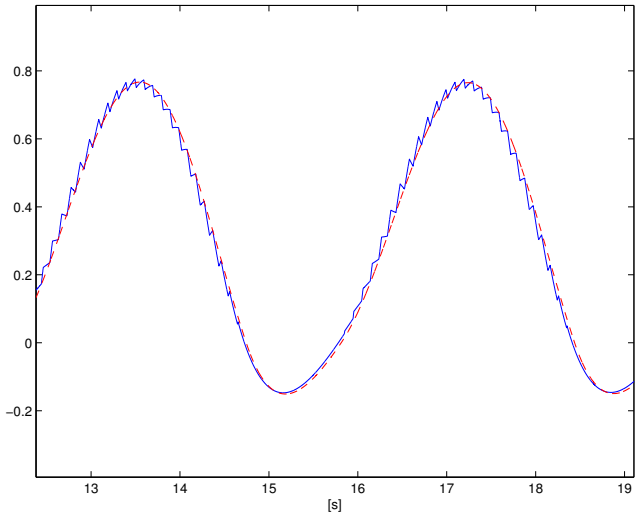

Figure 4.9: Zoom of Figure 4.8.

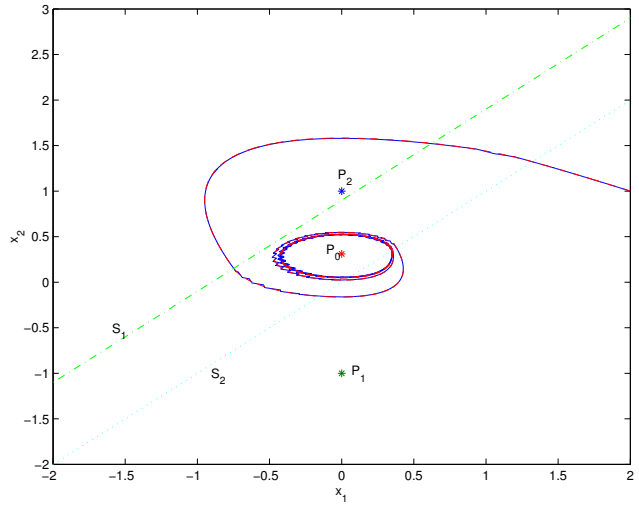

Figure 4.10: Phase plane of the simulation corresponding to Figure 4.8.

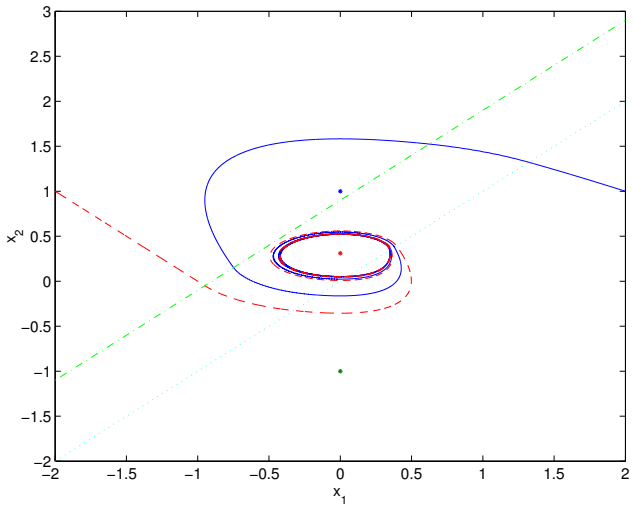

Figure 4.11: Phase plane of the simulation corresponding to Figure 4.8 with different initial conditions.

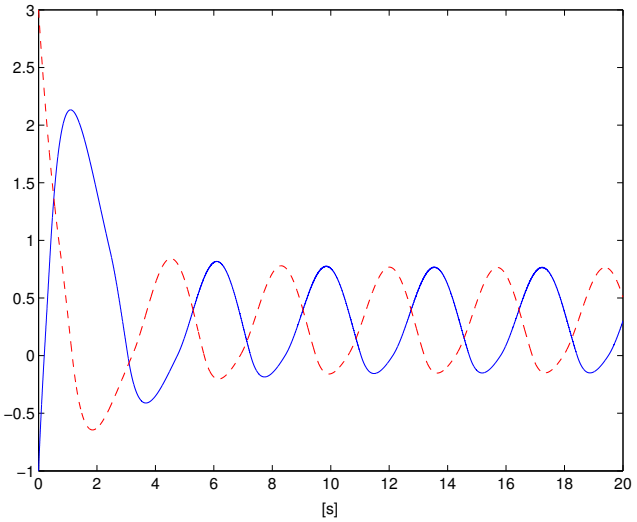

Figure 4.12: Simulation corresponding to Figure 4.8 with different initial conditions.

Chapter 5

Design

In this chapter we use Theorems 4.1.1 and 4.2.1 to tune the dither signal. The purpose can for example be to stabilize an oscillating system. We also use Corollary 5.2.1 to obtain an LMI based design methodology of the dither parameters. This results in an exponentially stable system with a state vector that can track the state vector of the smoothed system with arbitrary precision. We finally present a heuristic method, which can give less conservative designs. The design methods are illustrated on the example in Section 3.4. We consider the case with triangular dither. Analogous tuning rules can be derived for the case of, for example, sawtooth dither.

5.1 A first tuning algorithm

The dither design choice will necessarily be a compromise between conflicting consequences of the dither amplitude A and period p on the control performance. Based on our theoretical results we obtain the following algorithm for tuning the parameters of the dither signal.

Step 1 Choose A based on (4.39) in Corollary 4.2.1, so that the smoothed system in (4.1b) is exponentially stable.

Step 2 Estimate α_0, β_0 and let $T = -\ln(0.1/\beta_0)/\alpha_0$, where α_0, β_0 are the exponential stability parameters for the smoothed system. Choose p_0 based on T and the smoothed dynamics.

A few comments are in place. In Step 1 we need to choose the amplitude A of the dither signal large enough to allow the smoothed system to be stable and to have fast enough exponential decay rate. At the same time we want to keep A as small as possible in order to avoid injecting a large signal in the control loop.

In Step 2 the estimates of α_0 and β_0 can be derived based on the Kalman–Yakubovich–Popov Lemma, as discussed in Section 4.2. Then we can compute time interval length T, which is an auxiliary variable in the proof of Theorem 4.2.1. The parameter T gives a bound on the period of the dither signal through (4.30) in the proof of Theorem 4.1.1. Better bounds can be derived if we use the structure of the saturation nonlinearity and that the smoothed dynamics is chosen to be exponentially stable. The bound derived in Theorem 5.2.1 is taking several of these structural aspects into account.

5.2 A second tuning algorithm

We first improve the bound on p_0 obtained in the proof of Theorem 4.1.1. A much tighter bound can be obtained when the smoothed system is incrementally stable.

Theorem 5.2.1 *Assume $r(t)$ is globally Lipschitz with Lipschitz constant M_r and suppose there exists $P = P^T > 0$ and $\gamma > 0$ such that*

$$\begin{pmatrix} L^T P + PL & Pb + c^T & 0 \\ b^T P + c & -2A & c \\ 0 & c^T & -\gamma I \end{pmatrix} \leq 0. \tag{5.1}$$

Then the bound p_0 on the dither period in Theorem 4.1.1 can be chosen to be

$$p_0 = \min\left(\frac{4A}{7M}, \Gamma^{-1}\varepsilon\right) \tag{5.2}$$

where

$$\Gamma = c_3 T + 2c_1 + \sqrt{\gamma/\lambda_{\min}(P)}\sqrt{\frac{1}{3c_3}\left(\left(c_3 T + 2c_1\right)^3 - 8c_1^3\right)} \tag{5.3}$$

and

$$c_1 = \sup_{t\in[0,T]} |e^{Lt}b|, \quad c_2 = \sup_{t\in[0,T]} |Le^{Lt}b|, \quad c_3 = \frac{1}{2}\left(\frac{9M}{A}c_1 + 3c_2\right).$$

and $M = \sup_{t\in[0,T]}[|cLe^{Lt}x_0| + \int_0^t |cLe^{Ls}b|ds + |cb|] + M_r$.

Proof: The differential form of (4.25) is

$$\dot{x}(t) - \dot{w}(t) = L(x(t) - w(t)) + b[N(cx(t) + r(t)) - N(cw(t) + r(t))] + bv(t),$$

where $v(t) = n(cx(t) + r(t) + \delta(t)) - N(cx(t) + r(t))$. This system can equivalently be written

$$x(t) - w(t) = \int_0^t e^{L(t-s)}b(N(cx(s) + r(s)) - N(cw(s) + r(s)))ds + e(t), \tag{5.4}$$

where $e(t) = \int_0^t e^{L(t-s)}bv(s)ds$.

Lemma 5.2.1 *We have*

$$|e(t)| \leq \left(\left(\frac{9Mt}{2A} + 2\right)c_1 + \frac{3t}{2}c_2\right)p = (c_3 t + 2c_1)p$$

for all $t \in [0,T]$. Moreover,

$$\int_0^t |e(s)|^2 ds \leq \frac{1}{3c_3}\left(\left(c_3 t + 2c_1\right)^3 - 8c_1^3\right)p^2$$

where

$$c_1 = \sup_{t\in[0,T]} |e^{Lt}b|, \quad c_2 = \sup_{t\in[0,T]} |Le^{Lt}b|, \quad c_3 = \frac{1}{2}\left(\frac{9M}{A}c_1 + 3c_2\right).$$

Proof: This will be derived in a similar fashion as the proof of Theorem 4.1.1. Let $m = \lfloor T/p \rfloor$, then $e(t) = e_1(t) + e_2(t) + e_3(t)$

$$
\begin{aligned}
e_1(t) &= \int_{mp}^{t} e^{L(t-s)} b[n(cx(s) + r(s) + \delta(s)) - N(cx(s) + r(s))]ds \\
e_2(t) &= \sum_{k=0}^{m-1} \int_{kp}^{(k+1)p} [e^{L(t-s)} bn(cx(s) + r(s) + \delta(s)) \\
&\qquad - e^{L(t-kp)} bn(cx(kp) + r(kp) + \delta(s))]ds \\
e_3(t) &= \sum_{k=0}^{m-1} e^{L(t-kp)} bN(cx(kp) + r(kp))p - \int_{0}^{mp} e^{L(t-s)} bN(cx(s) + r(s))ds
\end{aligned}
$$

For the first term we have

$$|e_1(t)| \leq 2c_1 p, \quad \text{where} \quad c_1 = \sup_{t \in [0,T]} |e^{Lt} b|$$

Each term of e_2 can be split into two terms: $e_2 = \sum_{k=0}^{m-1} \left(e_{2_{ka}} + e_{2_{kb}} \right)$,

$$
\begin{aligned}
e_{2_{ka}} &= \int_{kp}^{(k+1)p} (e^{L(t-s)} - e^{L(t-kp)}) bn(cx(s) + r(s) + \delta(s))ds \\
e_{2_{kb}} &= \int_{kp}^{(k+1)p} e^{L(t-kp)} b[n(cx(s) + r(s) + \delta(s)) - n(cx(kp) + r(kp) + \delta(s))]ds
\end{aligned}
$$

For the first we get the bound

$$|e_{2_{ka}}| \leq c_2 p^2, \quad \text{where} \quad c_2 = \sup_{t \in [0,T]} |Le^{Lt} b|$$

and for the second we get

$$|e_{2_{kb}}| \leq c_1 4 \frac{M}{A} p^2, \quad p \leq \bar{p}$$

which follows from (4.20) in the proof of Theorem 4.1.1. If we put these bounds together and sum we get

$$|e_2(t)| \leq (c_2 + c_1 4 \frac{M}{A}) tp.$$

for all $t \in [0, T]$. Finally, since the Lipschitz constant of $H(s) = e^{L(t-s)} bN(cx(s) + r(s))$ can be bounded as

$$\text{Lip}[H] \leq c_2 + c_1 \frac{M}{A}$$

A similar argument as in equations (4.22)-(4.24) gives

$$|e_3(t)| \leq (c_2 + c_1 \frac{M}{A}) \frac{t}{2} p$$

for all $t \in [0, T]$. If we put everything together, we get

$$|e(t)| \leq \left(\left(\frac{9Mt}{2A} + 2 \right) c_1 + \frac{3t}{2} c_2 \right) p$$

for all $t \in [0,T]$. ∎

A state space realization of (5.4) is

$$\begin{aligned} \dot{z}(t) &= Lz(t) + bu(t), \quad z(0) = x(0) - w(0) = 0 \\ u(t) &= N(cx(t) + r(t)) - N(cw(t) + r(t)) \\ x(t) - w(t) &= z(t) + e(t) \end{aligned}$$

We will use the slope condition on the saturation nonlinearity N, which gives the relation

$$(c(z+e) - Au)u \geq 0 \tag{5.5}$$

Now, let us multiply the linear matrix inequality with $\begin{pmatrix} z^T & u & e^T \end{pmatrix}$ on the left and its transpose on the right. This gives

$$\frac{d}{dt} z^T P z + 2(c(z+e) - Au)u - \gamma e^T e \leq 0$$

If we integrate this inequality and use that the second term is positive due to (5.5) then we get

$$z(t)^T P z(t) \leq z(0)^T P z(0) + \gamma \int_0^t |e(s)|^2 ds$$

Hence, using $z(0) = 0$,

$$\begin{aligned} |z(t)| &\leq \sqrt{\lambda_{\max}(P)/\lambda_{min}(P)}|z(0)| + \sqrt{\gamma/\lambda_{\min}(P)}\sqrt{\int_0^t |e(s)|^2 ds} \\ &\leq \sqrt{\gamma/\lambda_{\min}(P)}\sqrt{\int_0^T |e(s)|^2 ds} \\ &\leq \sqrt{\gamma/\lambda_{\min}(P)}\sqrt{\frac{1}{3c_3}\left(\left(c_3 T + 2c_1\right)^3 - 8c_1^3\right)} \cdot p \end{aligned}$$

We see that $|x(t) - w(t)| \leq \varepsilon$ on $t \in [0,T]$ if

$$|z(t)| + |e(t)| \leq \varepsilon,$$

which is the case if

$$p \leq \Gamma^{-1}\varepsilon$$

where

$$\Gamma = c_3 T + 2c_1 + \sqrt{\gamma/\lambda_{\min}(P)}\sqrt{\frac{1}{3c_3}\left(\left(c_3 T + 2c_1\right)^3 - 8c_1^3\right)}$$

the bound on p in the statement of the theorem holds. ∎

By combining Theorem 4.3.1 and the previous theorem we obtain much better bounds for the dither frequency also in the case of infinite time horizon. We state this as a corollary. Here we assume that we have an estimate on the norm $\|w\|_\infty = \sup_{t\in[0,\infty)} |w(t)|$. Such a bound is easy to obtain for a given reference signal. If we have a class of reference signals then we can obtain a bound by exploiting the incremental exponential stability of the smoothed system.

Corollary 5.2.1 *Let $\varepsilon > 0$ and $x_0 \in \mathbb{R}^n$ be given. Suppose that the smoothed system* (4.1b) *is incrementally exponentially stable with gain β and decay rate α. Assume further that $r(t)$ is globally Lipschitz with Lipschitz constant M_r and that the bound on the smoothed system state is $\|w\|_\infty$. Then $|x(t,x_0) - w(t,x_0)| \leq \varepsilon$ for all $t \in [0,\infty)$ if the dither period is chosen in $p \in (0, p_0)$, where*

$$p_0 = \min\left(\frac{4A}{7M}, \frac{\varepsilon}{(1+\frac{\beta}{\mu})\Gamma(P,\alpha,\beta,\mu,\|w\|_\infty)}\right) \tag{5.6}$$

Here $\mu \in (0,1)$,

$$\Gamma(P,\alpha,\beta,\mu,\|w\|_\infty) = \frac{c_3}{\alpha}\ln\left(\frac{\beta}{1-\mu}\right) + 2c_1 + \sqrt{\frac{\gamma}{\lambda_{min}(P)}}\cdot\sqrt{\frac{1}{3c_3}\left(\left(\frac{c_3}{\alpha}\ln\left(\frac{\beta}{1-\mu}\right)+2c_1\right)^3 - 8c_1^3\right)}, \tag{5.7}$$

where $P > 0$ solves the LMI in (5.1) and

$$c_1 = \sup_{t\in[0,T^*]}|e^{Lt}b|, \quad c_2 = \sup_{t\in[0,T^*]}|Le^{Lt}b|, \quad c_3 = \frac{1}{2}\left(\frac{9M}{A}c_1 + 3c_2\right).$$

where $M = |cL|(\|w\|_\infty + \varepsilon) + |cb| + M_r$, and $T^* = \frac{1}{\alpha}\ln\frac{\beta}{1-\mu}$.

Proof: The proof follows by using Theorem 5.2.1 in an analogous reasoning as in Remark 4.3.1 in the proof of Theorem 4.3.1. ∎

The parameter M is a bound on the Lipschitz constant of $cx(t) + r(t)$. The bounds suggested in Theorem 5.2.1 and Corollary 5.2.1 are generally conservative. The more knowledge we have about the trajectory of the smoothed system and the reference signal, the better bound we are able to obtain.

We will here use Corollary 5.2.1 to derive a tuning algorithm that gives an exponentially stable dither system, which tracks the state of the smoothed system over an infinite time horizon with any desired accuracy. We assume that we have derived a bound $\|w\|_\infty = \sup_{t\in[0,\infty)}|w(t,r,x_0)|$. This can often be done by solving an LMI. For given tracking accuracy, ε, Corollary 5.2.1 gives the bound (5.6) with (5.7). Here $P > 0$ and $\gamma > 0$ solve the LMI (5.1) and the parameters α and β can be obtained from the LMI (4.41). We would like to optimize the free parameters such that p_0 becomes as small as possible. This is hard since the dependence on the free parameters is nonconvex. One way to obtain a reasonable solution is to pick some $\mu \in (0,1)$, then a dither amplitude A and desired exponential decay rate such that the LMI's (5.1) and (4.41) are feasible. From (5.6) and (5.1) we see that β and $\gamma/\lambda_{\min}(P)$ should be as small as possible (which also makes c_1 and c_2 small). This can done by solving

$$\min \beta^2 \tag{5.8a}$$

s.t.

$$\begin{pmatrix} L^TQ + QL + 2\alpha Q & Qb + c^T \\ b^TQ + c & -2A \end{pmatrix} \leq 0 \tag{5.8b}$$

$$Q \geq \lambda_{\min} I$$

$$\lambda_{\min}\beta^2 I \geq Q.$$

by bisection on β^2 and

$$\min \bar{\lambda} \tag{5.9a}$$

$$s.t.$$

$$\begin{pmatrix} L^TP+PL & Pb+c^T & 0 \\ b^TP+c & -2A & c \\ 0 & c^T & -\gamma I \end{pmatrix} \leq 0 \tag{5.9b}$$

$$\bar{\lambda}P \geq \gamma I$$

$$\gamma > 0.$$

by bisection on $\bar{\lambda}$. From the last optimization problem we obtain $\gamma/\lambda_{\min}(P) \leq \bar{\lambda}$. Note that the constraints of these two optimization problems are LMI's for fixed β^2 and $\bar{\lambda}$, respectively.

We have arrived at the following tuning algorithm:

Step 1 Choose $\mu \in (0,1)$.

Step 2 Choose a desired exponential decay rate α and then select the dither amplitude A so that the LMI's (5.8b) and (5.9b) are feasible.

Step 3 Solve the optimization problem (5.8a), which gives Q and β and then problem (5.9a), which gives P and $\gamma/\lambda_{\min}(P)$.

Step 4 Compute p_0 from (5.6).

5.3 A heuristic tuning algorithm

A practical issue that can be taken into account when tuning the dither period is how much fluctuations on the output we get due to the dither signal. We derive a heuristic bound on these fluctuations.

Assume the transients have decayed and signals are small enough, so that we can consider the linear range of the smoothed nonlinearity. Then the transfer function

$$G_{\text{cl}}(s) = \left(1 + \frac{G(s)}{A}\right)^{-1} \frac{G(s)}{A},$$

where $G(s) = -c(sI-L)^{-1}b$, approximately describe the mapping from the dither signal to the output $y = -cx$. Choose $\omega_0 > 0$ such that

$$|G_{\text{cl}}(j\omega)| \leq \frac{\mu}{A}, \quad \forall \omega \geq \omega_0, \tag{5.10}$$

for some small $\mu > 0$. Then we can expect $|y(t)| \leq \mu$ for sufficiently large t, if the dither period is chosen such that $p_0 \leq 2\pi/\omega_0$. The following heuristic tuning rule follows:

Step 1 Choose an output bound $\mu > 0$. Choose A based on (4.39) in Theorem 4.2.1.

Step 2 Choose p_0 such that $p_0 \leq 2\pi/\omega_0$, where ω_0 satisfies (5.10).

We have assumed the dither signal to be approximately sinusoidal while deriving this bound. Analytical expressions for the stationary periodic oscillation in a dithered relay system can be derived using the results in Section 4.4. This allow exact computation of the size of the dither ripple.

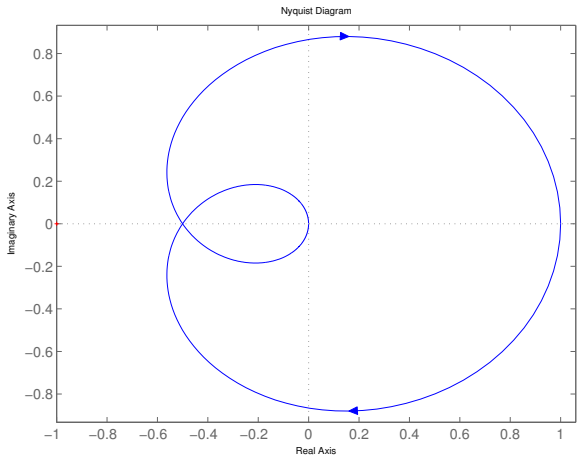

Figure 5.1: Nyquist curve of $G(s) = (1-s)(s+1)^{-2}$.

5.4 An example

Let us continue discussing the example in Section 3.4. Recall that

$$G(s) = -c(sI - L)^{-1}b = \frac{1-s}{(s+1)^2}.$$

In all the tuning algorithms the first step is to choose the dither amplitude A. Consider Theorem 4.2.1 with $H(s) = 0$, which corresponds to the circle criterion. We see from the Nyquist curve of G in Figure 5.1 that for $A > 0.56$

$$\mathrm{Re}\, G(j\omega) + A \geq 0,\ \forall \omega \in \mathbb{R}.$$

Hence, the dithered system is practically stable for $A > 0.56$ and p sufficiently small. By using Theorem 4.2.1 instead with $H(s) = -(s+1)^{-1}$, we can prove practical stability for $A > 0.501$. In order to choose the dither period, the first two tuning algorithms while providing a rigorous bound on p_0, still lead to a conservative result (with $A = 1$ the first algorithm gives $p_0 \simeq 1/10^8$, the second one gives $p_0 \simeq 1/10^4$). A useful guess value of the dither period can be obtained by using the heuristic tuning algorithm (for $A = 1$ and the same approximation error we have $p_0 \simeq 1/3$).

We now analyse the effects of the dither parameters A and p on the responses of the dithered and smoothed systems through some simulations. Figure 5.2 shows a simulation for $A = 0.502$ and $p = 1/10$. The system is close to the stability boundary. Recall that the smoothed system is unstable for $A < 0.5$.

Figure 5.3 shows the effect of the dither amplitude on the stability of the smoothed system: it is possible to obtain a fast convergence by increasing A. Figure 5.4 shows finally the effect of the dither frequency on the approximation between the dithered system and the smoothed system: it is possible to obtain a response very close to the output of the smoothed system by decreasing the dither period. Compare the figure in Section 3.4.

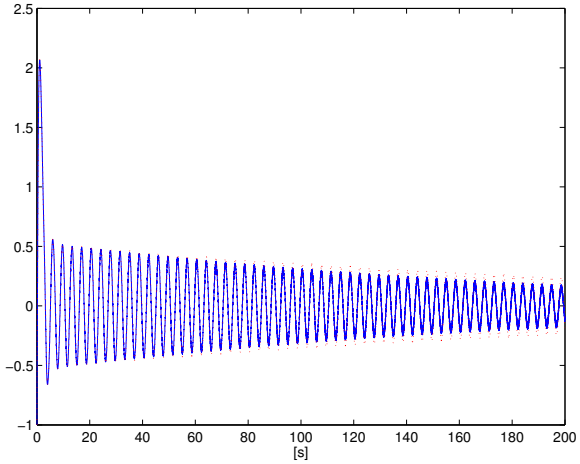

Figure 5.2: Outputs of the dithered (solid) and smoothed (dotted) systems close to the stability boundary predicted by Theorem 4.2.1. Note that in this figure the time axis extents to $t = 200s$.

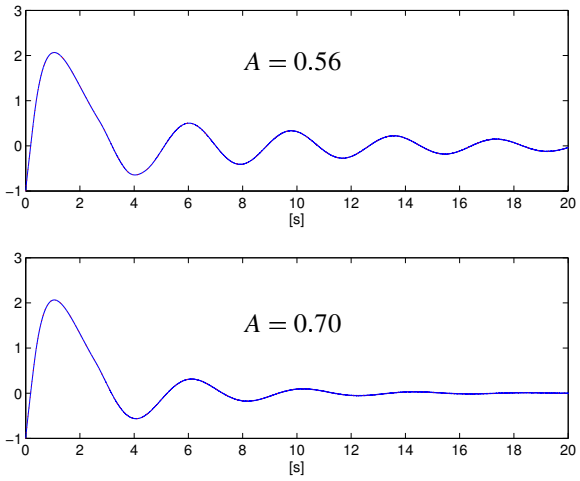

Figure 5.3: Output of the dithered system with δ having period $p = 1/50$. The amplitude is $A = 0.56$ (upper) and $A = 0.70$ (lower), respectively. A smaller A gives thus a less oscillating response.

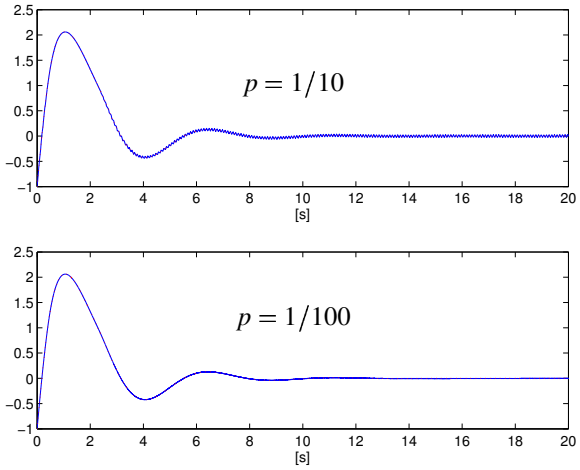

Figure 5.4: Output of the dithered system with δ having amplitude $A = 1$. The period is $p = 1/10$ (upper) and $p = 1/100$ (lower), respectively. A smaller p gives a better agreement between the responses of the dithered and smoothed systems.

Chapter 6

Applications

In this chapter we will present two applications of the averaging technique for the analysis of dithered relay feedback systems. We discuss the DC/DC buck converter and the position control of a DC motor. In both cases the actuator is essentially a switch (a transistor for the buck converter and a H-bridge driver for the DC) so it is modeled as a signum function. In power electronics the basic operations of circuits such as DC/DC converters consist in a toggling among different configurations. This switching operation is realized by using Pulse Width Modulation technique. So we will show that in some cases PWM systems can be viewed as dithered relay feedback systems in which the dither signal is a periodic sawtooth waveform.

6.1 DC/DC buck converter

Let us consider the basic topology of a buck converter reported in Figure 6.1. This circuit realizes a DC/DC conversion controlling the voltage on the load identified by the resistance R in the circuit. The circuit operates in closed loop since the voltage on the load is compared with the reference signal and amplified by a constant gain. This signal (control voltage) is then compared with a periodic sawtooth waveform and the comparator switch on or switch off the transistor S depending on the result of the comparator. In this way the circuit switches from a configuration with input voltage E to a configuration with input voltage zero if the diode D conducts when the switch S is OFF.

In the following we will assume that the buck converter is operating in *Continuous Conduction Mode* (the inductor current never becomes zero so the diode conducts when the switch S is OFF). The buck converter is governed by the following equations:

$$C_c \frac{dv_C}{dt} = i_L - \frac{v_C}{R} \tag{6.1a}$$

$$L_i \frac{di_L}{dt} = v_{\text{in}} - v_C \tag{6.1b}$$

where $v_{\text{in}} = E$ if the switch is ON and $v_{\text{in}} = 0$ if the switch is OFF.

If we introduce the state vector x whose components are $x_1 \equiv v_C$ and $x_2 \equiv i_L$, we

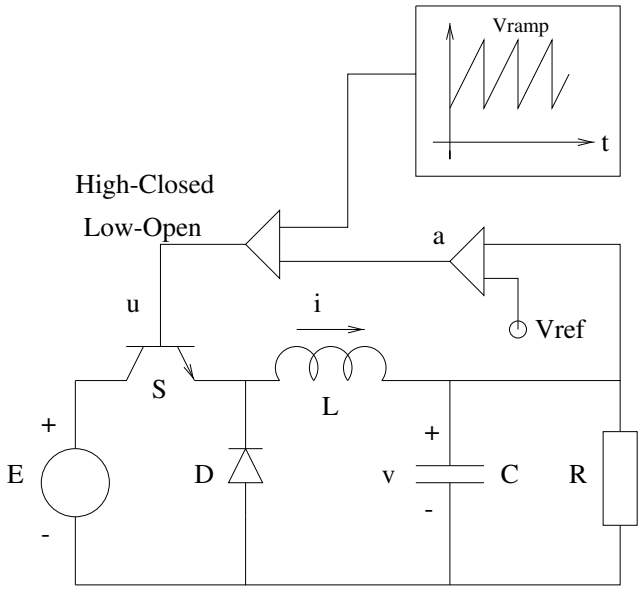

Figure 6.1: Circuit topology of a DC/DC buck converter.

can write $\dot{x} = Lx + b'u$ with

$$L = \begin{pmatrix} -\frac{1}{RC_c} & \frac{1}{C_c} \\ -\frac{1}{L_i} & 0 \end{pmatrix}, \quad b' = \begin{pmatrix} 0 \\ \frac{E}{L_i} \end{pmatrix} \tag{6.2}$$

and $u = 0$ if the switch is OFF and $u = 1$ if the switch is ON. The switch is pulse-width modulated in the following mode: a controlled voltage $v_{\text{con}} = k(v_C - V_{\text{ref}})$ (with $k > 0$) is compared with a sawtooth signal V_{ramp} that varies between V_l and V_u. If the controlled voltage v_{con} is smaller than the sawtooth, the switch is ON and conducts. So we can write

$$\begin{cases} u = 0, & \text{if} \quad V_{\text{ramp}} - k(v_C - V_{\text{ref}}) < 0 \\ u = 1, & \text{if} \quad V_{\text{ramp}} - k(v_C - V_{\text{ref}}) \geq 0. \end{cases} \tag{6.3}$$

This means that $\dot{x} = Lx + b'\eta(V_{\text{ramp}} + k(V_{\text{ref}} - v_C))$ where $\eta(\cdot)$ is the step function.

6.1.1 Converter model as dithered RFS

The buck converter model can be represented as in Figure 6.2

It is possible to do some blocks moving and transformations for obtaining a Relay Feedback System dithered with a sawtooth signal. In fact the step function can be viewed as $\eta(z) = 0.5(1 + \text{rel}(z))$ (of course it occurs to redefine $\text{rel}(0) = 1$) and the V_{ramp} can be viewed as the sum of $(V_u - V_l)/2 + V_l$ and $\delta(t)$ where $\delta(t)$ is the sawtooth signal (defined in 3.15) of amplitude $(V_u - V_l)/2$.

In this way Figure 6.2 is equivalent to the scheme of Figure 6.3.

In practice the buck converter is the following RFS dithered with a sawtooth signal $\delta(t)$ of amplitude $A = (V_u - V_l)/2$:

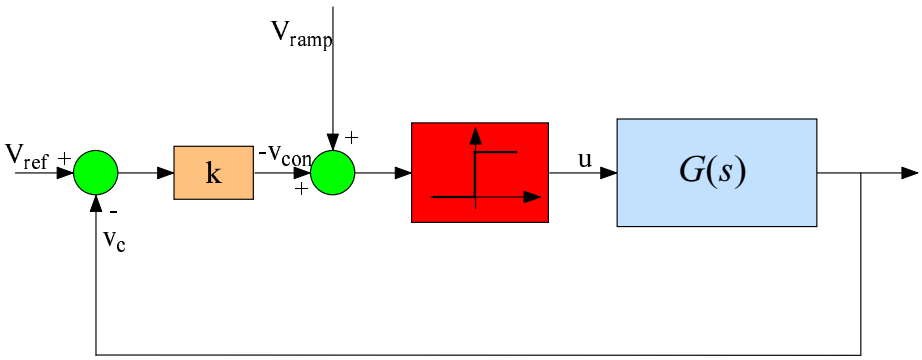

Figure 6.2: Block diagram of a buck converter.

$$\dot{x}(t) = Lx(t) + bn(cx(t) + \delta(t) + r(t)) + b \tag{6.4}$$

where the system matrix L has been written above,

$$b = \frac{1}{2}b' = 0.5 \cdot \begin{pmatrix} 0 \\ \frac{E}{L_i} \end{pmatrix}, \quad c = -k \begin{pmatrix} 1 & 0 \end{pmatrix} \tag{6.5}$$

and

$$r(t) = kV_{\text{ref}} + \frac{V_u - V_l}{2} + V_l. \tag{6.6}$$

The physical variable v_c is now equal to $-cx(t)/k$. It is not difficult to show that the smoothed system corresponding to Equation (6.4) is the following:

$$\dot{w}(t) = Lw(t) + bN(cw(t) + r(t)) + b. \tag{6.7}$$

In fact if we introduce the error $x - w$ we can write

$$\dot{x}(t) - \dot{w}(t) = L[x(t) - w(t)] + b[n(cx(t) + r(t) + \delta(t)) - N(cw(t) + r(t))] \tag{6.8}$$

that is equivalent to Equation (4.5) in the proof of the averaging theorem. So we can apply whole the theory derived in Chapter 4 and Chapter 5.

Let us consider a constant reference $r(t) = r$. If we look at the smoothed system (6.7) we can see that it is a PWL system in which the three configuration are affine in w. We have three cells:

$$\begin{aligned} W_1 &= \{w \ : \ cw + r > A\} \\ W_2 &= \{w \ : \ |cw| \leq A\} \\ W_3 &= \{w \ : \ cw + r < -A\}. \end{aligned}$$

The corresponding systems are

$$\begin{aligned} &\dot{w}(t) = Lw(t) + 2b \quad \text{for } w \in W_1, \\ &\dot{w}(t) = \left(L + \frac{bc}{A}\right) w(t) + b\left(1 + \frac{r}{A}\right) \quad \text{for } w \in W_2 \\ &\dot{w}(t) = Lw(t) \quad \text{for } w \in W_3. \end{aligned}$$

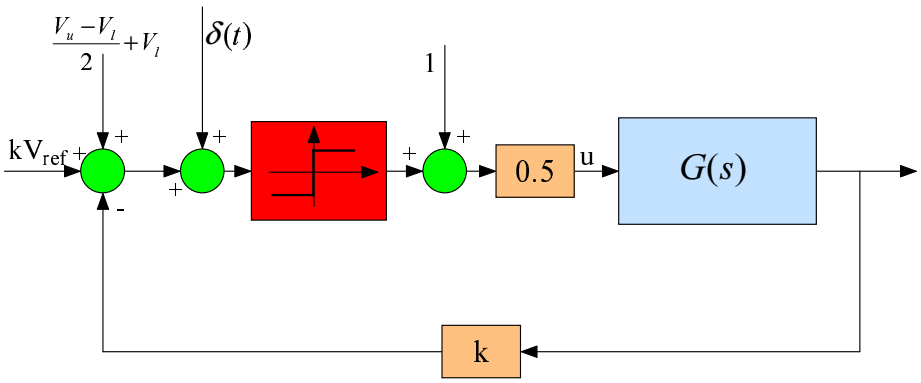

Figure 6.3: Block diagram of a buck converter as a dithered RFS.

The switching surfaces are

$$S_1 = \{w \,:\, cw + r = +A\}$$
$$S_2 = \{w \,:\, cw + r = -A\}.$$

It is clear that the origin is not an equilibrium point since it does not lies in W_3 (here we have the relation $-kw_1 + r < -A \Rightarrow w_1 > (r+A)/k$ that does not hold for $w_1 = 0$ and r, $A > 0$). On the other hand the point $\bar{w}_1 = -L^{-1}2b = \begin{pmatrix} E & E/R \end{pmatrix}^T$ is an equilibrium point only if relation $-kE + r > A$ is satisfied, that is

$$-kE + kV_{\text{ref}} + A + V_l > A \Rightarrow V_{\text{ref}} > E - \frac{V_l}{k}.$$

Otherwise we have only the equilibrium point in the linear region (cell W_2).

6.1.2 Simulations

Let us consider a DC/DC buck converter with the following parameters: $R = 22\Omega, L_i = 20mH, C_c = 47\mu F, E = 25V, V_{\text{ref}} = 12V, V_l = 0.3V, V_u = 10V, k = 8.4, f = 6kHz$ where $f = 1/p$ is the switching frequency. We present some simulations results comparing the output of the buck converter (the capacitor voltage v_c) with the output of the corresponding smoothed system.

In Figure (6.4) we can see both the signal. The corresponding phase plane portrait is reported in Figure (6.5).

If we decrease the switching frequency we would expect a larger ripple in the output of the buck converter. And in fact in Figure 6.6 we can appreciate the difference. The corresponding phase plane portrait is reported in Figure 6.7. Dither theory validates these results.

6.2 Position control of a DC motor

In this section we will present another application in which the PWM control system can be viewed as a dithered relay feedback system.

Let us consider a DC motor that we can supply with a voltage V_a. Our control objective is to put the motor shaft at a desired angular position. The DC motor is

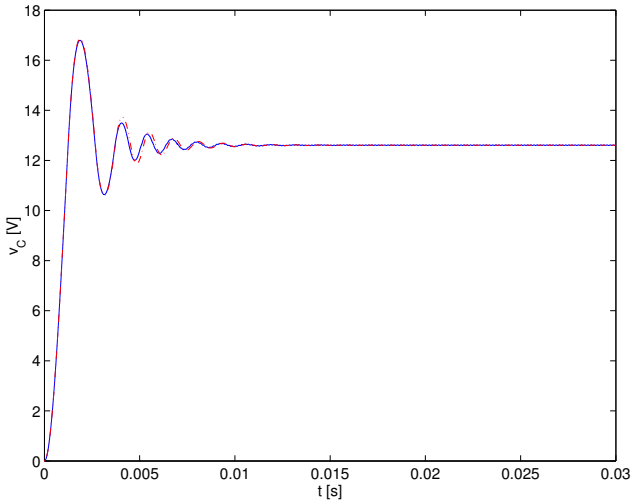

Figure 6.4: Output voltage v_c (solid line) of the buck converter with a step input of amplitude $V_{\text{ref}} = 12V$. The dash-dotted line is the corresponding signal of the smoothed system. The switching frequency is $f = 6kHz$.

modeled as an electric (armature) circuit with a given armature resistance (R_a) and inductance (L_a) and a mechanical subsystem with a inertia J and a viscous coefficient β. The motor provides a torque proportional to the armature current i_a.

We can write the differential equations that describe our physical system:

$$\frac{d\theta(t)}{dt} = \omega(t) \tag{6.9a}$$

$$J\frac{d\omega(t)}{dt} = k_t i_a(t) - \beta\omega(t) - T_L(t) \tag{6.9b}$$

$$L_a\frac{di_a(t)}{dt} = v_a(t) - Ri_a(t) - k_e\omega(t) \tag{6.9c}$$

In the following we will neglect the load torque: $T_L = 0$. By introducing the state vector $x = \begin{pmatrix}\theta & \omega & i_a\end{pmatrix}^T$ we can write

$$\dot{x} = \begin{pmatrix} 0 & 1 & 0 \\ 0 & -\frac{\beta}{J} & \frac{k_t}{J} \\ 0 & -\frac{k_e}{L_a} & -\frac{R}{L_a} \end{pmatrix} x + \begin{pmatrix} 0 \\ 0 \\ \frac{v_a}{L_a} \end{pmatrix}. \tag{6.10}$$

In order to control the position of the motor shaft we need a position transducer. We can use a potentiometer supplying it with a constant voltage V_s (we realize a voltage divider) in such a way that the voltage at two terminals of the potentiometer is proportional to the position of the motor shaft. The control action is performed by providing a constant voltage V_a to the motor by using a H-bridge driver. This device has a logic input that select a positive or negative (in the same way as we invert the motor terminals) supply voltage for the DC motor. The control loop is closed by amplifying the position error and comparing this signal with a sawtooth waveform, like a PWM converter. The

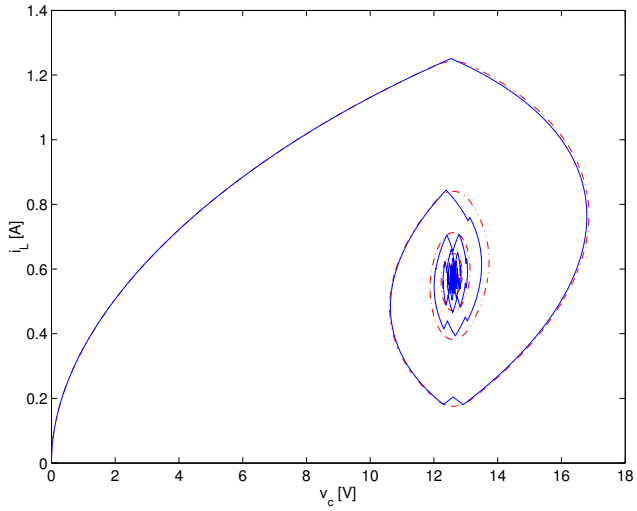

Figure 6.5: Phase plane diagram (solid line) of the buck converter with a step input of amplitude $V_{\text{ref}} = 12V$. The dash-dotted line is the corresponding trajectory of the smoothed system. The switching frequency is $f = 6kHz$.

output of the comparator is the input of the H bridge driver (see Figure 6.8). In this case the input of the linear system is positive or negative, so we have essentially a dithered relay feedback system without the sum of a constant term at the output of the relay input (as for the case of the buck converter in the previous section).

The transducer constant k_{pot} is function of the supply voltage V_s and the resistance of the potentiometer. For example if we use a potentiometer that allows a maximum of 10 revolutions and has a total resistance of $5k\Omega$ (the resistance varies 500Ω per revolution) and we choose a dual supply voltage of $\pm 5V$, we have

$$k_{\text{pot}} = \frac{500}{2\pi} \cdot \frac{1}{5000} \cdot 10 = \frac{1}{2\pi} \frac{\text{V}}{\text{rad}}. \tag{6.11}$$

6.2.1 Simulations

Let us consider a DC motor with the following parameters: $R = 260\Omega, L_a = 30mH, k_t = k_e = 14.325mV/(rad \cdot s^{-1}), \beta = 2.175mN \cdot cm/(rad \cdot s^{-1}), J = 34.8g \cdot cm^2$. The transducer has the constant (6.11). The motor supply voltage is chosen $V_a = 10V$ and the dither signal is chosen as a sawtooth swinging between $-1V$ and $+1V$. Moreover we use a proportional gain $k = 0.42$. The desired position angle is $\theta_{\text{ref}} = -20°$, so that we have $V_{\text{ref}} = -20\frac{\pi}{180} \cdot \frac{1}{2\pi} V$.

In Figure 6.9 the performances of a simple relay control system (without PWM) are reported. The output is oscillatory and the system has a limit cycle of amplitude 0.25° (see zoom in Figure 6.10).

In Figure 6.11 it is reported the step response of the closed loop system when the dither frequency f is chosen equal to $50Hz$.

It is possible to appreciate the presence of a ripple on the position signal due to the low switching frequency. If we use a frequency $f = 500Hz$, the ripple is much more attenuated (see Figure (6.12)).

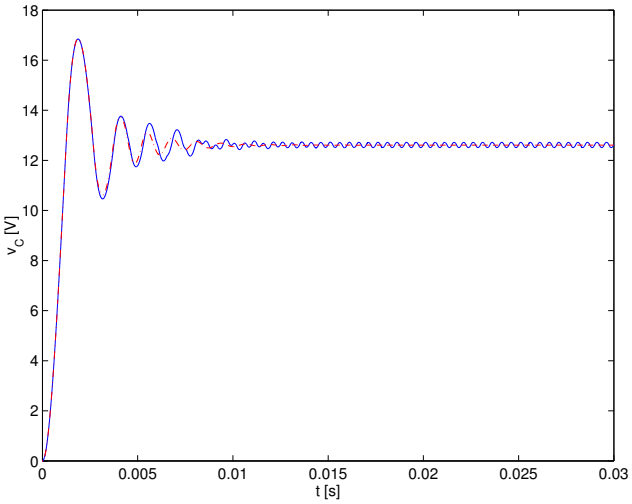

Figure 6.6: Output voltage v_c (solid line) of the buck converter with a step input of amplitude $V_{\text{ref}} = 12V$. The dash-dotted line is the corresponding signal of the smoothed system The switching frequency is $f = 2kHz$.

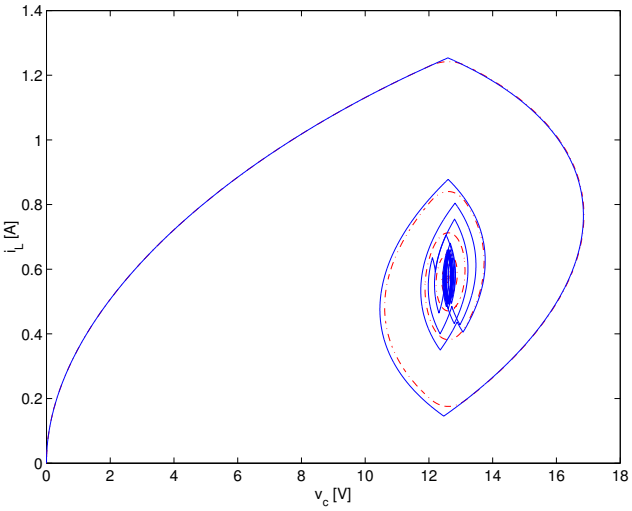

Figure 6.7: Phase plane diagram (solid line) of the buck converter with a step input of amplitude $V_{\text{ref}} = 12V$. The dash-dotted line is the corresponding trajectory of the smoothed system. The switching frequency is $f = 2kHz$.

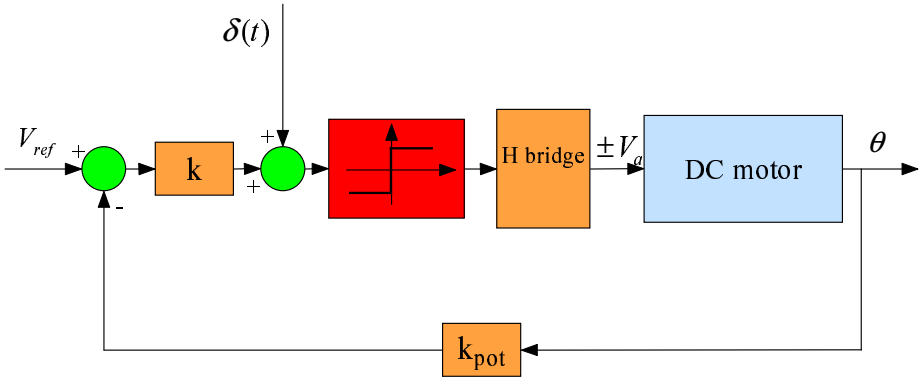

Figure 6.8: Block diagram of the motor position control system.

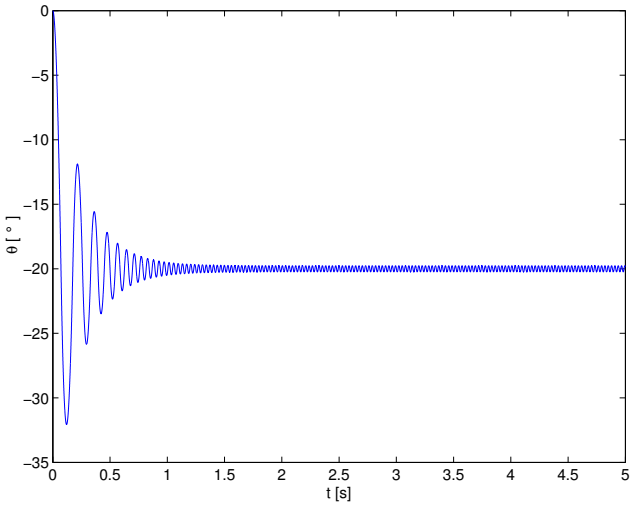

Figure 6.9: Step response of the position control system without PWM.

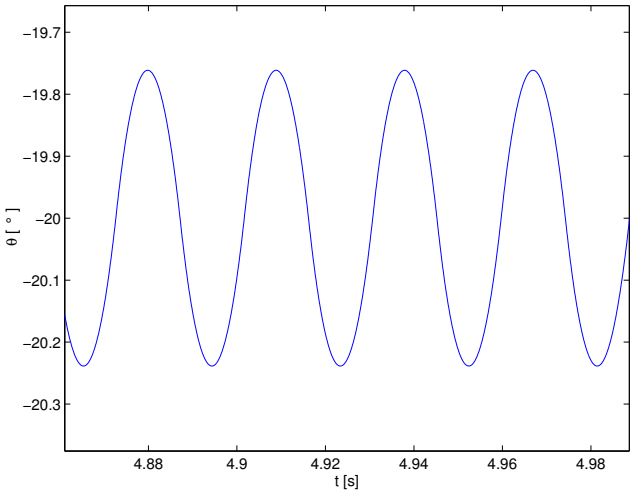

Figure 6.10: Zoom of the Figure 6.9

.

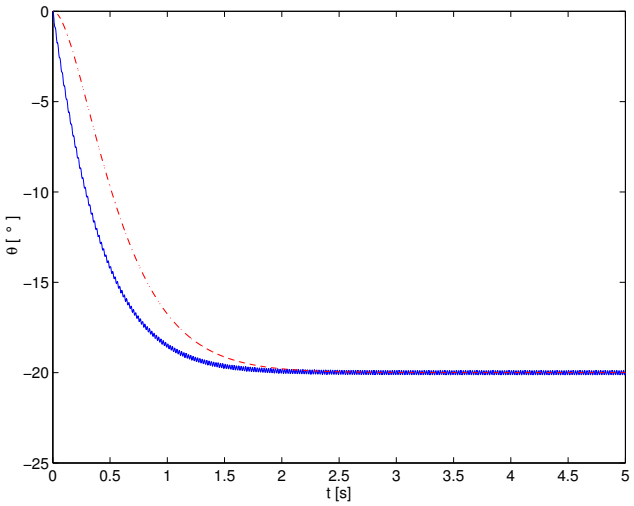

Figure 6.11: Step response of the position control system (solid line) and the corresponding smoothed system output (dash-dotted line). The switching frequency is $f = 50Hz$.

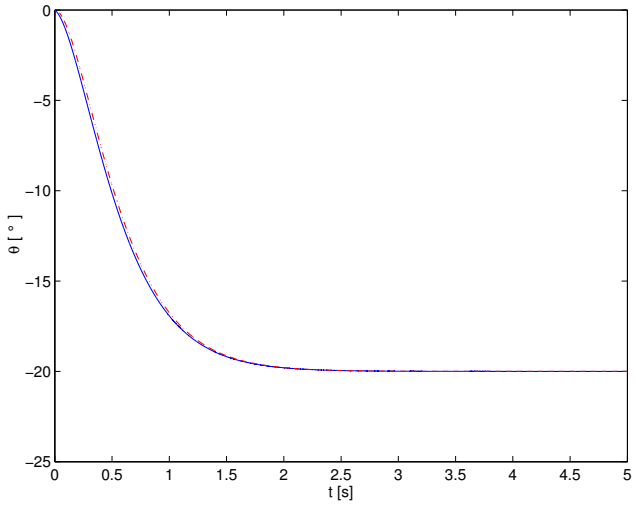

Figure 6.12: Step response of the position control system (solid line) and the corresponding smoothed system output (dash-dotted line). The switching frequency is $f = 500Hz$.

Chapter 7

Conclusions

7.1 Summary

This thesis has focused on the problem of analysing relay feedback systems in which the relay nonlinearity is forced with periodic high frequency waveforms (known as dither signals). The aim of this technique, widely used in the practice, is to attenuate nonlinear effects (limit cycle, sub-harmonics, chaos, etc.). Although dithering is not a new idea, its effects in nonsmooth feedback systems are still not well understood.

This thesis gave some ideas and tools for studying such class of problems. The main result is that a relay feedback system with a triangular dither signal at the input of the hard nonlinearity can be viewed as a feedback system (without dither) in which the relay is replaced by a saturation. While the amplitude of the dither signal affects the slope of the saturation, the approximate equivalence between the dithered and smoothed systems depends on the frequency of the dither signal. Studying a saturated system is certainly simpler than studying a dithered relay feedback system.

Results given for triangular dither are valid also for sawtooth dither signals (applicative examples have been presented in chapter 6). Other types of dither signals have been discussed in the thesis. In particular it has been shown how the shape of dither can affect the behaviour of the dithered relay feedback system. Periodic signals with time interval during which they are constant (zero-slope dither) does not satisfy averaging principle and the can induce some strange phenomena in dithered systems.

A particular class of trajectories, called smooth-switching trajectories, has been discussed and an averaging theorem that relates this type of trajectories with the existence of a limit cycle in the smoothed system has been derived.

On the other hand, looking at a design problem, explicit relations to achieve a desired approximation error have been given. Furthermore analytical and practical guidelines to design dithered systems have been presented.

7.2 Future work

The work presented in this thesis has investigated some problems that are far from being totally understood. Thus future research is certainly possible on this topic. In the following some interesting ideas are given.

- It would be worth to investigate the extension of averaging theorems for other

types of piecewise linear systems in which, for example, the dynamic matrix changes through a switching rule relay-like. Then a generalization of averaging theory for nonlinear systems (not necessarily piecewise linear) with relay nonlinearities would be very interesting.

- Design procedures derived by theoretical results and by using optimization techniques such as LMIs are quite conservative. It would be interesting to investigate different approaches in order to make more practical the bound on approximation error. Maybe it would be useful approaching with a mean-case analysis rather than a worst case.

- Stochastic dithering seems to be quite straightforward to analyse by using tools presented in Chapter 3, but it could be worth to get deeper into the problem and to exploit this approach in order to get some other interesting design procedures.

- All results derived in this thesis are valid for dynamic systems described by differential equations. It would be very nice to find analogous results for discrete time systems. Probably it is the most challenging problem among the listed points and it would open the door at very interesting applications such as analysis and design of sigma-delta converters.

Bibliography

Andronov, A.A., S.E. Khaikin and A.A. Vitt (1965). *Theory of Oscillators*. Pergamon Press. Oxford, UK.

Armstrong-Helouvry, B. (1991). *Control of Machines with Friction*. Kluwer Academic Publisher. Boston.

Armstrong-Helouvry, B., P. Dupont and C. Canudas de Wit (1994). A survey of models, analysis tools and compensation methods for control of machines with friction. *Automatica* **30**(7), 1083–1138.

Åström, K. J. (1995). Oscillations in systems with relay feedback. In: *Adaptive Control, Filtering, and Signal Processing* (K. J. Åström, G. C. Goodwin and P. R. Kumar, Eds.). Vol. 74 of *IMA Volumes in Mathematics and its Applications*. pp. 1–25. Springer-Verlag.

Åström, K. J. and T. Hägglund (1995). *PID Controllers: Theory, Design, and Tuning*. second ed.. Instrument Society of America. Research Triangle Park, NC.

Åström, K.J. and B. Wittenmark (1989). *Adaptive Control*. Addison-Wesley. Reading, MA.

Atherton, D. (1975). *Nonlinear Control Engineering*. Van Nostrand Reinhold Co.. London.

Carbone, P. and D. Petri (2000). Performance of stochastic and deterministic dithered quantizers. *IEEE Transactions on Instrumentation and Measurement* **49**(2), 337–340.

di Bernardo, M., K. H. Johansson and F. Vasca (2000). Self-oscillations and sliding in relay feedback systems: Symmetry and bifurcations. *International Journal of Bifurcations and Chaos* **11**(4), 1121–1140.

Elia, N. and S. K. Mitter (2001). Stabilization of linear systems with limited information. *IEEE Transactions on Automatic Control* **46**(9), 1384–1400.

Feeny, B.F. and F.C. Moon (2000). Quenching stick-slip chaos with dither. *Journal of Sound and Vibration* **237**(1), 173–180.

Fuh, Chyun-Chau and Pi Cheng Tung (1997). Experimental and analytical study of dither signals in a class of chaotic systems. *Physics Letters A* **229**(4), 228–234.

Gelb, A. and W. Vander-Velde (1968). *Multiple Input Describing Functions*. McGraw-Hill.

Gelig, A. Kh. and A. Churilov (1998). *Stability and Oscillations of Nonlinear Pulse Modulated Systems*. Birkhäuser. Berlin.

Gonçalves, J. M., A. Megretski and M. A. Dahleh (2001). Global stability of relay feedback systems. *IEEE Trans. on Automatic Control* **46**(4), 550–562.

Gonçalves, J.M.M.S. (2000). Constructive Global Analysis of Hybrid Systems. PhD thesis. Massachussets Institute of Technology. Cambridge, Massachussets, USA.

Gray, R.M. and D.L. Neuhoff (1998). Quantization. *IEEE Transactions on Information Theory* **44**(6), 2325–2383.

Gray, R.M. and T.G. Stockham (1993). Dithered quantizers. *IEEE Transactions Information Theory* **39**(3), 805–812.

Imura, J. and A. van der Shaft (2000). Characterization of well-posedness of piecewise-linear systems. *IEEE Transactions on Automatic Control* **45**(9), 1600–1619.

Johansson, K. H., A. Barabanov and K. J. Åström (2002). Limit cycles with chattering in relay feedback systems. *IEEE Transactions on Automatic Control*.

Johansson, K. H., A. Rantzer and K. J. Åström (1999). Fast switches in relay feedback systems. *Automatica* **35**(4), 539–552.

Johansson, M. (1999). Piecewise Linear Control Systems. PhD thesis. Lund Institute of Technology. Lund, Sweden.

Khalil, H.K. (2002). *Nonlinear Systems*. third ed.. Prentice-Hall.

Lehman, B. and R. Bass (1996). Extensions of averaging theory to power electronics. *IEEE Transactions on Power Electronics* **11**(4), 542–553.

Ljung, L. (1999). *System Identification. Theory for the User*. second ed.. Prentice-Hall. New Jersey, USA.

Megretski, A. and A. Rantzer (1997). System analysis via integral quadratic constraints. *IEEE Transactions on Automatic Control* **42**(6), 819–830.

Morgül, Ö. (1999). On the control of some chaotic systems by using dither. *Physics Letters A* **262**, 144–151.

Morse, A. S. (1995). Control using logic-based switching. In: *Trends in Control. A European Perspective* (A. Isidori, Ed.). pp. 69–113. Springer.

Mossaheb, S. (1983). Application of a method of averaging to the study of dither in non-linear systems. *International Journal of Control* **38**(3), 557–576.

Norsworthy, S.R., R. Schreier and G.C. Temes (1996). *Delta Sigma Data Converters*. John Wiley & Sons Inc.

Papoulis, A. (1991). *Probability, Random Variables and Stochastic Processes*. third ed.. McGraw-Hill.

Pervozvanski, A. A. and C. Canudas de Wit (2002). Asymptotic analysis of the dither effect in systems with friction. *Automatica* **38**(1), 105–113.

Peterchev, A. V. and S. R. Sanders (2001). Quantization resolution and limit cycling in digitally controlled PWM converters. In: *Proc. IEEE Power Electronics Specialists Conf.*. Vancouver, Canada.

Sastry, S. (1999). *Nonlinear Systems: Analysis, Stability and Control*. Springer-Verlag. New York.

Taylor, S.J. (1966). *Introduction to Measure and Integration*. Cambridge University Press.

Tsypkin, Ya. Z. (1984). *Relay Control Systems*. Cambridge University Press. Cambridge, UK.

Utkin, V.I. (1992). *Sliding Modes in Control and Optimization*. Springer Verlag. Berlin.

Varigonda, S. and T.T. Georgiou (2001). Dynamics of relay relaxation oscillators. *IEEE Transactions on Automatic Control* **46**(1), 65–77.

Vidyasagar, M. (1993). *Nonlinear Systems Analysis*. second ed.. Prentice Hall. Englewood Cliffs, New Jersey.

Wagdy, M.F. (1989). Effects of various dither forms on quantization errors of ideal a/d converters. *IEEE Transactions on Instrumentation and Measurement* **38**(4), 850–855.

Wagdy, M.F. and M. Goff (1994). Linearizing average transfer characteristics of ideal adc's via analog and digital dithering. *IEEE Transactions on Instrumentation and Measurement* **43**(2), 146–150.

Wannamaker, R.A. (1997). The Theory of Dithered Quantization. PhD thesis. University of Waterloo. Dept. of Applied Mathematics.

Wannamaker, R.A., S.P. Lipshitz and J. Vanderkooy (2000*a*). Stochastic resonance as dithering. *Physical Review E (Statistical Physics)* **61**(1), 233–236.

Wannamaker, R.A., S.P. Lipshitz, J. Vanderkooy and J.N. Wright (2000*b*). A theory of nonsubtractive dither. *IEEE Transactions on Signal Processing* **48**(2), 499–516.

Zames, G. and N. A. Shneydor (1976). Dither in non-linear systems. *IEEE Transactions on Automatic Control* **21**(5), 660–667.

Zames, G. and N.A. Shneydor (1977). Structural stabilization and quenching by dither in non-linear systems. *IEEE Transactions on Automatic Control* **22**(3), 352–361.

Zames, G. and P.L. Falb (1968). Stability conditions for systems with monotone and slope-restricted nonlinearities. *SIAM Journal of Control* **6**(1), 89–108.

Appendix A

Mathematical review

In this appendix we introduce several mathematical concepts and tools that will be used throughout the thesis. We also include a short introduction to dynamic systems, including equilibrium points and limit cycles. Most of the concepts are derived from (Khalil 2002).

A.1 Basic concepts

Let the field of real numbers be denoted by $\mathbb{R}$, the set of $n \times 1$ vectors with elements in $\mathbb{R}$ by $\mathbb{R}^n$ (n-dimensional Euclidean space), and the set of all $m \times n$ matrices with elements in $\mathbb{R}$ by $\mathbb{R}^{m \times n}$. Let I denote the identity matrix and superscript (^{T}) denote transpose. A matrix A is Hurwitz if the real part of each eigenvalue of A is negative.

A.1.1 Vector and matrix norms

The norm $\|x\|$ of a vector x is a real-valued function with the following properties:

- $\|x\| \geq x$ for all $x \in \mathbb{R}^n$, with $\|x\| = 0$ if and only if $x = 0$.
- $\|x+y\| \leq \|x\| + \|y\|$, for all $x,\ y \in \mathbb{R}^n$ (**triangle inequality property**).
- $\|\alpha x\| = |\alpha|\|x\|$, for all $\alpha \in \mathbb{R}$ and $x \in \mathbb{R}^n$.

The p-norm of a vector $x = \left(x_1, x_2, \cdots, x_n\right)^T \in \mathbb{R}^n$ is given by

$$\|x\|_p = \left(\sum_{i=1}^{n} |x_i|^p\right)^{\frac{1}{p}},\ 1 \leq p < \infty \tag{A.1}$$

and

$$\|x\|_\infty = \max_i |x_i|. \tag{A.2}$$

The most commonly used norms are $\|x\|_1$, $\|x\|_\infty$ and the Euclidean norm $\|x\|_2 = \sqrt{x^T x}$. In this thesis, we reserve the notation $|\cdot|$ for the Euclidean norm of a vector.

The induced p-norm of a matrix A is defined by

$$\|A\|_p = \sup_{x \neq 0} \frac{\|Ax\|_p}{\|x\|_p} = \max_{\|x\|_p = 1} \|Ax\|_p \tag{A.3}$$

where sup denotes the least upper bound (such as inf denotes the greatest lower bound).

For $p = 1, 2, \infty$ we have

$$\|A\|_1 = \max_j \sum_{i=1}^{m} |a_{ij}|, \quad \|A\|_2 = \sqrt{\lambda_{\max}(A^T A)}, \quad \|A\|_\infty = \max_i \sum_{j=1}^{n} |a_{ij}|$$

where $\lambda_{\max}(A^T A)$ is the maximum eigenvalue of the matrix $A^T A$.

A.1.2 Signals norms

We will consider the space of signals $u(t) : [a,b] \mapsto \mathbb{R}^m$. We denote with $\mathcal{L}_p^m$ the space of all the real signals $u(t)$ with norm

$$\|u(t)\|_{\mathcal{L}_p} = \left(\int_0^\infty \|u(t)\|^p dt \right)^{\frac{1}{p}} < \infty.$$

So we have, for the space of piecewise continuous, bounded functions,

$$\|u(t)\|_{\mathcal{L}_\infty} = \sup_{t \geq 0} \|u(t)\| < \infty,$$

while for the space of piecewise continuous, square-integrable functions,

$$\|u(t)\|_{\mathcal{L}_2} = \sqrt{\int_0^\infty u^T(t) u(t) dt} < \infty.$$

A.1.3 Positive definite matrices

A matrix $P \in \mathbb{R}^{n \times n}$ is called symmetric if $P = P^T$ and positive definite (positive semidefinite) if $x^T P x > 0$ ($x^T P x \geq 0$) for all nonzero $x \in \mathbb{R}^n$. $P > 0$ on S stands for $x^T P x > 0$ for all nonzero $x \in S \subseteq \mathbb{R}^n$. We will write $P > Q$ ($P \geq Q$) if the matrix $P - Q$ is positive definite (semidefinite). For a real symmetric matrix A it can be shown that A is positive definite (semidefinite) if and only if the eigenvalues of A are positive (nonnegative).

Moreover for all matrices $A \in \mathbb{R}^{n \times n}$ (not necessarily symmetric and positive definite) the following inequality holds:

$$\lambda_{\max}(A) \cdot I \geq A \geq \lambda_{\min}(A) \cdot I$$

and $\lambda_{\max}(A)$ is the minimum λ such that $\lambda I \geq A$. Analogously $\lambda_{\min}(A)$ is the maximum λ such that $A \geq \lambda I$.

A.2 Sets and neighborhoods

Definition A.2.1 *A* neighborhood *of a point x is a set $N_\varepsilon(x)$ of all points y such that $|x - y| < \varepsilon$. The number ε is the radius of $N_\varepsilon(x)$.*

Definition A.2.2 *A point x is called* limit point *of the set X if every neighborhood of x contains a point $y \neq x$ such that $y \in X$.*

Definition A.2.3 *The set X is* closed *if every limit point of X is a point of X. The* closure *of X is the set $\bar{X} = X \cup \{x : x \text{ is a limit point of } X\}$.*

A point x of X is an interior point *of X if there is a neighborhood $N_\varepsilon(x)$ of x such that $N_\varepsilon(x) \subset X$. X is* open *if every point of X is an interior point of X.*

X is bounded *if there exists a real number $M > 0$ and a point $y \in \mathbb{R}^n$ such that $X \subseteq N_M(y)$.*

A.3 Gronwall-Bellman inequality

Let $\lambda : [a,b] \mapsto \mathbb{R}$ be continuous and $\mu : [a,b] \mapsto \mathbb{R}$ be continuous and nonnegative. If a continuous function $y : [a,b] \mapsto \mathbb{R}$ satisfies

$$y(t) \leq \lambda(t) + \int_a^t \mu(s)y(s)ds$$

for $a \leq t \leq b$, then on the same time interval

$$y(t) \leq \lambda(t) + \int_a^t \lambda(s)\mu(s) \exp\left[\int_s^t \mu(\tau)d\tau\right] ds.$$

In particular, if $\lambda(t) \equiv \lambda$ is a constant, then

$$y(t) \leq \lambda \exp\left[\int_a^t \mu(\tau)d\tau\right].$$

If, in addition, $\mu(t) \equiv \mu \geq 0$ is a constant, then

$$y(t) \leq \lambda e^{\mu(t-a)}.$$

A.4 Dynamical systems

A time continuous dynamical system is described by the following differential equation

$$\dot{x} = f(t,x)$$

with $x \in \mathbb{R}^n$. The previous mathematical model is used to describe a variety of physical problems. Of course it is an interesting point if the mathematical model has a solution $x(t)$ that satisfies the initial-value problem

$$\dot{x} = f(t,x), \quad x(t_0) = x_0 \tag{A.4}$$

for $t > t_0$.

The question of existence and uniqueness of solution is addressed by the following theorem:

Theorem A.4.1 *Suppose that $f(t,x)$ is piecewise continuous in t and satisfies*

$$\|f(t,x) - f(t,y)\| \leq L\|x - y\|$$

$\forall x,y \in \mathbb{R}^n$, $\forall t \in [t_0,t_1]$. Then, the state equation $\dot{x} = f(t,x)$, with $x(t_0) = x_0$, has a unique solution over $[t_0,t_1]$.

A special case of dynamic system is when the function f does not depend explicitly on time:

$$\dot{x} = f(x). \tag{A.5}$$

In this case we speak about a *autonomous* or *time-invariant* dynamical system.

A.5 Equilibrium points

An *equilibrium point* x^* of the system (A.5) is a point such that when the system starts from the initial condition x^* it will remain in x^* for all future time. Then equilibrium points x^* are the roots of equation $f(x) = 0$.

Definition A.5.1 *The equilibrium point x^* of system* (A.5) *is said* stable *if, for each $\varepsilon > 0$ there exists a $\delta > 0$ such that*

$$|x(0) - x^*| < \delta \Rightarrow |x(t) - x^*| < \varepsilon, \ \forall t \geq 0.$$

A stable equilibrium point x^* is called asymptotically stable *if*

$$|x(0) - x^*| < \delta \Rightarrow \lim_{t \to \infty} x(t) = x^*.$$

Moreover it is globally asymptotically stable *if it is asymptotically stable for every initial condition $x(0) \in \mathbb{R}^n$. We will say an equilibrium point x^* to be* exponentially stable *if there exist a α and β such that*

$$|x(t) - x^*| \leq \beta e^{-\alpha t} |x(0) - x^*|.$$

A.6 Limit cycles

Definition A.6.1 (Periodic orbits and limit cycles) *A system oscillates when it has a* nontrivial *(we exclude constant solutions)* periodic solution

$$x(t + T) = x(t), \quad \forall t \geq 0$$

for some $T > 0$. The image of a periodic solution in the state space is called a periodic orbit *or* closed orbit. *An* isolated *periodic orbit is called* limit cycle.

Definition A.6.2 (Invariant sets) *Let $x(t)$ be the solution of* (A.5). *A point p is said to be a* positive limit point *of $x(t)$ if there is a sequence $\{t_n\}$, with $t_n \to \infty$ as $n \to \infty$, such that $x(t_n) \to p$ as $n \to \infty$.*

A set M is said to be an invariant set *with respect to* (A.5) *if*

$$x(0) \in M \Rightarrow x(t) \in M, \quad \forall t \in \mathbb{R}.$$

In the previous definition, if a point belongs to an invariant set M, it belongs to M for all time instants in the past and in the future. If we look only at future, we will say

Definition A.6.3 *A set M is said to be a* positively invariant set *if*

$$x(0) \in M \Rightarrow x(t) \in M, \quad \forall t \geq 0.$$

Definition A.6.4 *We say that $x(t)$ approaches a positive limit set M as t approaches infinity if, for each $\varepsilon > 0$ there is a $T > 0$ such that*

$$\mathrm{d}(x(t), M) < \varepsilon, \quad \forall t > T$$

where

$$\mathrm{d}(p, M) = \inf_{x \in M} \|p - x\|.$$

In this framework a stable limit cycle is the positive limit set of every solution starting sufficiently near the limit cycle (it is not necessarily globally stable). It is worth to note that it is not necessary the existence of $\lim_{t\to\infty} x(t)$ although $x(t)$ approaches the positive limit set M.

We can define stability of limit cycles analogously as for equilibrium points:

Definition A.6.5 *A neighborhood of a limit cycle γ of* (A.5) *is the set $U_\varepsilon(\gamma) = \{x \in \mathbb{R}^n : \mathrm{d}(x,\gamma) < \varepsilon\}$. A limit cycle γ is said* stable *if, for each $\varepsilon > 0$ there exists a $\delta > 0$ such that*

$$x(0) \in U_\delta \Rightarrow x(t) \in U_\varepsilon,\ \forall t \geq 0.$$

A stable limit cycle γ is called asymptotically stable *if*

$$x(0) \in U_\delta \Rightarrow \lim_{t\to\infty} \mathrm{d}(x(t),\gamma) = 0.$$

Moreover it is globally asymptotically stable *if it is asymptotically stable for every initial condition $x(0) \in \mathbb{R}^n$. We will say a limit cycle γ* exponentially stable *if there exist a α and β such that*

$$\mathrm{d}(x(t),\gamma) \leq \beta e^{-\alpha t}\, \mathrm{d}(x(0),\gamma).$$